INVESTIGATION OF CEMENTED TAILINGS BACKFILL AND WELLBORE STABILITY FOR NARROW VEIN MINING BY DRILLING

by
© JAVAD SOMEEHNESHIN

A thesis submitted to the School of Graduate Studies in partial fulfillment of the requirements for the degree of

Master of Engineering

Faculty of Engineering and Applied Science

Memorial University of Newfoundland

October 2020

St John’s, Newfoundland, Canada

Abstract

In this thesis, a comprehensive investigation of using tailings in backfilling material and the percentage of Portland cement and binder composition (a combination of Portland cement and fly ash) with the proportion of (80:20) is studied. Curing time and curing strength of the backfilling material after 7 days, 14 days, and 28 days were the main objective of this thesis. The freestanding vertical face of the void space by inclined stope method was calculated. Specimens were made with Portland cement as the first binder, which was composed of 6%, 8%, and 10% of the solid content of the mixture and 20% water content of the backfilling mixture. The Curing time and curing strength of the specimens in this first binder were measured by Geo-mechanical Loading Frame in Drilling Technology Laboratory (DTL). The second series of the specimens were made with binder composed of regular Portland cement 80% type GU and fly ash 20% class C with 6%, 8%, and 10% of the solid content of the mixture and 20% water content of the backfilling mixture. Then the curing time and curing strength of the specimens were measured. Finally, the results were compared and the effect of binder dosage on Unconfined Compressive Strength (UCS), the effect of binder composition on UCS, the effect of curing time on UCS, and the stiffness of backfilling materials for both binders were presented.

In addition, an analytical study and Discrete Element Method (DEM) simulation were conducted to evaluate the wellbore stability of steeply mining using various wellbore failure criteria. Mining site data of surface and subsurface in-situ stress and rock mechanics properties was collected to support the study. The dimensions of the studied wellbore were 100m maximum depth, 1.3m maximum diameter, and 45 degrees inclination. The wellbore rock failure was analyzed, and the critical wellbore pressure after drilling in four essential azimuths (i.e. 0°, 90°, 180°, and 270°) using pure water was calculated. The results of the

individual and the analytical-DEM coupled study demonstrated that the wellbore stability. The critical wellbore pressure is negative all along the wellbore; also, all applied stresses around the wellbore are between minimum wellbore pressure and maximum wellbore pressure, which indicates the stability of the well.

Acknowledgements

I would like to thank my supervisor Prof. Stephen Butt, for their consistent support and guidance during the running of this project. Furthermore, I would like to thank Dr. Abdelsalam Abugharara and the rest of the postgraduate research team (DTL Group) for their collaborative effort during data collection. I would also like to ac-knowledge Memorial University of Newfoundland and Labrador for their participation and engagement in the study.

In addition, I would also like to mention about my fellow group members Zijian Li, Daiyan Ahmad, Dipesh Maharjan and Shaheen Shah, without whom this journey would be not so comfortable.

I would like to recognize Anaconda Mining Inc. and MITACS Accelerate Program for providing the research fund and giving us the opportunity to learn from the field and industry.

I am grateful to my parents, my siblings, who have been there for me all the way of my graduate life. I am truly thankful for having them all in my life.

Table of Contents

List of Figures

List of Tables

List of Nomenclature

σ_h	Minimum Horizontal Stress
σ_H	Maximum Horizontal Stress
σ_v	Normal Vertical Stress
ARD	Acid Rock Drainage
BHP	Bottom Hole Pressure
CCS	Confined Compressive Strength
CPB	Cemented Paste Backfill
DTL	Drilling Technology Laboratory
FW	Foot Wall
G	Gravitational Accelerate
GSI	Geological Strength Index
HW	Hanging Wall
NVM	Narrow Vein Mining
PC	Portland Cement
PPF	Pore Pressure Factor

SD NVOB	Steeply Dipping Narrow Vein Ore Bodies
SMD	Sustainable Mining by Drilling
UCS	Uniaxial Compressive Strength
UNEP	United Nations Environment Program

Chapter 1: Introduction

1.1 Overview of Sustainable Mining by Drilling (SMD)

The Drilling Technology Laboratory (DTL) group has an industrial partnership with a Newfoundland Gold Mine, also known as Anaconda mining, who focuses on making steeply dipping narrow vein ore bodies feasible for ore extraction. Traditional mining techniques, like underground mining (cut and fill mining, shrinkage mining) and open pit, produce too large a stripping ratio for the mining to be economically successful. To combat the unfeasibility of the traditional mining techniques on steeply dipping ore bodies, SMD was developed. This novel mining technique uses drilling rigs to surgically remove the ore through directional drilling. The SMD technique involves detailed geophysical imaging of the boundary regions associated with the borehole. The goal of the imaging is to adjust the trajectory of a directional drill string to optimize the stripping ratio by steering the drill string within the ore body. Once the ore has been extracted, mining reclamation is performed by infilling the boreholes.

The SMD method is based on a two-pass drilling procedure using a high torque, high thrust drill rig that is custom modified for the mining equipment. For the first drilling pass, a pilot hole is drilled along the dip of the vein. This hole is directionally steered using downhole geophysical imaging tools to follow a trajectory that is halfway between the Hanging Wall (HW) and Foot Wall (FW) contacts of the vein. In the second drilling pass, the pilot hole is opened to the full width of the vein using a large diameter hole opener that follows the trajectory of the pilot hole. The holes will be drilled in primary and secondary sequencing. When primary holes are drilled in the intact rock, and secondary holes are drilled between

the primary holes. Primary holes need to be backfilled using cemented tailing backfill, while secondary holes do not.

To backfill the holes, mill tailings are suggested in this thesis since mill tailings are free and available in the mine site. Also, the transportation fee will be reduced. Using tailings of ore processor not only is more convenient to use but also the majority of the produced tailings will be placed into the holes, and it will decrease cost and time on planning to dispose of tailings out of the mine site.

The tailings have a suitable grain size distribution, which can increase the strength of the backfilling and will boost the pump ability of the backfilling through the pipeline to the holes. Mixing the tailings with Portland cement and fly ash as a binder will increase the strength of the backfilling material, and placing the backfilling will stabilize the wellbores. The wellbores are required to be filled after extraction to provide support for HW and prevent the collapse of jointed rocks into the wellbores.

1.2 Backfilling and wellbore stability

One of the most important tasks of the post-mining process is called mine backfilling. This is the process of replacing the soil or rock into the excavated area of the mine or trenches. Backfill is made from soil, overburden, mine tailings, or any kind of aggregate which can be imported as a filler and booster to emplace in the extracted area, which was excavated by a mining operation. Backfill material is placed into the previously extracted stopes to produce a stable platform for the miners to work on and ground support for the walls of the adjacent adits while the mining progresses by reducing the amount of open area that might be filled by a collapse of the encompassing pillars (Barret et al., 1978). Backfilling is the last operation of mining, and it requires skills and heavy equipment. Also, backfilling can be performed by using flow able fill. A flow able fill is a mixture made by aggregates and

binders with a low water binder ratio. The binder can be Portland cement or a combination of Portland cement and fly ash, or slag and any type of addition to suit different purposes. Additives are added to the binder to reduce the water-to-binder ratio and increase the strength of the backfilling. Depending on the type of the void space, and the required strength for the backfilling, the amount of the binder will vary. The cementitious material is delivered to the mine site by a ready-mix truck and will be pumped into the void space using a utility pipe.

Backfill material is categorized as hydraulic fill, paste fill, and rock fill. In order to increase the strength of the backfill material, a small amount of binder (Portland cement) is added to the mixture. Mine productivity could be enhanced by using underground paste backfill, because paste backfill not only supports the ground for the pillars and walls, but also helps stop caving, roof collapse, and improves pillar recovery (Coates 1981). Cemented paste backfill (CPB) is used in many cut and fill mines all around the world. This method is a significant inevitability of underground mining operations and is becoming a standard procedure in several mines (Landriault et al. 1997, Naylor et al. 1997).

Paste backfill consists of mill tailings generated throughout ore dressing that is mixed with additives like Portland cement, lime, powdered ash, and slag. The binding agents aim is to develop cohesion inside CPB, so that exposed fill faces have enough strength to tolerate the load (Mitchell 1989). The material of the CPB is usually made by the mill waste tailings that have lost water. The mill tailings are in the form of a slurry. After dewatering, the mill tailings will be filtered to thicken them (70–85 wt. % solids). To bind the tailing particles and raise the strength of the CPB, usually, one or two types of cement such as standard Portland cement, sulphate-resistance cement, ground granulated blast furnace slag (fine-grained smelter slag), will be added to the mixture as a hydraulic binder. If the mix satisfies

pozzolanic behavior and is able to make 18-25 cm slump height, then the CPB is ready to transport as a backfill to the underground voids. (Helmes, 1988; Brackebusch, 1994; Benzaazoua et al., 1999; Fall et al., 2005; Orejarena and Fall, 2011; Yilmaz et al., 2014).

Every year, 500 million tonnes of tailing and waste rock are produced in Canada. The tailing contains very fine, fine, and course proportion grains, some of which are acid generators (reactive), and the rest are non-reactive.

Many companies use coarse grains for backfilling purposes, while the fine grains must be disposed of on the surface in a tailing pond. However, by utilizing the paste fill method, which is relatively recent, fine grains (10–30% by weight finer than 45 microns) are used to make paste fill materials (Brummer and Moss, 1991). In Canada, large amounts of tailings and waste rocks are produced annually. According to a report from the United Nations Environment Program (UNEP), Canada has more mine tailings than most other countries in the world. In the traditional method, most mining companies discharged tailings into the nearby watercourses, which have caused many environmental issues, such as water pollution, landslides, leaching, and dust. Gradually, backfilling has attracted more and more attention, and the percentage of tailings being sent underground has increased. In order to extract a very small portion of ore, a huge amount of waste material needs to be removed from the ground. Also, a large fraction of tailings are produced after ore processing. Tailings are the worthless remaining material after ore separation, which is not economical. This waste material (gangue) must be disposed of at the ground, while they may cause environmental issues such as dam failure and acid rock drainage (ARD). Usually, tailings have the potential to be contaminated by radioactive and toxic elements. ARD will happen when the acidic water outflows from coal and metal mines. Recently, tailings utilization has become more popular in the backfilling industries since it is

available on a large scale, cheap, and easy to transfer. Also, using tailings as backfill material can reduce tailings pond accumulation, ARD, and environmental issues.

To minimize the percentage of the Portland cement, paste fill can be mixed with sand and a chemical additive, which acts as a glue. The obtained mixture is called a gel fill. The maximum possible, solid content for the Paste fill method is 75 – 80%, and in this thesis, the calculation is based on 80%, solid content and 20% water. Solid content is the mass ratio of solid over the total mass. Also, a small dosage of binder (Portland cement) is used to enhance the strength of the backfilling. The binder dosage is the mass of cement over the mass of solids. Depend on the backfill design and required strength, 2 - 10% binder is used to increase the strength and the free-standing of the backfilling material.

This thesis will test 6%, 8%, and 10% binder combined with waste tailings and water to produce backfill slurries. The water-to-binder ratio has an inverse ratio to its compressive strength. When the water percentage increases, with a normal range of the binder, the compressive strength of the backfill will decrease. Since the mill tailings are mixed with water and found in the form of a slurry, the moisture content of the tailings needs to be taken in to account.

The conventional development of steeply dipping narrow vein ore bodies (SD NVOB) is always a challenge due to extensive costs, high environmental impacts, and higher risk exposure. As an efficient alternative, the drilling method was introduced to overcome such challenges. In this method, the SDNVOB will be crushed and transported to the surface in the process of directional drilling. The stability of the wellbores during and after drilling is critical for the safety of the HW in highly deviated intervals of narrow vein mining and, therefore, requires intensive analysis to be maintained. In the mining industry, the

occurrence of wellbore stability problems are frequent, leading to increasing drilling costs and overall non-operational time.

To ensure the wellbore's stability, several factors must be considered, including rock mechanical properties, wellbore trajectory, pore pressure, drilling fluid and pore fluid chemicals, temperature, time, mud weight, and principal far-field stresses. Moreover, the wellbore formation bedding and natural fracture discontinuities and spacings, as well as the influx of the drilling mud into these fractures, could initiate instability in rock masses. (Aoki et al., 1994; Chen et al., 1998; Last et al., 1995; Okland and Cook, 1998). The borehole diameter is another main parameter that affects the stability of the wellbore. According to the wellbore stability definition, as long as the wellbore and the drill bit have the same diameter, and the drill bit keeps its shape constant, the well will be stable. Zhou et al. (1996) studied the deviated wellbore based on principal horizontal stress and reported that an inclined wellbore could be more stable than a vertical one when $\sigma_v > \sigma_H, \sigma_h$ (extensional stress regime). In other words, when the normal vertical stress (σ_v), is greater than the minimum horizontal stress (σ_h) and the maximum horizontal stress (σ_H), an inclined wellbore is more stable.

Recently, energy demand is intensively increasing. Due to the limited amount of near-surface ore bodies, developing mining resources efficiently and rapidly has become an important research topic for drilling engineering. Nowadays, the open stope mining method with a simple structure is widely used. This method grants simple investor operation, high production efficiency, small dilution, and low cost.

However, the over break and dilution caused by the stope HW will damage the activity and economy of underground mines. Therefore, the efficiency of open stope mining is generally determined by the capacity with minimal dilution to achieve maximum extraction (Villaescusa, 2004). It is important to predict HW stability precisely and to understand its influencing variables to prevent HW instability and support stable stope design. Wellbore stability requires a proper balance between the uncontrollable factors of earth stresses, rock strength, pore pressure, well-bore fluid pore pressure, wellbore fluid pressure, and mud chemical composition (J.B. Cheatham Jr. 1984).

Several methods have been developed for the study of HW stability. Mathews et al. in 1980 proposed a stability graph approach based on the Mathews stability number and the hydraulic radius to estimate HW stability. The stability of the wellbores during and after drilling is critical in narrow vein mining. In particular, the HW must be stable to avoid wall collapse during drilling caused by inclination and the gravity force. The numerical method calculates the stress around the wellbore at different distances and different azimuths; by using a failure criterion, the wellbore stability can be examined.

The support of the HW in inclined wells is fundamental to the operation and safety of the mine site and surrounding areas. Bolting is the primary method of support in many modern mines. However, in some cases and for several reasons, rock bolts alone may not be sufficient to support the HW, and secondary support must also be installed.

1.3 Research objective and approach

I. Simulating the backfill material by the waste tailing of the gold mine of Anaconda mine, Portland cement, and water.

II. Investigation of designing backfill material by using tailing with 80% solid content of total mass and different cement dosage of the solid content.

III. Analyzing the cured strength and cured time of the backfilling

The most important part of using and preparing the backfill mixture in the SMD project is to calculate the required strength of the material. This parameter is the basis of backfill design and is used to select the type of backfilling and the binder percentage. Different methods can calculate the vertical free-standing face. These methods and calculations are discussed in detail in Chapter Four. The inclined stope method is the most suitable method for computing the vertical free-standing face, and having this information would guide us to design the specimens and to perform the curing strength and curing time.

By knowing the required strength of the backfilling, two types of binders were designed to test. Portland cement and a combination of Portland cement and fly ash with the proportion of 80:20 were used to make the specimens. The specimens were made with waste tailings from the mine and a binder with 80% solid content and 20% water content. Both types of binders were cast with 6%, 8%, and 10% binder, and the curing time and curing strength were tested after 7 days, 14 days, and 28 days. Using the grinder machine, the surface of the specimens was smoothed, and by utilizing the geomechanical loading frame, the UCS of the specimens was measured. Finally, the stiffness of backfilling materials, the effect of binder dosage, the effect of the binder composition, and the effect of curing time on UCS were analyzed and compared.

In order to recognize the stability of the wellbores during and after drilling, the stress distribution around the wellbore needs to be studied. The area with a radius of 5 times the radius of a wellbore is the area affected by stress. All stresses around the wellbore, including axial, radial, and tangential stresses, as well as shear stresses, were calculated using tensile and shear stress formulas. The entire perimeter of the wellbore at every 10 degrees and the entire length of the wellbore at a distance of one meter were studied. This analysis was repeated for distances of 5 times the well radius up to 10 meters from the wellbore. Maximum and minimum wellbore pressure from the bottom to the top of the wellbore were calculated, and using different failure criteria such as modified Hoek and Brown, the stability of the wellbore was analyzed.

1.4 Thesis outline

CHAPTER 1 is an introduction to the thesis; **CHAPTER 2** provided a literature review, and **CHAPTER 3** focuses on the research methodology.

CHAPTER 4 presents a paper titled "AN ASSESSMENT OF THE FREESTANDING VERTICAL FACE FOR THE BACKFILL USING THE RUN OF THE MINE TAILINGS AND PORTLAND CEMENT" and was submitted to the ARMA 2020 conference, and mostly focuses on the vertical free-standing face and preparation of the tests.

CHAPTER 5 presents a paper titled "THE BACKFILL ANALYSIS AND PARAMETRIC EVALUATION OF THE CEMENT BINDER ON CURED STRENGTH AND CURING TIME" and was submitted to the GeoCalgary 2020 conference, and

analysis the curing time and curing strength of the specimens made by the waste tailings and different binders.

CHAPTER 6 presents a paper titled "WELLBORE STABILITY OF HIGHLY DEVIATED WELL INTERVALS FOR LARGE DIAMETER BOREHOLES" and was submitted to the GeoCalgary 2020 conference, and studies the stability of the wellbores and analysis of the wellbore failure criterion.

CHAPTER 7 summarizes all the outcomes of this study, indicating the contribution of this research to mining by drilling method and provides recommendations for the future works.

Chapter 02: Literature review

2.1 Backfilling

By starting to exploit the valuable minerals from the ground and penetrating deeper, there will be more voids containing stops. The volume and number of voids will increase gradually as extracting continues. The extracted ore-body will convert to waste rocks after milling and mineral processing, which have to be dumped on the ground surface of the mining fields. (Wang et al. 2013).

These voids would cause instability and subsidence hazards which is dangerous. One of the main reasons for rockburst in mining, or any potential land settlement, is the collapse of voids and free space such as stops. (Jiránková, 2007; Helm et al. 2013; Wang et al. 2013).

Water is used as the transportation medium in the hydraulic backfill method to make backfill material transmission easier. Hydraulic backfill is a type of renewable high engineering technology comprise of hydraulic water slag, mountain sand, river sand, waste tailing, and crushing sand, which is utilized to fill the empty space beneath the mines (Yao et al. 2012).

As hydraulic backfill material contains considerable water, by increasing the height of the backfill material, free water will be gathered on the top of the backfill after emplacement. The emplacement procedure is usually performed inside the voids from the top of the stops. Finally, this extra water must be drained as seepage water, although 20-30% of the water will be trapped inside the backfill for a very long time. (Potvin et al., 2005). CPB is used in many cut and fill mines all around the world. This method becomes a significant

inevitable section of the underground mining operations and is becoming a standard procedure in several mines. (Landriault et al. 1997, Naylor et al. 1997).

Paste backfill consists of mill tailings generated throughout ore dressing that is mixed with additives like Portland cement, lime, powdered ash, and slag. The aim of the binding agents is to develop cohesion inside CPB, so that exposed fill faces have enough strength to tolerate the load.

Hydraulic backfill properties are as follows: most particle sizes are smaller than 1µm, and fine particles, which are usually removed to make the backfill material permeable. So those particles that are 10 µm or less than 10 µm ought to be less than ten percent (Potvin et al., 2005).

For instance, the hydraulic backfill was used to backfill an underground mine, which was a room and pillar, or board and pillar method in the coal mines Wyoming State in the USA. It was applied to stop surface subsidence within the type of sinkholes or trough subsidence in abandoned coal mines (Karfakis and Topuz 1991).

Typically the CPB method acts as an ideal solution to use waste tailings, and for waste rock and sand disposal, rock backfill and hydraulic backfill are used. CPB is used to fill the extracted voids in underground mining, especially in Australia and Canada (Mehmet Yumlu, 2010).

All of the voids in the Hannah mine in the United States were filled by hydraulic backfill exploitation using granular material from abandoned coal mines. The obtained analytical results from hydraulic backfilling in the United States proved that hydraulic backfilling is more suitable for the wet voids and provides higher strength in voids with below groundwater table than dry voids. Since mining areas with lower rubblized zones settle for

a lot of backfill material, it would be more accessible to drain the water (Karfakis and Topuz 1991).

By performing grain size distribution of Hydraulic backfill grain, it was noticed that sometimes it contains sandy silt, silty sand (SM-ML). To remove the clay fraction, there is a method called desliming; in this method, whole backfill material passes through hydrocyclones by circulation, and therefore the clay portion is removed to be deposited into the tailings dam. The Hydrocyclone containing silty sandy backfill material is moved within a suspension, called slurry, by pipelines to underground voids (Sivakugan et al., 2006).

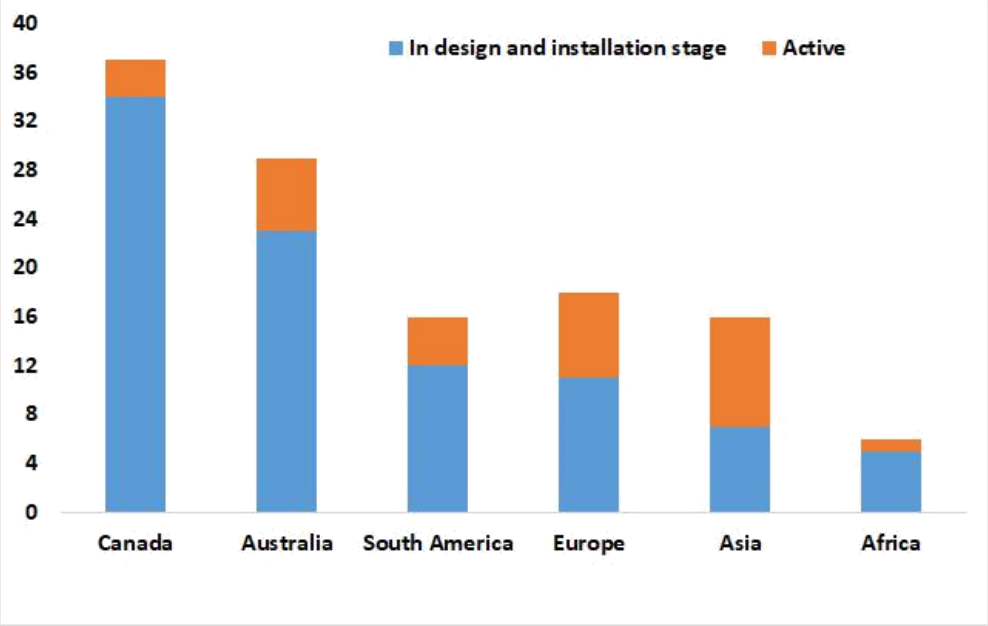

Figure 1 Use of paste backfill technology worldwide (Mehmet Yumlu, 2010)

For designing backfill and barricades, there are strict rules applied within the procedure of the backfill process. Progressively, CPB is being replaced by hydraulic backfill wherever

strength is needed from backfill or a waste product contain a better quantity of very fine particles (Potvin et al., 2005).

The material of the CPB is usually made by the mill waste tailing that has lost water. The mill tailings are in the form of a slurry. After dewatering, the mill tailing will be filtered to get thicker (70–85 wt. % solids). To bind the tailing particles and raise the strength of the CPB, usually, one or two types of cement such as standard Portland cement, sulphate resistance cement, ground granulated blast furnace slag (fine-grained smelter slag), solid pulverized fly ash will be added to the mixture as a hydraulic binder. If the mix satisfies pozzolanic behavior and is able to make 18-25 cm slump height, then the CPB is ready to transport as a backfill to the underground voids (Helmes, 1988; Brackebusch, 1994; Benzaazoua et al., 1999; Fall et al., 2005; Orejarena and Fall, 2011; Yilmaz et al., 2014).

When the CPB is cured and hardened enough, it will convert to a strengthened pillar. This pillar acts as ground support for the other close part of the underground mining operations (Grice, 2001; Kesimal et al., 2003; Yilmaz et al., 2004; Fall and Pokharel, 2010; Mahlaba et al., 2011; Pokharel and Fall, 2013; Ghirian and Fall, 2013).

In order to treat low-grade ores extracted from the mine, flotation operation is used as a part of mineral processing methods. However, typically 95-98% of the feed ore will be generated after flotation operation (Ercikdi et al. 2012). Today's much stricter environmental and administrative restrictions need reliable and sustainable handling of tailings. Tailings are today managed by:

- Disposal into tailings dams,
- Produced during the processing of the ore,
- Discharge into deep sea areas available,
- Backfill into an underground mine,

Practically, deep-water discharges are sometimes used, but the mine site must be very close to the shore in order to have a suitable area for the disposal of tailings. (Cetiner et al. 2006). Alternatively, well-constructed, monitored, and managed tailings dams are commonly used worldwide for tailings management/disposal. Chambers and Higman (2011) estimated that there are more than 3,500 dams located worldwide for tailings. Nevertheless, there has been a range of accidents at the tailings dam, especially between 1960–1980 and 1980–2011, which is an average of 2–5 events every year, respectively. Such events have resulted in the loss of human lives, structural destruction, agricultural and forestry land degradation and adverse environmental effects (for example, water pollution) (Rico et al. 2008). A total of 198 tailing dam disasters occurred before 2000, and 22 worldwide after 2000. (Azam and Li 2010; WISE 2016). Such accidents derive from: (a) inappropriate designs, construction, operation and management of the tailings dams; (b) adverse climatic conditions (such as heavy rainfall); (c) inadequate height of the body of the dam and excessive disposal; (d) soil conditions, liquefaction, slope instability and displacement; and (e) the drainage conditions, leakage, and pore water pressure (Azam and Li 2010) Paste backfill processing, first used effectively in 1980 at the Bad Grund mine in Germany, is a secure way to pack tailings into deep mined-out voids. (Landriault 2006) However, the performance of a tailings backfill concept and activity essentially depends on the characteristics and flowability properties of the tailings content as well as the underlying voids' environmental conditions. Several considerations, such as the preparation process of the paste backfill mixture, the transport of the paste backfill to the underground openings, the barricade size, the paste backfill stability and strength, the flow properties of the paste backfill, the impact on the water quality, and the expense of the backfilling all affect the design of a paste backfill system (Belem and Benzaazoua 2008).

In underground stops, the necessary feature of CPB decides the planned value of its unconfined strength. For instance, a minimum of 0.15 MPa is needed in the early stages of curing to avoid liquefaction hazard and barricade failure (Beenet al. 2002; Roux et al. 2004). Paste backfill content inserted in underground voids offers protection during mining of nearby stops in mines where cut and fill and sublevel mining methods have been employed. To this end, after 28 days of curing, CPB is suggested to have a minimum strength of 0.7 MPa (Brackebusch 1994; Landriault 1995).

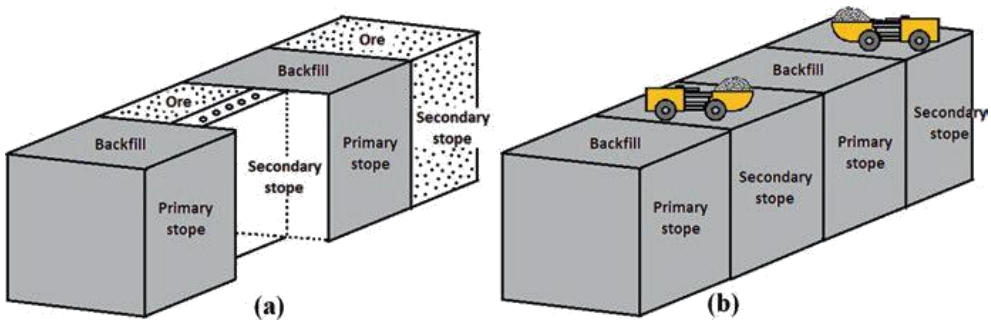

Figure 2 Function of paste backfill in underground mining voids (modified after Hassani and Bois 1992; Belem and Benzaazoua 2008)

Furthermore, CPB, which acts as a worksite for equipment and staff, is said to have a strong rise in strength in the early stages of curing (Belem and Benzaazoua 2008). CPB is, therefore, necessary to have a uniaxial compressive strength (UCS) value of at least 4 MPa for roof protection (Grice 1998). The rate of production of target strength has real value to the waiting time for the corresponding stops to be extracted. Thus, acceptable engineering design is needed for CPB to attain the necessary strength. Studies have shown that for use with other mine tailings, the CPB design used for a particular type of mill tailings cannot be generalized. Therefore, every type of tailings needs a suitable and separate mix design

with an appropriate binder form and mixing ratio (Kesimal et al. 2004; Tariq and Nehdi 2007; Ercikdi et al. 2009a, b, 2010a, b; Nasir and Fall 2010; Cihangir et al. 2012).

2.1.1 Backfill function

Backfilling is one of the indispensable procedures in SMD and is used for three primary functions, including ground stabilization, provision of a working floor, and disposal of the waste tailings.

As a function of ground stabilization, backfill can be used for regional support. In particular, the backfill prevents the breakup and sloughing of the HW and FW in rockburst mining situations. The performance of backfill for regional support has been the main research subject in South Africa, where the mining of deep, shallow dipping, narrow, and gold-bearing reefs presents many challenges. Jager (1992) reported that in 1990, approximately 55% of all fatalities were rock-related, and of these fatalities, 52% were attributed to rock bursts in three major South African districts.

Gurtunca and Gay (1993) concluded that backfilling is capable of providing adequate regional support to monitor seismic events. They also claimed that since the stabilizing pillars are considerably more rigid than backfills, backfill cannot, at least in the short term, affect regional seismicity. Besides supporting the HW and FW, backfill is capable of improving mining recoveries and decreasing dilution by providing stable support. Webbstock, Keen and Bradley (1993) presented that backfill, which was at the Randfontein Estates Gold Mining Company's Cooke 3 shaft, increased extraction from 78% to 95% while keeping the working conditions safe.

In cyclical mining methods, such as the cut and fill method, backfill can be used to provide the working floor. The important property of the backfill for this function is its bearing strength, which increases with cement content. However, cement affects the drainage characteristics of the fill, which in turn affects how soon the equipment can operate on the floor. For cyclical mining, the curing time must be short, and the backfill must provide new strength to support personnel and mechanized equipment. Krauland (1989) reported that Boliden Mineral AB, (a Swedish mining company) in thirteen of sixteen mines, had developed highly efficient cut and fill practices to achieve high mining recoveries from deposits with small, irregular orebodies and unfavorable rock conditions.

Backfill also performs many environmental benefits to the mining industry. The capacity of the tailings pond was difficult to meet the requirements of expanding future production, and the discharged tailings caused many environmental issues, such as water pollution, landslides, leaching, and dust. The mining industry has been under increasing pressure to develop waste management practices, which has resulted in a greater focus on the role of backfill in waste disposal. With the development of backfill technology, the tailings have become the main material used as backfilling material to fill the underground voids. Backfill with tailings will reduce the tailings pond's accumulation on land, and the costs associated with constructing and reclaiming tailings the ponds during mining are also reduced. Therefore, backfill can not only solve the safety and environmental issues caused by mine production and tailings discharge but also maximize the recovery of resources, which is of great significance for the development of SMD.

2.1.1 Backfill types

The paste backfills can obtain a similar strength in rock backfills by using less cement than hydraulic backfills. It utilizes a different size distribution of tailings and consists of high solid contents, resulting in the reduction of the surface tailing's impoundment requirements. In comparison, rock and hydraulic backfills prefer less solid content or larger size distribution of tailings.

2.1.3 Rheology

One of the most important properties of CPB is rheology. The transportability of the CPB can be determined by measuring the rheology of the backfilling materials. The CPB mixture should have sufficient consistency throughout its transport through a pipeline network throughout underground openings mined out (Simon 2005). If the amount of solid material deposited in underground output voids is maximized with limited usage of resources, a reliable and cost-effective method of transporting paste backfill is feasible. However, by increasing the solid content of the mixture, the fluidity of the backfilling will decrease, which can cause friction loss. Therefore, the efficiency of the backfilling and material transfer rate will reduce (Huynh et al. 2006).

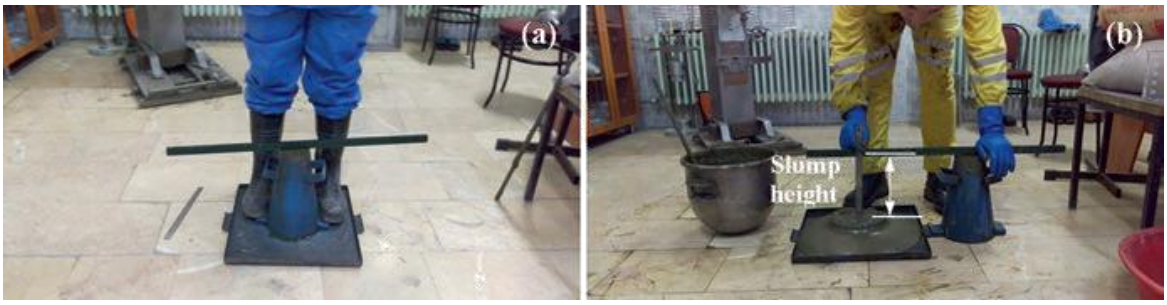

Figure 3 Schematic of the cone slump test (Erol Yilmaz and Mamadou Fall, 2017)

Solid ratio, water-to-binder ratio (W/C), percentage and the type of binder, additives and chemical materials, particle shape, grain size distribution, density, the surface area of the aggregates (tailings), and ion and the PH of the water are the most significant factors of the CPB, which affect the flowability and fluidity (Nguyen and Boger 1998; Clayton et al. 2003; Henderson et al. 2005; Huynh et al. 2006). The quality of the water (ion and the PH) that is used for making CPB, can have an impact on the yield stress of the backfilling. flowability is quality or degree of (fluids and loose particulate solids) being flowable while fluidity is the state of being fluid rather than viscous. Slump testing is a common method to assess the flowability properties of the CPB. In practice, the slump cone test is a simple and useful method that can be applied to the mine site and in the lab. A range of 6-10 in slump value is suitable for the CPB applications. A standard slump cone is a frustum shape of a height of 12 in, the top and a base diameter of the frustum are 8 and 4 in, respectively (Landriault et al. 1997; Cooke 2007). In order to measure the slump of any mixture, the material is poured into the slump cone, and the difference between the original height of the mixture and the height level after the collapse (when the slump cone is removed) is measured.

By increasing the water-to-binder ratio, the slump value will increase as well. Therefore the mixture can be transported through the pipelines and underground easily (Brackebusch, 1994; Grabinsky et al. 2002). Although additional water would extend the curing time and decrease the strength of the CPB, Huynh et al. 2006 claimed that flowability properties could be increased by adding chemical plasticizers to the CPB, which can help to transport a low water-cement CPB into the underground voids. Excess water would cause higher segregation that leads to loss of uniformity of the backfill mixture, and water separation from the mixture affects the mechanical and durability characteristics of the backfilling.

2.1.4 Freestanding vertical face

To minimize backfilling failure, the development of the stresses is essential to understand. We expect to have more stresses at the bottom of the mine, while evidence shows that the stresses at the bottom of the stope mines are much less than calculated. Traditionally, for calculating the stress at any section of the mine, the unit weight of the backfill multiple to the depth will result in the stress at that section (Grice, 2011).

More details are provided in chapter 04, and the application are covered in this chapter.

2.1.5Arching effect

When the yielding backfill is emplacing down to the holes in the mine, the movement is opposite to the stable unyielding rock on the wall. Therefore, this movement is against the shear resistance along with the interface between rock and backfill materials. The generated

shear stress in the contacted area tends to keep the backfill in its place and opposes its movements. Figure 4 shows a schematic diagram of the process (Terzaghi, 1943).

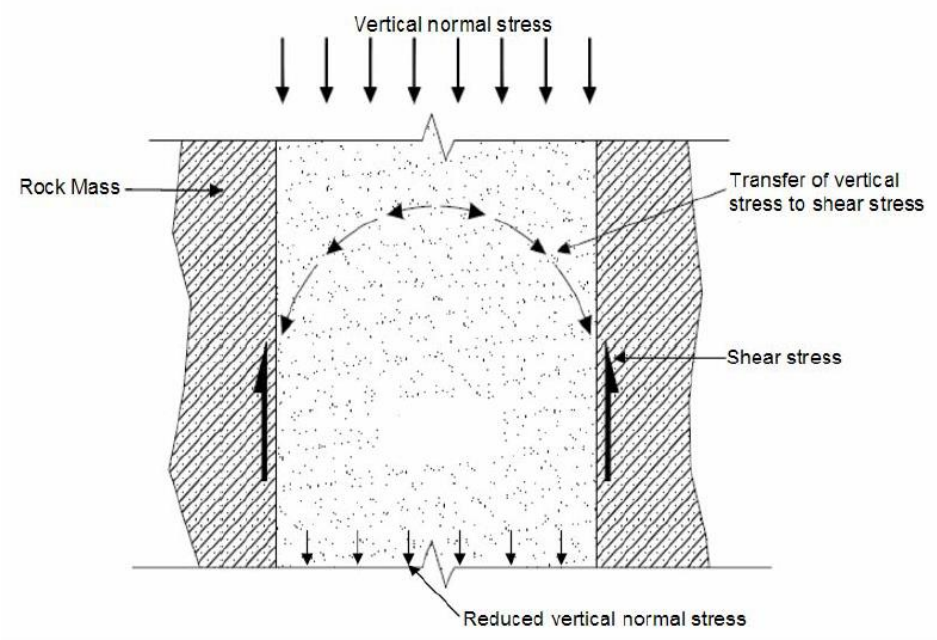

Figure 4 Arching effect (Pirapakaran, K. 2008. Load-deformation characteristics of mine fills with particular reference to arching and stress developments. J. James Cook University)

2.2 Wellbore stability

To ensure the wellbore stability, several factors must be considered, including rock mechanical properties, wellbore trajectory, pore pressure, drilling fluid and pore fluid chemicals, temperature, time, mud weight and principal far-field stresses. Moreover, the wellbore formation bedding and natural fracture discontinuities and spacings, as well as the influence of the drilling mud into these fractures, could initiate instability in rock masses, (Aoki et al., 1994; Chen et al., 1998; Last et al., 1995; Okland and Cook, 1998). The borehole diameter is another main parameter that affects the stability of the wellbore.

According to the wellbore stability's definition, as long as the wellbore and the drill bit have the same diameter, and the drill bit keeps its shape constant, the well will be stable. Zhou et al. (1996) studied the deviated wellbore based on principal horizontal stress and reported that an inclined wellbore could be more stable than a vertical one when $\sigma v > \sigma H, \sigma h$ (extensional stress regime).

Recently, energy demand is increasing intensively. Due to the limited amount of near-surface ore bodies, developing mining resources efficiently and rapidly has become an important research topic for drilling engineering. Nowadays, the open stope mining method with a simple structure is widely used. This method grants simple investor operation, high production efficiency, small dilution, and low cost. However, the over break and dilution caused by the stope HW will damage the activity and economy of underground mines. Therefore, the efficiency of open stope mining is generally determined by the capacity with minimal dilution to achieve maximum extraction (Villaescusa, 2004). It is important to predict HW stability precisely and to understand its influencing variables to prevent HW instability and support stable stope design. Wellbore stability requires a proper balance between the uncontrollable factors of earth stresses, rock strength, pore pressure, wellbore fluid pore pressure, wellbore fluid pressure, and mud chemical composition (J.B. Cheatham Jr. 1984).

Several methods have been developed for the study of HW stability. Mathews et al. (1980) proposed a stability graph approach based on the Mathews stability number and the hydraulic radius to estimate HW stability. The stability of the wellbores during and after drilling is critical in narrow vein mining. In particular, the HW must be stable to avoid wall collapse during drilling caused by inclination and the gravity force. The numerical method

calculates the stress around the wellbore at different distances and different azimuths; by using a failure criterion, the wellbore stability can be examined.

Freezing (if there is water) or cement can be used; however, for the majority of the slopes and HWs, the installation of (mega long bolts) cable bolts is the standard and most effective method of support.

The discrete element method (DEM) simulation is a good method to estimate the stress condition in a wellbore stability study. It has the advantage of monitoring the stress of every particle in the model and therefore provides a more precise result. For the wellbore instability, distributed stress, and rock strength, two major failure modes can be observed, which are shear and tensile failures. Shear fractures occur because of wellbore fluid pressure. When the pressure of the wellbore fluid is more than BHP, shear fracture will occur. Shear fracture and tensile fracture occur as a result of the excessive wellbore fluid pressure applied parallel to the minimum horizontal stress (σh max), and tensile fractures occur as a result of the excessive wellbore fluid pressure applied parallel to the maximum horizontal stress (σH max). This thesis studies the stresses around the wellbores in different locations and analyzes their impact on the wellbore stability utilizing a numerical analysis and DEM simulation.

A failure criterion has also been applied after calculation of the stress around the wellbore to examine the wellbore stability.

2.2.1 Well control

Well, control is a procedure in drill planning to prevent unwanted conditions like:

1. Kick, which occurs when the formation fluids enter the wellbore
2. Wellbore integrity, which is the wellbore failure by fracturing Both Kick and well integrity is related to the bottom hole pressure (BHP)

When the BHP is less than the formation pore pressure, Kick will happen, and when the BHP is greater than the formation fracture pressure, wellbore fracturing is expected.

Formation pore pressure is the pressure of groundwater held within a soil of rock in gaps between particles and can be estimated by:

$$Pore\ Pressure = \rho_{brine} \times g \times h \times PPF \tag{2.1}$$

Where:

ρ_{brine} is the brine density, formation average water density ≈ 1000 kg/m^3

g is gravitational acceleration=9.81 m/s2

h is the depth below ground surface

PPF is the pore pressure factor

- PPF>1 Over Pressured
- PPF=1 Normally Pressured
- PPF<1 Under Pressured

2.2.2 In-situ stress

In-situ stress is the natural, local stress within a rock mass formation. In-situ stress defines the quantity and direction of compression that is being applied to a rock at a specific location. It is a property of rock mass studied by trenchless construction planners in order

to assess potential geotechnical challenges. Most in-situ stresses are due to body forces (gravity).

The stress within a rock can be resolved into three principal stresses. A formation will fracture when the pressure in the borehole exceeds the least of the stresses within the rock structure. Normally these fractures will propagate in a direction perpendicular to the least principal stress.

Four components of the in-situ stress are σv, σH, σh, and Pore Pressure. The vertical stress σv can be approximated by the hydrostatic stress using the weighted average density of overlying formations as follows:

σ_v is the normal vertical stress

$$\sigma_v = \rho_{average} \times g \times h \tag{2.2}$$

σ_H is the Maximum horizontal stress

$$\sigma_H = K_{max} \times \sigma_v \tag{2.3}$$

σ_h is the minimum horizontal stress

$$\sigma_h = K_{min} \times \sigma_v \tag{2.4}$$

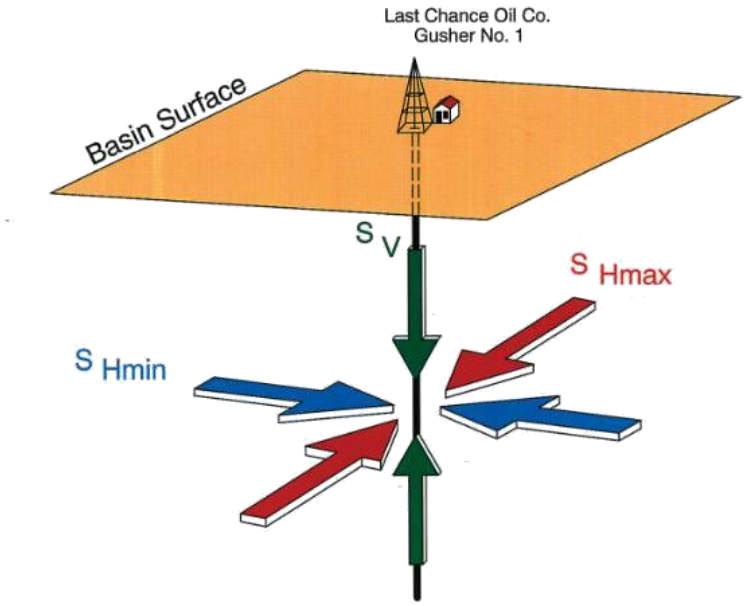

Figure 5 In-situ stress (Erling Fjar, 2008)

σ_H and σ_h are estimated using horizontal stress coefficient K_{Max}, K_{min}, that can be measured from a leak off test (LOT) and mini-frac.

$$0.25 < K_{min}, K_{Min} < 0.75 \qquad (2.5)$$

The pressure of the drilling fluid (Pmud) in the annulus of the wellbore depends on several factors such as hydraulic mud pressure, annular friction pressure (AFP), and dynamic pressure fluctuations (surge pressure and swab pressure).

In order to stabilize the wellbore while drilling, mud pressure must be between formation pore pressure and formation fracture pressure.

Formation Pore Pressure < Mud Pressure < Formation Fracture Pressure Formation

Fracture pressure is the pressure in the wellbore at which a formation will crack. The fracture pressure is a function of in situ stresses, Ppore, and the formation tensile strength σt.

$$P_{frac} = 3\sigma_h - \sigma_H - P_{pore} + \sigma_t \quad (2.6)$$

σ_t is the tensile strength and can be estimated by UCS , σ_t=0.1 × UCS. The tensile strength of the formation σ_t is estimated beforehand, or it can be assumed to be zero to give a conservative estimate.

2.2.3 Wellbore wall failure modes

Minimum well pressure (Pw-min) and Maximum well pressure (Pw-max), or fracture pressure, are two essential parameters that must be measured to study the wellbore stability. Pw-min is generally less than pore pressure, and for weak formations and high in-situ stress zones (deep formations), it has a significant role in most drilling design. Therefore, if the bottom hole pressure (BHP) is less than the minimum well pressure, then shear fractures or compressive fractures will occur parallel to the minimum horizontal stress σ_h. When the BHP is greater than the maximum well pressure, tensile fractures will happen parallel to the maximum horizontal stress σ_H (FJÆR et al. 2008).

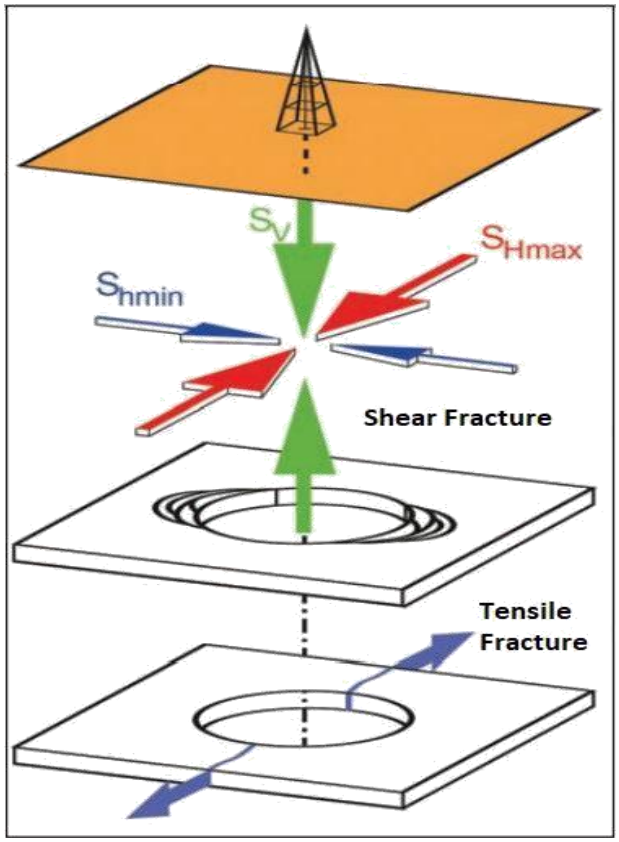

Figure 6 Wellbore wall failure (Erling Fjar, 2008)

2.2.4 Failure criterion

The Mohr-Coulomb and Drucker Prager criterion is the most famous failure criterion used for analyzing wellbore stability. However, it does not consider the effect of intermediate principal stress on rock strength. Modified Lade criterion can provide a closed-form solution for critical wellbore pressure and, consequently, the critical mud weight. It also reflects the influence of intermediate principal stress. In this thesis, the Mohr-Coulomb, Ducker Parger (Inner circle, Middle circle, and outer circle), the Modified Lade criterion, and the Modified Hoek and Brown are analyzed. The summary of the failure criterion can be found in the results section. However, the Modified Hoek and Brown failure criterion will be discussed in detail.

2.2.5 Modified Hoek and Brown criterion

Hoek and Brown (1980) developed a failure criterion to estimate jointed rock mass strength. The limitations were derived in 1983 using laboratory triaxial tests on samples of intact rocks. The modified Hoek and Brown criterion was later presented for heavily jointed rock masses. To estimate the strength and characteristic deformation of the rock mass, which are fractured and jointed heavily, the Hoek and Brown criterion, as well as associated GSI, are used worldwide.

In order to consider the effect of the shale matrix on the strength of the bulk rocks in the wellbores, the modified Hoek and Brown criterion was used since it can describe the effect of in-situ stress on the compressive shearing stress at a depth of the wellbores (Liu, C., Han, Y., Liu, H. H., & Abousleiman, Y. N. 2019).

The GSI was developed by Hoek 1994 and Hoek et al. 1995 in order to link engineering geology observations in the field and the Modified Hoek & Brown criterion. GSI is the rock mass characterization system based on the structure and the condition of the joints. GSI can roughly estimate the rock strength by quantifying the fractures and joints. The strength of the host rock has a significant effect on the stability of the wellbores and HW.

Chapter 3: Research methodology

3.1 Backfilling using waste tailings

One of the essential tasks of the post-mining process is called mine backfilling. Back-fill is made from soil, overburden, mine tailing or any kind of aggregate which can be imported as a filler and booster to emplace in the extracted area that was excavated by mining operations. Starting to exploit the valuable minerals from the ground and penetrating deeper, there will be more voids. The volume and number of voids will increase gradually as extracting continues, while at the same time, the extracted orebody will be converted to waste rocks after milling and mineral processing and have to be dumped on the ground surface of the mining fields. These voids can cause instability and subsidence hazards, which is dangerous. One of the main reasons for rockburst in mining, or any potential land settlement, is the collapse of voids and free spaces. There are multiple backfilling methods, and the two most popular types are hydraulic fill and paste fill. Backfill materials are categorized as hydraulic fill, paste fill, and rock fill. In order to increase the strength of the backfill material, a small amount of binder (Portland cement) is added to the mixture. For designing backfill and barricades, there are strict rules applied throughout the entire process. Progressively, CPB is being replaced by hydraulic backfill wherever strength is needed from the backfill or a waste product contain a better quantity of very fine particles. Every year, an extensive amount of tailing and waste rock are produced in Canada. The tailing contains very fine, fine, and course proportion grains, some of which are acid generators (reactive), while the rest are non-reactive. Coarse grains are used by many companies for backfilling purposes, while the fine grains must be disposed of on the surface in a tailing pond. However, by utilizing the paste fill method, which is relatively recent,

fine grains (10–30% by weight finer than 45 microns) are used to make paste fill materials. CPB is made by mixing waste tailings, water, and cement. It is a non-homogenous material that is between 70 and 85 percent solid; the utilized water can be either clean water or mine-processed water, and usually, a hydraulic binder is added to the mixture to increase the strength of the CPB. The binder fraction is mostly between 3–7% of the total weight. In the mining industry, CPB is improving and expanding every day, because it helps to manage the waste tailing in an economical method.

Furthermore, it provides safety and support for mine and mine workers in the underground. Additionally, CPB develops technology to help solve environmental issues. CPB is used in many cut and fill mines all around the world. This method is becoming an inevitability of underground mining operations and is becoming a standard procedure in several mines.

3.1.1 Proposed mixture

In the paste fill method, a small dosage of binder, mostly 2-10% (mass of cement/mass of solids), is added to the backfill material to enhance the strength of the CPB. In this thesis, we will evaluate the effect of the cement percentage on the strength of the CPB and its cured time and cured strength on its 7th, 14th, and 28th, days according to ASTM standard C 1157.

Amaratunga (1997) studied the effect of binder dosages on the UCS of the backfilling and stated that by increasing the binder dosage, the UCS would increase. His study showed that a 7% binder dosage will give a suitable performance on the UCS's development. Therefore, in considering 80% solid content of the paste fill, we propose cement as 6%, 8%, and 10% of the solid content to test a different range of backfill strengths.

Table 1: Cement, tailings, and water percentage

Binder %	6%	8%	10%
Mass of Tailings %	75.2%	73.6%	72%
Mass of Cement %	4.8%	6.4%	8%
Mass of Water %	20%	20%	20%

The binder is Portland cement and in a combination of Portland cement and fly ash. Therefore, 2 series of tests are conducted in this thesis. First, we tested Portland cement as a binder and next, the combination of Portland cement and fly ash with the proportion of 80% Portland cement to 20% fly ash was used as a binder. Note that the binder percentage is the solid content of the mixture. Table 1 shows the proposed cement dosage, waste tailing, and water content as percentages.

Amaratunga (1997) presented the effect of the partial replacement of Portland cement with fly ash class C on a UCS. Generally, fly ash are categorized by two types: fly ash Class C and fly ash Class F. Class C fly ash typically made from the combustion of younger lignite or subbituminous coal while class F fly ash produced from the burning of harder bituminous coal and older anthracite. In contrast to Class F, self-cementing Class C fly ash does not need an activator. The proportion of PC: FA (80%:20%) attained a higher UCS after 28 days. Using fly ash in the binder composition not only improves the strength of the backfill but will also reduce the cost of backfilling. In this study, utilizing 20% of fly ash in the binder, the dosage will be investigated. Table 2 provides the proposed cement dosage, fly ash, waste tailing, and the water content as percentages.

Table 2: Cement, fly ash, tailings, and water percentage

Binder %	6%	8%	10%
Mass of Tailings %	75.2%	73.6%	72%
Mass of Cement %	3.8%	5.1%	6.4%
Mass of Fly Ash %	1%	1.3%	1.6%
Mass of Water %	20%	20%	20%

3.1.2 Material and equipment

Portland cement

Portland cement is the most common type of cement, which is used as a fundamental component of concrete, and it is used in the backfill mixture as a binder to increase the strength of the backfilling. Considering its high costs in purchasing and transport to the mine site, cement adds considerable expense to backfills, even when used in small dosages on the order of 2–10%. Consequently, and with considerable success, the mines have been trying to replace cement with blended cement, which consists of cement mixed with fly ash and/or slag.

Portland cement has four main compounds that get the strength from chemical reactions between water and the compounds. The Portland cement is made by crushing, milling and proportioning of tricalcium silicate ($3CaO \cdot SiO2$), dicalcium silicate ($2CaO \cdot SiO2$), tricalcium aluminate ($3CaO \cdot Al2O3$), and a tetra-calcium aluminoferrite ($4CaO \cdot Al2O3Fe2O3$).

Tailings

One of the primary purposes of this thesis is to evaluate the usage of tailings instead of aggregates in the backfilling material. Anaconda Mining provided a considerable amount of the waste tailings that are stored in the DTL's storage and will be used as a main component of the backfill mixture. Tailings from a milling operation are usually discharged as a dilute slurry. Excess water may be recovered for recycling in the milling operation by use of a tailings thickener, but the tailings slurry is always too wet to be considered a paste. Therefore, the dewatering of the tailings slurry is usually the first step in preparing a paste backfill mixture. Table 3 provides the mineral composition and chemical composition of the tailing.

Table 3 Mineral composition and chemical composition of the tailing.

SAMPLE	FE	AS	MO	ZN	CU	SB	AG	PB	CO	NI	MN
NUMBER	%	ppm	ppm	ppm	ppm	ppm	ppm	ppm	ppm	ppm	ppm
BLANK	0.01	5	1	1	1	5	0.5	2	1	1	5
STD LKSD-2	3.18	8	1	185	37	5	0.8	31	17	20	1596
J BULK-01	1.90	5	4	12	33	7	0.5	2	10	12	235
J BULK-02	1.56	5	3	9	32	7	0.5	2	8	9	221
J BULK-03	1.62	5	3	9	21	6	0.9	2	8	9	207
J BULK-04	1.41	5	3	9	26	7	0.5	2	7	9	188
J BULK-05	2.02	5	3	11	19	5	0.5	2	10	10	262
J BULK-06	1.51	5	3	8	19	7	0.5	2	8	10	204
J BULK-07	1.12	5	3	7	26	6	0.5	2	6	8	147
J BULK-08	1.79	5	3	11	23	5	0.5	2	9	9	249
J BULK-09	1.19	5	3	7	27	6	0.5	2	6	9	162
J BULK-10	1.41	5	4	9	47	6	0.5	2	8	9	190
J BULK-11	1.64	5	4	8	17	6	0.5	2	8	10	209
J BULK-11 DUP-P	1.74	5	4	9	19	6	0.5	2	9	11	223
J BULK-12	1.20	5	2	6	30	6	0.5	2	6	7	164
J BULK-13	1.44	5	3	10	35	6	0.5	2	7	9	201
J BULK-14	1.19	5	4	7	32	6	0.5	2	7	8	167
J BULK-15	1.45	5	3	8	34	6	0.5	2	7	9	193
J BULK-16	1.14	5	3	6	22	7	0.5	2	6	8	156
J BULK-17	1.61	5	6	9	26	5	0.5	2	8	10	220
J BULK-18	1.53	5	3	8	32	6	0.5	2	8	9	205
J BULK-19	1.86	5	4	10	22	7	0.5	2	10	12	241
J BULK-20	1.56	5	3	8	23	7	0.5	2	8	10	207
J BULK-21	1.27	5	4	6	20	7	0.5	2	7	9	172
J BULK-21 DUP-C	1.32	5	5	7	22	7	0.5	2	7	10	179
J BULK-22	1.26	5	4	6	17	8	0.5	2	6	10	164
J BULK-23	1.29	5	4	7	23	7	0.5	2	7	8	173
J BULK-24	1.80	5	4	9	13	5	0.5	2	9	9	241
J BULK-25	1.54	5	4	11	36	7	0.5	2	8	9	214
J BULK-26	1.17	5	4	7	24	6	0.5	2	6	8	156
J BULK-27	1.38	5	3	8	24	7	0.5	2	7	9	189
J BULK-28	1.43	5	4	9	26	6	0.5	2	7	9	184

Mold

According to the ASTM Standard C192/C192M-15 and C39/C39M-12, the mixture must be cast in a 2” by 4” (5.08 cm by10.16 cm) paper molds. The specimen length to diameter ratios is between 2.0:1 and 2.5:1. Also, the minimum diameter can be 47 mm (ASTM D4543). After blending the backfill material via a mixer, the combination will be moved to the standard molds. By utilizing a tamping rod, the molds will be tamped and will be covered by a plastic bag. Curing is performed in the DTL lab according to ASTM standard C192/C192M-15, in which the curing temperature is 23 ± 2° for 24 hours. After, the specimens will be removed from the molds and will be kept underwater or in the moisture room until the test date.

Electric hand concrete mixer

These tests will be performed with less than 20 kg of tailings, but the smallest concrete mixer machine has a capacity of 100 kg. Therefore, for this experiment, we will use a large bucket and an electrical hand concrete mixer to mix the material.

Other equipment

- Standard Personal Protective Equipment (PPE).
- Small shovel for moving the mixture into the molds.
- large bucket for mixing the material and keeping specimens underwater
- Digital scale for measuring tailings, cement, and water

Grinder

This machine is used to grind concrete specimens, natural stones, tiles, block pavers, ceramic materials etc. Based on the ASTM standard D7012-10 and ASTM C39/C39M-12, after coring and cutting the samples, cores must have a smooth surface on their tops and bottoms. The Grinder provides the final step in preparing test specimens with parallel and flat ends according to the ASTM and the ISRM specifications.

Figure 7-Grinder machine

Geomechanical loading frame

Figure 7 shows the geomechanical loading frame used for UCS measurements. The frame is equipped with a Data Acquisition System (DAQ-Sys) that records the main parameters required for constructing stress-strain relationship, including load in Kilo Newton and displacement in millimeters. The DAQ-Sys utilizes LabVIEW software that records at a 100 Hz sampling rate for these tests. The compression hydraulic pump is manually operated; however, a fixed loading rate was maintained in all tests. The tests of the same sample types, percent-age, parameters, and conditions are repeated at least three times, and the strength was then estimated based on the average.

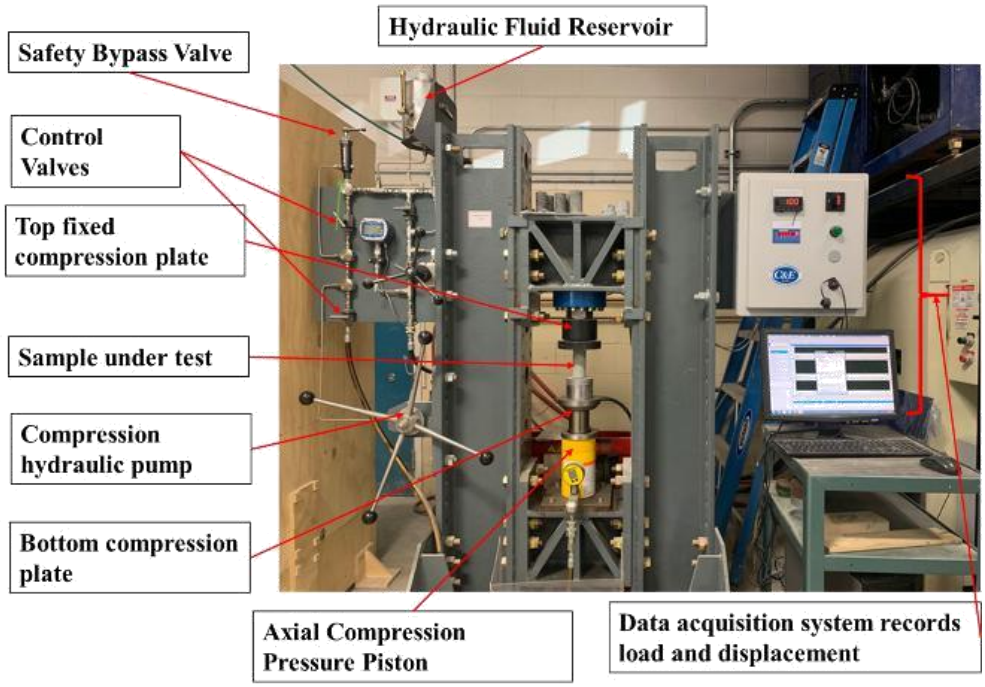

Figure 8-Geomechanical Loading Frame

3.1.3 Test procedure

Moisture content

The cement-water ratio has an essential impact on concrete strength. In this project, we propose 20% water by total mass, and it was kept constant for the entire test. Since the waste tailings are wet, the moisture content must be calculated, and the percentage of tailings and water in tables 3.1 and 3.2 were changed according to the amount of moisture in the tailings.

2000 grams of the waste tailings are measured and kept it in the oven with 120 degrees Celsius for 10 hours to make sure they are completely dried. Then the dewatered tailings were measured. The difference between wet and dry mass over wet mass is the moisture content percentage.

$$Moisture\ content = \left(\frac{Mass\ of\ wet\ tailings - Mass\ of\ dry\ tailings}{Wet\ tailings}\right) \times 100 \qquad (3.1)$$

$$Moisture\ content = \left(\frac{2000 - 1852.1}{2000}\right) \times 100 = 7.395\%$$

Bulk density

In the first step for estimating the amount of mixture, the bulk density of the waste tailings need to be measured. 100 gr of dried tailings are measured and will was then be added to a beaker containing a certain amount of water. The increased volume of water can be considered equal to the volume of tailings. The measured mass over the volume is the bulk density of the tailings (BW Ramme, 2005).

Pulp density

Hydraulic fill and paste fill are often described in terms of their pulp density which is defined as (BW Ramme, 2005)

$$Pulp\ density = \left(\frac{dry\ weight\ of\ aggregates + binder}{dry\ weight\ of\ all\ solid + weight\ of\ all\ liquids}\right) \qquad (3.2)$$

Procedure

The weights of all materials must be measured before mixing them. Based on tables 3.1 and 3.2, and using a scale, tailings, Portland cement, fly ash, and water for each batch were measured and using Equation 3.2, the pulp density can be calculated. In this equation, the tailings are used as aggregates, and the binder is the combination of Portland cement and fly ash. Since the tailings have the moisture content, to calculate the dry weight of aggregates, moisture content must be subtracted from the weight of the tailings and must be added to the weight of the liquid.

Wet and dry density

The dry density of backfill materials can be expected to be substantially less than that of the wet density due to water loss. When the mixture is ready to cast, using a standard measuring cup, the wet density of the mixture can be measured (BW Ramme, 2005).

$$Wet\ density = \left(\frac{Mass\ of\ cup\ full\ of\ backfilling - Mass\ of\ empty\ cup}{Voulume\ of\ the\ cup}\right) \qquad (3.3)$$

Procedure

First, the weight and volume of the standard cup are measured. Then the cup was filled with backfill mixture and was weighed again. Finally, using Equation 3.3, wet density can be calculated. Dry density can be calculated by measuring the weight and volume of a dried specimen after 28 days. Equation 3.4 is used to calculate the dry density of the backfilling materials.

$$Dry\ density = (\frac{Mass\ of\ dry\ sepcimen\ after\ 28\ days}{Volume\ of\ the\ specimen}) \qquad (3.4)$$

Solid Relative density

Solid relative density is the density ratio of a fill unit volume compared to the density of a unit volume of water. By having the backfill sample density and comparing it with the density of water, which is 1000 Kg/m^3, the Solid Relative Density can be calculated. This can be calculated for both the wet and dry density of the backfilling mixture (BW Ramme, 2005).

Flowability

Flowability enables the materials to be self-levelling, to flow into and readily fill a void, and be self-compacting without the need for conventional placing and compacting equipment. Flowability can be varied from stiff to fluid, depending upon requirements. One method of expressing the workability of the mixture is the standard concrete slump cone (ASTM C 143) (BW Ramme, 2005). Flowability of mixture is measured by the slump flow or v-funnel test.

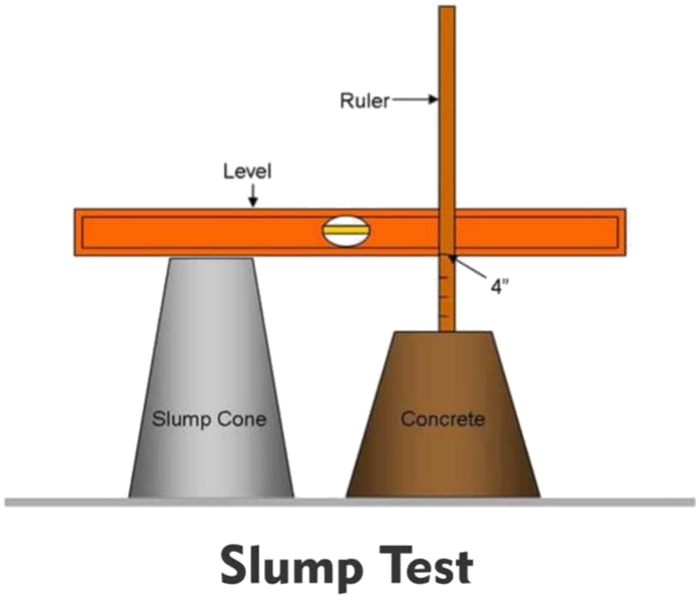

Figure 9-slump test

Slump Cone

"Slump" is the distance, measured in inches, the concrete settles after the slump cone is removed. Workability ranges associated with the slump cone can be expressed as follows:

- Low workability: less than 150 mm (6 in.);
- Normal workability: 150 to 200 mm (6 to 8 in.);
- High workability: greater than 200 mm (8 in.)

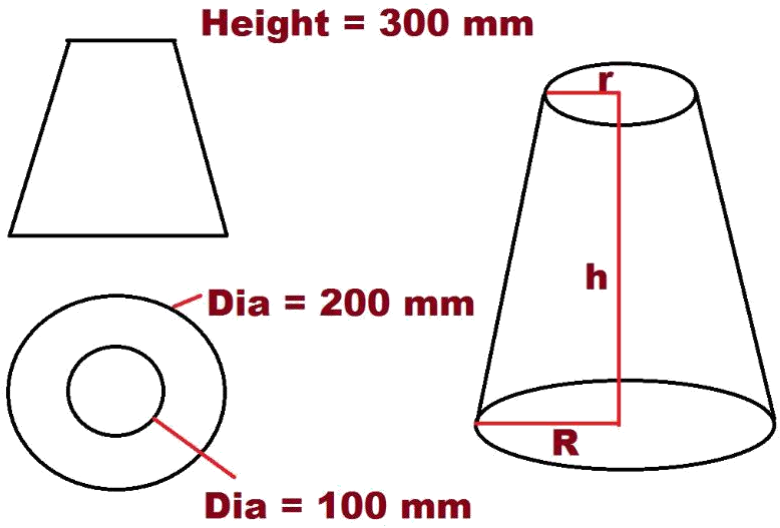

Figure 10-Slump size

Procedure

After mixing backfill materials, the slump cone was filled with the mixture. Then the cone is flipped on the surface and removed. When the material is stable, using a level and a ruler, the distance between the top of the material and the slump cone is measured. Figure 10 shows this procedure.

The volume of the slump cone

Before starting the flowability test, the volume of the slump cone needs to be measured to prepare the backfill material (BW Ramme, 2005).

Figure 11-Slump procedure

Void Ratio

The ASTM Standard C1688 determined the void ratio or void content. It is defined as the total percentage of voids present by volume in a specimen. For example, a void ratio of 85% can be considered as a good density, because only a little binder is required to fill the voids, making more binder available for coating particles. Therefore, the cohesion was enhanced. The void ratio can be calculated using equation 3.5 (ASTM C192. ASTM C192/C192M, 2016)

$$Void\ content\ \% = \frac{T-D}{T} \times 100 \qquad (3.5)$$

And density is

$$D = \frac{M_c - M_m}{V_m} \qquad (3.6)$$

And theoretical density

$$T = \frac{M_s}{V_s} \qquad (3.7)$$

Where:

M_c is the mass of measure filled with concrete

M_m is the net mass of concrete by subtracting the mass of measure

V_m is the volume of measure

M_s is the total mass of materials batched

V_s is the total absolute volume of materials

Internal vibration test

In order to conduct compaction tests, an internal vibrator and four 6×12 in molds are needed. All required materials must be weighted accurately; then dry materials are mixed together. After that, the measured water should be added to the mixture, and it was mixed by the drill and mixer for 3 minutes. Then, the mixture was poured into the mold. The mixture inside the mold was tapped at each 1/3 of the height until the mold is full of mixture. Then, the density of the mixture was measured. In order to compact the mixture and to measure the effect of the vibrator, the vibrator was slowly inserted into the second mold, and the vibrator is not allowed to rest on or touch the bottom or sides. Generally, no more than 5 s of vibration should be required for each insertion to consolidate the mixture adequately. Longer times may be required for lower slump concrete, but the vibration time should rarely have to exceed 10 s per insertion. Over-vibration may cause segregation. Usually, sufficient vibration has been applied when the surface of the mixture becomes relatively smooth and large air bubbles cease to break through the top surface. The vibration should be continued only long enough to achieve proper consolidation of the mixture. After vibration, the vibrator is slowly withdrawn so that no large air pockets are left in the specimen. The decreased height of the mixture inside the mold was measured. Then, weight and density need to be calculated. This process should be repeated for the third and fourth molds but with fewer times using the vibrator. Finally, the results of density

and height decrease between the specimens can be compared. The specimens must stay in the room temperature covered with a plastic bag for 24 hours and after that must be kept in the moisture room for 28 days. The UCS test, after 28 days, can measure the strength of the specimens regarding the effect of the internal vibrator and compaction.

Figure 12-Concrete needle vibrator

Curing time

The purpose of this research is to measure the cured time and cured strength of the backfilling. We proposed a range of cement dosages of 6%, 8% and 10% based on the ASTM standard C 1157; the strength of the backfill material made by cement and the waste tailings after 7, 14, 21, and 28 days can be measured. After casting and shaking the concrete in the molds, the molds were kept in 23 degrees Celsius for 24 hours and then were removed from the molds and kept under the water to start coring and performing the tests.

3.1.4 Standard Test Method for UCS

The most important test for measuring the strength of the concrete is UCS. By using a loading frame machine, we can measure the UCS. The given data can be used to draw the Mohr's circle. Modulus of elasticity can be obtained from the UCS test.

The initial object of the unconfined compressive test is to achieve the compressive strength of the rocks or soils. A sufficient degree of cohesion in the specimen is required to be able to conduct the UCS test. The UCS is the compressive stress at which an unconfined cylinder shape specimen fails under compressive stress. In this method, due to safety requirements based on ASTM standard D2166/ D2166M-16, the maximum attained load per area (P/A) at 15% axial strain is the UCS. Also, shear strength can be calculated as 12 of the compressive stress at failure. The laterally unconfined specimen were loaded axially at an axial strain rate between 0.5% and 2% per minute. Brittle or stiff materials should be tested at a lower rate of strain since they show small deformations at failure, while softer materials should be tested at a higher rate of strain.

Calculation

- Calculate the axial strain, ϵ_1 , to the nearest 0.1%

$$\epsilon_1 = \frac{\Delta L}{L0} \times 100 \qquad (3.8)$$

where

ΔL is the length change of specimen, mm [in.],

L_0 is the initial length of the test specimen, mm [in.].

- Calculate the compressive stress ,σ_c, to three significant figures or nearest one kPa [0.01 ton/ ft2],

$$\sigma_c = \frac{P}{A} \qquad (3.9)$$

where

P is the given applied load, kN [lbf],

A is the corresponding average cross-sectional area mm^2 [$in.^2$].

Chapter 4: Assessment of Freestanding Vertical Face for the Backfill Using the Run of the Mine Tailings and Portland Cement

Javad.Someehneshsin[a]
Memorial University of Newfoundland, St. John's, Newfoundland and Labrador, Canada
Weizhou.Quan[a]. and Abdelsalam.Abugharara[a,b]. Stephen.Butt[a].
a: Memorial University of Newfoundland, St. John's, Newfoundland and Labrador, Canada
b: Sebha University, Sebha, Libya

This chapter is a paper accepted in the ARMA 2020 conference and authored by Javad Someehneshin, Weizhou Quan, Dr. Abdelsalam Abugharara & Dr. Stephen Butt, and was published on OnePetro numbered "1882". The MEng candidate was involved with the planning and calculation of the experiments, method selection, the data analysis, and the writing of the paper.

4.1 Abstract

Exploiting very thin but valuable ore bodies that are uneconomical to extract by conventional mining methods is being noticed nowadays. Some methods are used to mine stranded, steeply dipping ore veins, which are too small or isolated to mine economically using conventional methods since the dilution is minimized. This novel mining technique uses drilling rigs to extract the ore through directional drilling surgically. This paper is focusing on utilizing the run of the mine tailings and Portland cement as backfill material to support the HW for providing safe mine operation and different methods, including Marston's theory and Terzaghi's theory, for calculating freestanding vertical face were proposed and compared. Also, the arching effect and inclination of stope were considered.

CPB is designed by mixing waste tailings, water, and cement of the precise percentage for optimal outcomes. It is a non-homogenous material that contains 70-85% solids. The vertical normal stress for a 2 meter diameter and 200 meter depth hole, filling with 2000 kg/m^3 waste tailings, will be 0.123 MPa and using a backfill material with 1 MPa compressive strength is suggested.

4.2 Introduction

One of the most important tasks of the post-mining process is mine backfilling. Typically, backfill is made of soil, overburden, mine tailings or any other kind of aggregate which can be used as a filler and booster in the extracted area, which was excavated by mining operations. Backfill material is placed into previously extracted stopes to produce a stable platform for the miners to work on and provide ground support for the walls of the adjacent adits while mining progresses. These backfills reduce the amount of open area that might be filled by a collapse if the encompassing pillars failed (Barret et al. 1978). Backfill material is categorized as hydraulic fill, paste fill, and rock fill. In order to increase the strength of the backfill material, a small amount of binder (Portland cement) is added to the mixture. Mine productivity could be enhanced by using underground paste backfill. Paste backfill not only supports the ground for the pillars and walls, but also helps stop caving, roof collapse, and improves pillar recovery (Coates 1981).

CPB is used in many cut and fill mines all around the world. This method is a significant inevitable section of underground mining operations and is becoming a standard procedure in several mines. (Landriault et al., 1997). Paste backfill consists of mill tailings generated throughout ore dressing that have lost water. They are mixed with additives like Portland

cement, lime, powdered ash, and slag. The aim of the binding agents is to develop cohesion inside the CPB, so that exposed fill faces have enough strength to tolerate the load (Mitchell 1989). The mill tailings are in the form of a slurry. After dewatering, the mill tailings will be filtered to get thicker (70–85 wt. % solids). To bind the tailings particles and raise the strength of the CPB, usually one or two types of cement, such as standard Portland cement, sulphate-resistance cement, ground granulated blast furnace slag (fine-grained smelter slag), and solid pulverized fly ash will be added to the mixture as a hydraulic binder. Tailings are the worthless remaining material after ore separation. This waste material (gangue) must be disposed of, even though it may cause environmental issues such as dam failure and acid rock drainage (ARD). Usually, tailings have the potential to be contaminated by radioactive and toxic elements. ARD happens when acidic water outflows from coal and metal mines. Recently, the use of tailings has become more popular in backfilling industries since it is available on a large scale, cheap, and easy to transfer. Also, using tailings as backfill material can reduce tailings pond accumulation, ARD, and environmental issues. The maximum possible, solid content in the paste fill method is 75 – 80 %. In this paper, the calculations are based on 80 solid content and 20 % water. Solid content is the ratio of the mass of solid over the total mass. Also, a small dosage of binder (Portland cement) is used to enhance the strength of the backfill. The binder dosage is the mass of cement over the mass of solids. Depending on the backfill design and the required strength, a 2-10% binder is used to increase the strength and the free-standing ability of the backfill. The water-to-binder ratio has an inverse ratio with the compressive strength. When the water percentage increases with a normal range of the binder, the compressive strength of the backfill will decrease. Since the mill tailings are mixed with water and found the form of a slurry, the moisture content of the tailings needs to be taken in to account.

The arching effect is one of the most common phenomena to be observed in soils both in the field and in the laboratory. Terzaghi confirmed the existence of the arching effect by trap door model tests (Terzaghi, 1943). The relative movements in the soil are affected by the resistance of the shear strength of soils, so that the pressure of the moving parts of soils decreases, while the pressure of the stationary parts increases. The arching effect in soils is different from the arch structure. The arch structure is to make the material into the shape of the arch and plays the role of bearing pressure under the action of load. However, the arching effect has its own forming process. Under the action of load or self-weight, the soil mass compresses and deforms, which results in an uneven settlement, the arching effect occurs in a certain range of soil layers. It worth mentioning that in addition to the arching effect in the vertical direction, there is also the arching effect in the horizontal direction. Using vertical and horizontal arching effects properly can make the redistribution of soil stress develop in a beneficial direction and make full use of the anti-deformation ability of soils.

With increasing recognition of arching effect, it has been identified in various applications, such as vertical stress and support requirements above tunnels and other underground situations (Terzaghi 1943, and Iglesia et al. 1999), underground conduit (Spangler 1962, and McCarthy 1988), and piled embankments (Low et al. 1994). This effect is most recognized in the underground. Underground openings can be built utilizing the arching action to account for the reduction in the overburden pressure. Currently, five main methods are used to investigate the arching effects, Free-Standing Vertical Face (Grice 2001), Vertical Slope (Grice 2001), 3-D Sliding Wedge Failure (Mitchell et al. 1982), Simple Arching Theory and its Modifications (Marston 1930, Aubertin et al. 2003), and Modified Simple Arching (Winch 1999).

The studied vein prospect is underlain by a sequence of relatively un-deformed, massive fine grained, locally vesicular pillow basalts. Fine-grained, mafic volcanic, and gabbroic intrusive rocks host the veins. The prospect consists of three northeast aligned quartz veined zones 1 to 2 meters thick, exposed over 300 meters, striking 20˚ and dipping 60˚. The veins are spatially associated with a north-northeast trending topographic lineament that continues for several kilometers to the north. Traditional mining techniques like underground (cut and fill mining, shrinkage mining) and open pit produce a stripping ratio too large to be economically successful. To combat the unfeasibility of the traditional mining techniques on steeply dipping ore bodies, a new drilling technique was developed. This novel mining technique uses drilling rigs to remove the ore surgically through directional drilling. This technique involves detailed geophysical imaging of the boundary regions associated with the borehole. The goal of the imaging is to adjust the trajectory of a directional drill string to optimize the stripping ratio within the ore body. Once the ore has been extracted, mining reclamation is performed by infilling the boreholes.

This paper will give the designed proportions of CPB by mixing waste tailings, water, and cement of the precise percentage for optimal outcomes. The test plans for all CPB specimens are based on American Society for Testing and Materials (ASTM) standards. The different methods for investigating arching effects for this vein are given and analyzed in the later part. The vertical normal stress of the stope and the compressive strength of backfill material is recommended from the calculations.

4.3 Materials and method

4.3.1 The grain size distribution of mine tailings

To design the backfill material, the waste tailings from the gold mine, Portland cement, and water are mixed. Grain (particle) size distribution can identify the tailings characterization. The particle size analyzes a distribution based on cumulative function. To perform the grain size distribution, the samples are dried in an oven at 115 $^{\circ}$C for 12 hours, stirred, and returned the oven at the same temperature for three more hours. After cooling, the samples are classified using mesh containing 2000, 630, 315, 250, 150, and 75 microns by an electric shaker. The shaker is active for 5 minutes at 70% power. Figure 13 shows the tailings samples before and after drying.

Figure 13-Tailings before (left) and after (right) drying

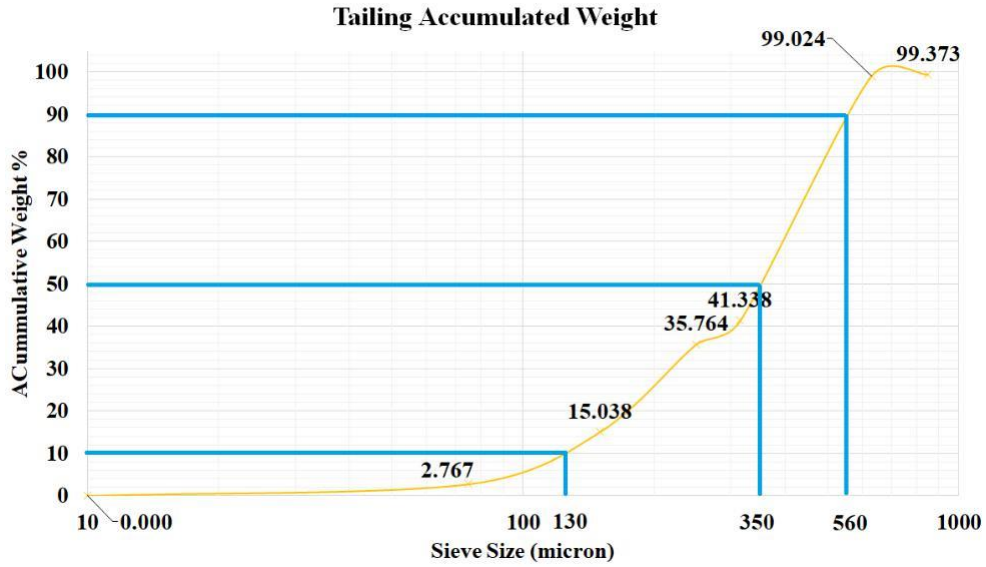

Figure 14-Tailings accumulated weight and grain size distribution

4.3.2 Materials

The mill tailings are well-graded. Figure 14 indicates that 90% of the tailings are below 560-micron, 50% are below 350-micron, and 10% are below 130-micron. Regular Portland cement type GU is used in this research.

4.3.3 Method

As mentioned before, backfill consists of three major types: hydraulic fill, rock fill, and paste fill. Paste fill has gained much attention in the past decade because of its certain operational and environmental advantages (Landrail, 1995). Paste fill has a higher solid content, containing both fine and coarse particles, which can reduce the surface tailings accumulation maximally. The backfill prepared using the paste fill method has the

comparative undefined compressive strength (UCS) of the rock fill. Furthermore, paste fill can facilitate the mining sequence because the UCS is achieved earlier when compared with hydraulic fill. Unlike hydraulic fill, there is no cost for dewatering.

Further, this method has a higher filling rate than hydraulic fill since it comprises a 3-6% by weight of the binder. Also, the combination of slurry velocity, slurry density, pipe diameter, and pipe gradient causes pipe wear. Paste fill is categorized into medium and fine depending on the resulting pulp densities:

- Coarse tailings: have a pulp density of 78% to 85% solids by weight; will produce fill with at least double the strength of similar slurry fill for the same cement content.
- Medium tailings: have a pulp density of 70% to 78% solids by weight.
- Fine tailings: have a pulp density of 55% to 70% solids by weight; high retention of water means suitable for transport but bad for overall strength.

To minimize the percentage of the cement, paste fill can be mixed with sand and a chemical additive. The obtained mixture is called a Gel Fill. The paste fill method is adopted in this research. This method contains mill tailings, a binder like Portland cement, and water. Paste fill is suggested for the vein extracted by the new drilling method. All of the mill tailings can be used, and there is no need to do a size separation.

4.3.4 Moisture content

The ore dressing process and waste tailings transportation will add water to the tailings. Since the tailings are usually stored in an open area, the water content can affect the accuracy of experiments. Moisture content is determined by removing the water in the tailings through the heating process. The difference in weight is the water content.

$$Moisture\ content = (\frac{Mass\ of\ wet\ tailings - Mass\ of\ dry\ tailings}{mass\ of\ wet\ tailings}) \times 100 \qquad (4.1)$$

The cement-water ratio has an essential impact on concrete strength. This paper proposes 20% water of the total mass, keeping it constant throughout the test. Since the waste tailings are wet, the moisture content must be calculated. The percentage of tailings and water will be changed according to the amount of moisture measured. 2000 grams of the waste tailings are heated in the oven at 120 ˚C for 10 hours to ensure it is completely dried. The dewatered tailings are then measured. The difference between wet and dry mass over wet mass is the moisture content percentage.

$$Moisture\ content = \left(\frac{2000-1852.1}{2000}\right) \times 100 = 7.395\% \qquad (4.2)$$

4.3.5 Test plan

The procedures and mixture for fabricating the backfilling material for this project are introduced. During the curing time (28 days in total) of the backfilling content, its increase in strength over time is tested and analyzed at 7 days, 14 days, and 28 days after the casting (ASTM standard C 1157). At each curing stage, density, and UCS tests are performed. The relationships between backfill strength and tailing grain size distribution, curing time, and

the backfill material recipe is proposed based on the experimental results. The most important test for measuring the strength of the concrete is UCS. By using a geomechanical loading frame machine, the UCS can be measured. The given data can be used to draw the Mohr's circle. Modulus of elasticity can be obtained from the UCS test.

4.4 Freestanding vertical face

To minimize the failure of the backfill, the development of stresses is essential to understand. Though it is expected to have more stresses at the bottom of the mine, evidence shows that the stresses at the bottom of the stope mines are much less than calculated. Traditionally, for calculating the stress at any section of the mine, the unit weight of the backfill multiplied by the depth will result in the stress at that section.

4.4.1 Arching effect

When the yielding backfill is emplacing down to the holes in the mine, the movement is opposite to the stable unyielding rock on the wall. Therefore, this movement is against the shear resistance along with the interface between rock and backfill materials. The generated shear stress in the contacted area tends to keep the backfill in its place and opposes its movements. Figure 15 shows a schematic diagram of the process of the backfill movement.

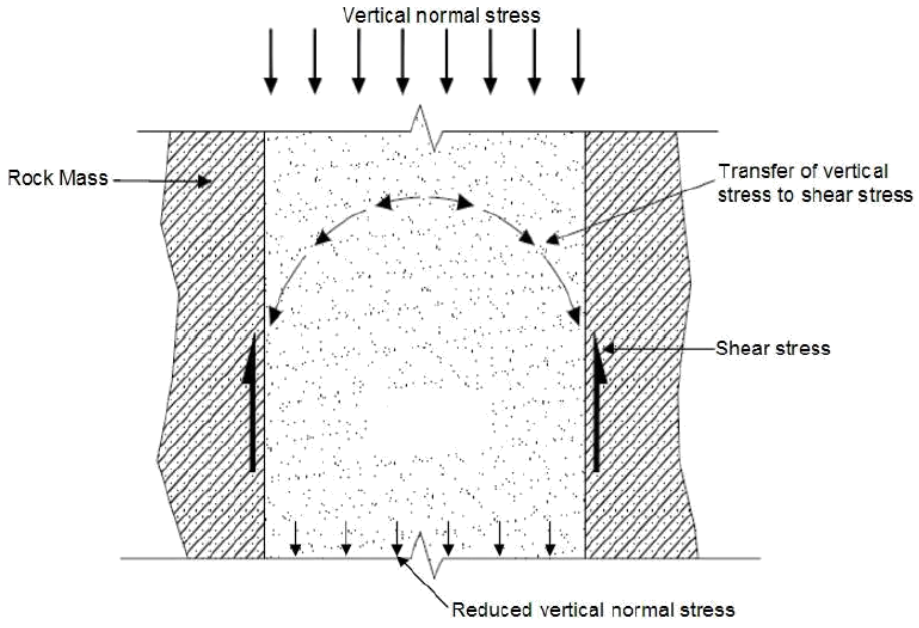

Figure 15-Arching effect (Pirapakaran, K. 2008. Load-deformation characteristics of mine fills with particular reference to arching and stress developments. J. James Cook University)

4.4.2 The necessity of considering the arching effect in backfilling

If the lateral confinement is neglected, the vertical normal stress at any depth can be calculated from equation 4.3.

$$\sigma_v = \gamma Z \qquad (4.3)$$

Where:

γ is the unit weight of the backfill (kN/m^3)

Z is the strata depth (m)

σv is the vertical normal stress (kPa)

Aubertin et al. (2003) used the modified Marston's theory, which considers the arching effect. The above equation calculates the vertical normal stress; however, it is overestimated since it does not consider the influence of the arching, while approximately 60% of the reduction of the stress occurs at the stope bottom. Neglecting the arching effect causes an overestimation of the strength of the backfill and will increase the dosage of binder and, consequently, the cost of the backfilling.

4.4.3 Freestanding

Conventionally, to withstand the pressure of the overburden due to the self-weight, free-standing walls of the cemented paste fill and hydraulic fill are designed for the specific depth. As expressed above, Eq. 4.3. Is used to compute the overburden pressure. Grice (2001) suggested the following relationship for designing the exposed face as a free-standing:

$$UCS = \gamma Z \qquad (4.4)$$

In this relationship, the increase of strength due to the lateral confinement is entirely discounted. Therefore calculating the free-standing of this narrow vein based on the 2 meter diameter and 200 meter depth holes filling with the waste tailing and cement with the bulk density of 2000 kg/m^3 is as follows: ρ=2000 kg/m^3

Z=200 m

UCS≥ 2000×9.81×200

UCS≥ 3.92 MPa

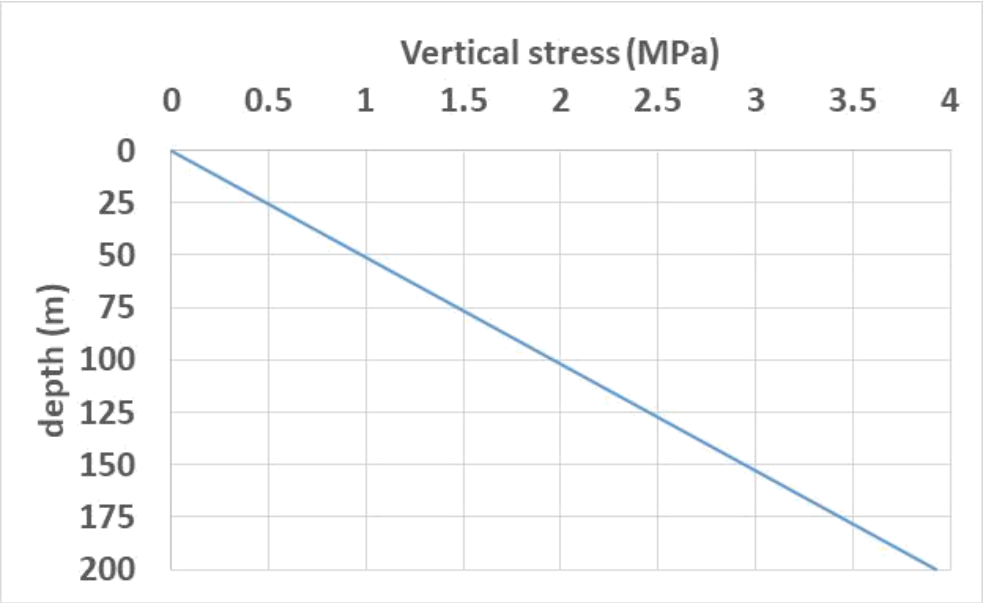

Figure 16-Freestanding method plot

The above calculated free standing is a conservative estimation that does not consider the confinement lateral and arching effect. Figure 16 shows the vertical stress versus depth plot of the freestanding method. The rate of vertical stress over depth is 0.0196 MPa per meter constantly.

4.4.4 Marston's theory

Marston (1930) developed a relationship for vertical and horizontal stresses with a specific solution to the arching concept. Marston's theory can be used to estimate the vertical and lateral loads forcing on the stope floor and walls correspondingly. The following relationships are a two-dimensional plane strain with a combination of the arching effect.

In this theory, the cohesion of the backfill was not considered. The vertical and horizontal normal stresses are expressed as follows:

$$\sigma_v = \frac{\gamma w}{2\mu K_a}\left[1 - exp\left(-\frac{2K_a\mu h}{w}\right)\right] \quad (4.5)$$

$$\sigma_h = \sigma_v . K_a \quad (4.6)$$

$$K_a = \tan^2(45° - {}^{\varphi}/_{2}) \quad (4.7)$$

Where:

σ_v is the vertical normal stress

σ_h is the horizontal normal stress

γ is the unit weight of the backfill (kN/m^3)

h is the stope depth (m)

w is the stope width (m)

φ is the friction angle of the backfill

δ is the angle of wall friction, (between 1/3φ and 2/3φ)

μ is frictional coefficient between a rock and fill, (μ is tan δ)

K_a is Rankines's active earth pressure coefficient

Bieniawski (1989) expressed that the shear strength of the rock mass depends on the cohesion and internal friction angle of the rock mass. Rock mass rating (RMR) can be used to estimate the cohesion and the internal friction angle of the rock mass. Both cohesion and

internal friction angle of the backfill material are functions of the binder percentage (Portland cement) and curing time. By increasing the percentage of binder and curing time, these parameters will increase. Besides, the required binder typically depends on the void space and applied stress in the mine. In the absence of any reliable laboratory tests or computer simulations and since a huge fraction of the backfilling is composed of tailings, which follows the rock behaviors, the RMR relation was used to approximate the cohesion and internal friction angle of the backfilling. Table 4 provides both cohesion and internal friction angle of the rock mass based on the RMR and is used to estimate these parameters for the backfill. Since the backfill uses a small dosage of binder, Brakebusch (1994) expressed that typically sufficient UCS for backfill is 0.7 MPa to 2 MPa (Amartunga, L. M. and Yaschyshyn, D. N., (1997)). Ulusay, Resat and Gokceoglu, Candan (2011) used the relationship between RMR and the UCS to indicate a rating chart of block punch strength and UCS for RMR and M-RMR rock mass classification systems. This formula was already expressed by Bieniawski (1989). Therefore, using Table 4, Figure 17, and Eq. 4.8, the cohesion and the internal friction angle of the backfill can be estimated as 0.1 MPa and 15˚, respectively.

$$RMR = \left(\frac{UCS}{3.67}\right)^{0.65} \qquad (4.8)$$

$$RMR = \left(\frac{2}{3.67}\right)^{0.65} = 0.67 \qquad (4.9)$$

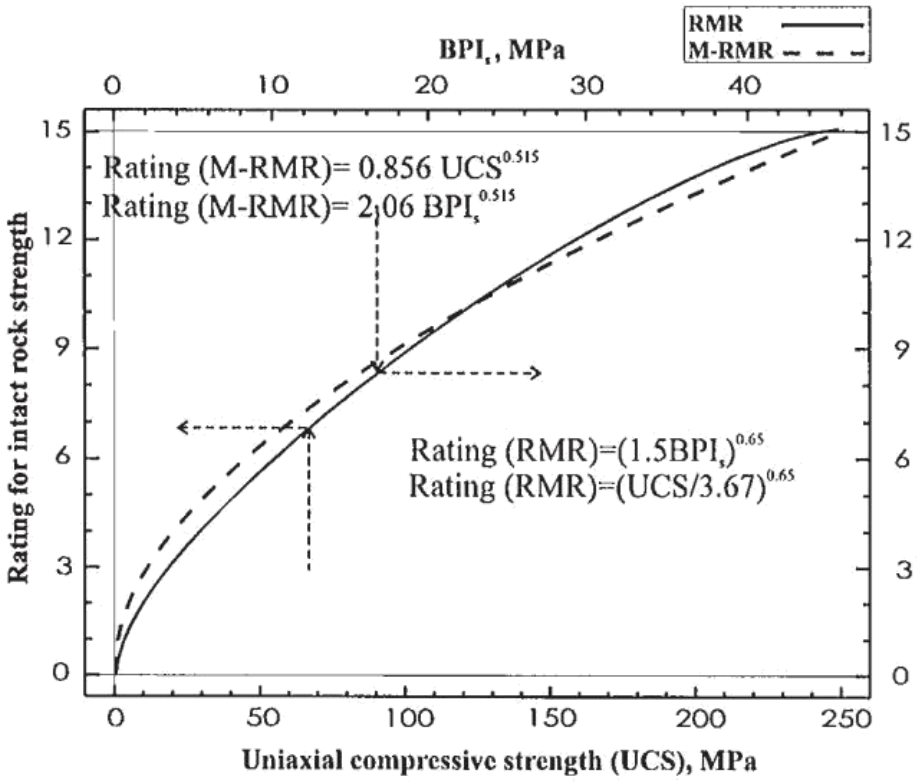

Figure 17-The relationship between RMR and UCS (Bieniawski, Z. T. 1989)

4.4.5 Calculation the freestanding by Marston's theory

Considering the angle of internal friction of the backfill as 15˚, Rankine's active pressure coefficient will be 0.588.

$$K_a = \tan^2\left(45° - {}^{15}/_{2}\right) = 0.588 \quad (4.10)$$

By applying the information of the vein, the vertical and horizontal normal stresses would be 0.253 MPa and 0.148 MPa, respectively.

$$\sigma_v = \frac{2000\times9.81\times2}{2\times0.13\times0.588}\left[1 - exp\left(-\frac{2\times0.588\times0.13\times200}{2}\right)\right] = 0.253\ MPa \quad (4.11)$$

$$\sigma_h = 0.253 \times 0.588 = 0.148\ MPa \qquad (4.12)$$

Table 4 RMR, Cohesion, and angle of internal friction of rock mass

No.	Parameter/ properties of rock mass	RMR (rock class)				
		100-81 (I)	80-61 (II)	60-41 (III)	40-21 (IV)	<20 (V)
1	The cohesion of rock mass (MPa)	>0.4	0.3-0.4	0.2-0.3	0.1-0.2	<0.1
2	Angle of internal friction of rock mass	>45 ˚	35-45 ˚	25-35 ˚	15-25 ˚	<15 ˚

The vertical stress which applies to the bottom of the backfilled stope, due to the arching effect, is significantly less than the overburden pressure (Marston, 1930; Terzaghi, 1943; Pirapakaran and Sivakugan, 2007; Nasir and Fall, 2008). Eq. 4.5 contains an exponential part $\left(\left[1 - exp\left(-\frac{2K_a\mu h}{w}\right)\right]\right)$ that is a function of the depth. At a lower depth (from surface h=0 to 25 meters), the exponential part is a number approximately between 0.07 and 0.7. However, by increasing the depth and after 80 meters, this part converges to approximately 1. Figure 18 shows the vertical stress versus depth using Marston's theory. It indicates that the vertical stress will increase until 80 meters depth, and after that, it shows a constant value of the vertical stress. This is because the second part of the formula converges to 1 and the first part ($[\frac{\gamma w}{2\mu K_a}]$) is not a function of the depth. Figure 19 shows the rate of stress over depth. Marston's method is a plateau or constant with respect to depth for (h) more than 80 meters.

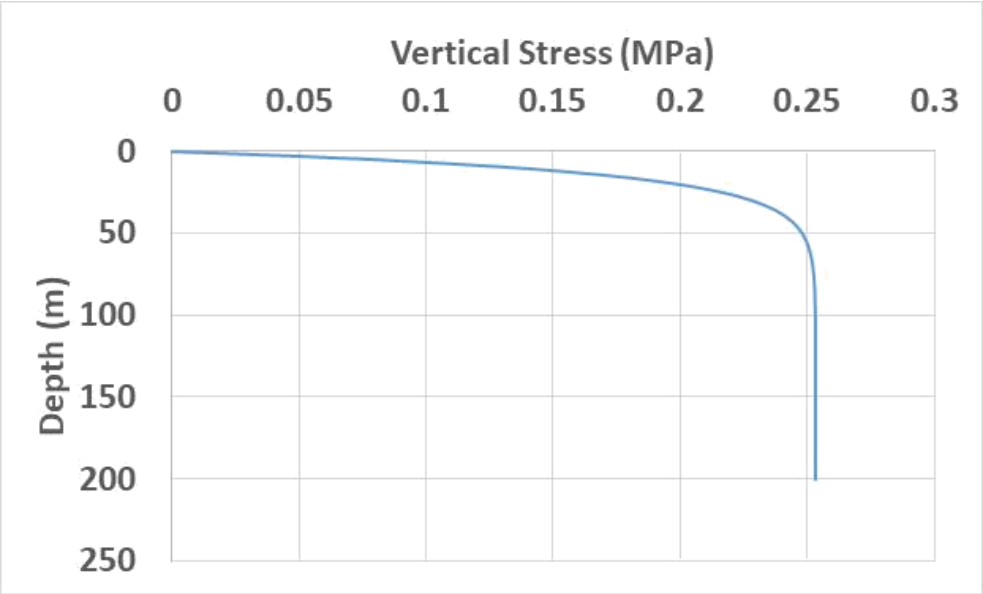

Figure 18-Marston's theory

4.4.6 Terzaghi's theory

In Marston's theory, the cohesion of the backfill was ignored. Terzaghi (1943) added the effect of cohesion to Marston's theory to predict the vertical and horizontal normal stresses. Including the cohesion in Marston's theory will reduce the amount of vertical and horizontal normal stresses.

$$\sigma_v = \frac{\gamma w - 2c}{2K \tan \varphi}\left[1 - exp\left(-\frac{2Kh \tan \varphi}{w}\right)\right] \qquad (4.13)$$

$$\sigma_h = \sigma_v . K \qquad (4.14)$$

$$K = \frac{1}{1+2\ tan^2\ \varphi} \qquad (4.15)$$

Where c and K are cohesion and earth pressure coefficient, respectively.

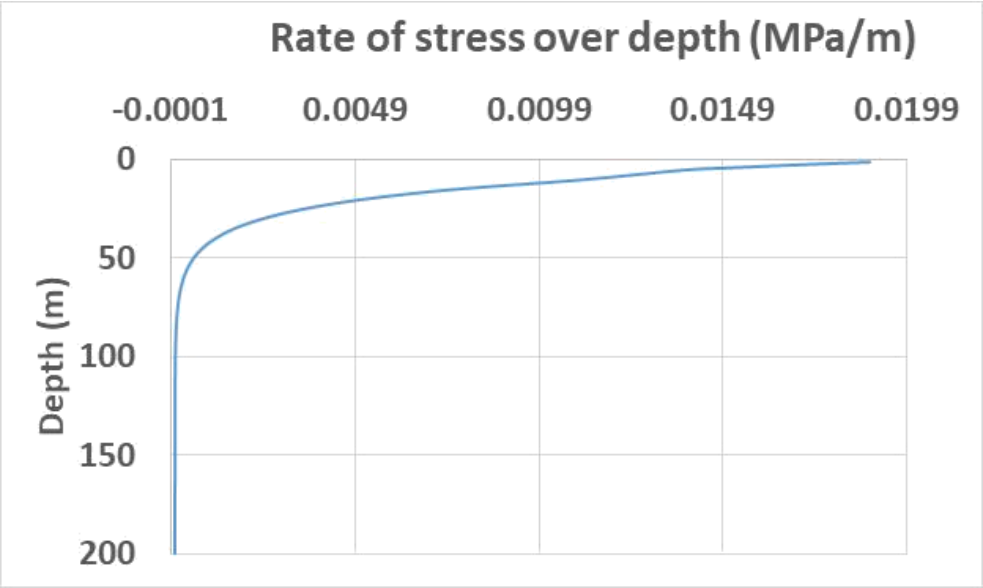

Figure 19-Rate of stress over depth

By applying the previous data of the vein and estimation of the cohesion of c=0.1 MPa on Eq. 4.13 to Eq. 4.15, the vertical and horizontal normal stresses would be -0.34 MPa and -0.3 MPa, respectively. In the rock mechanics theory, negative stress expresses tensile stress. For cohesion backfill, Aubertin et al. (2003) modified the relations of Marston's theory and, based on that, for c=0, Eq. 4.16 and Eq. 4.17, the vertical and horizontal normal stresses would be 0.083 MPa and 0.073 MPa, respectively.

$$\sigma_v = \frac{\gamma w}{2K \tan \varphi}\left[1 - exp\left(-\frac{2Kh \tan \varphi}{w}\right)\right] \quad (4.16)$$

$$\sigma_h = \sigma_v . K \quad (4.17)$$

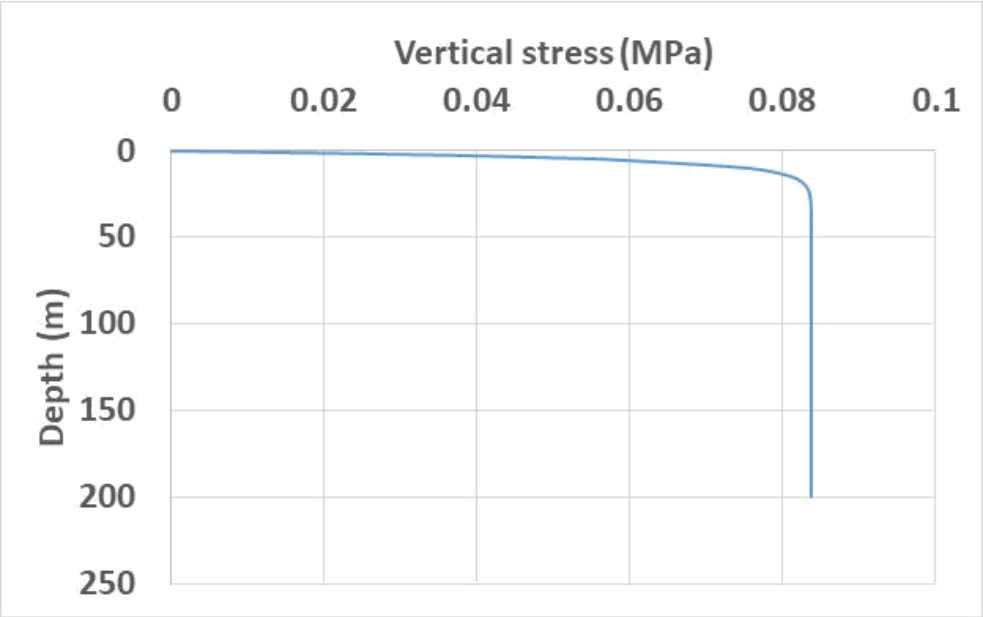

Figure 20-Abuertin et al. method

As explained above, Abuertin et al. method is the same as Marston's method with some improvements and consideration of cohesion. Figures 20 and 21 show the vertical stress versus depth and the rate of stress over depth, respectively. Due to having an exponential part in this formula ($\left[1 - exp\left(-\frac{2Kh\tan\varphi}{w}\right)\right]$), the stress after the depth of 25 meters converges to the maximum value of the vertical stress, i.e. Abuertin et al. method is a constant function equal to 0.083 MPa.

4.4.7 Inclined stope

The inclination of the stope may have a significant effect on stress development. The studied vein has an inclination of approximately 20-30 degrees. The orebody is located between HW and FW. HW and FW influence the distributed load while backfilling.

Knustsson (1981) expressed that if the inclination is less than 30˚, it would have a minimal effect of less than 10% on the distributed stress. Abuertin et al. (2003) extended Knustsson's idea and indicated that there is a difference between vertical and inclined stopes regarding the load distribution. The arching effects were not developed, but due to the weight of the backfill, there is a portion of the transferred pressure on the FW. Caceres (2005) studied the Musselwhite mine of Placer Dome and derived an analytical solution from modified Marston theory for backfilling an inclined narrow stope.

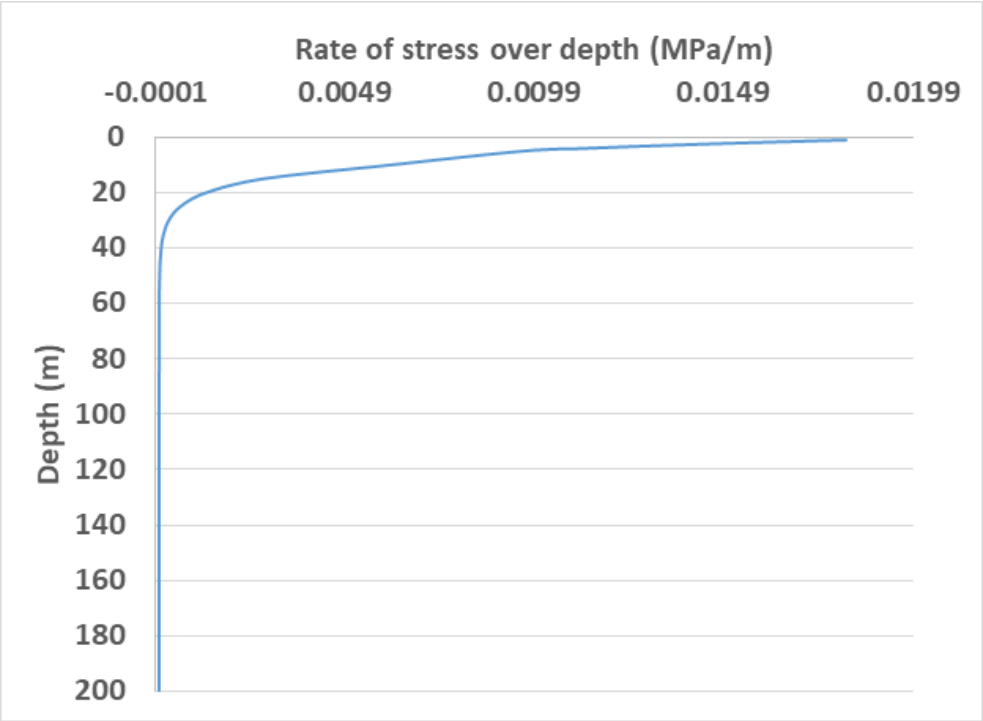

Figure 21-Rate of stress over depth

$$\sigma_v = \frac{\gamma w}{2K \tan \varphi} sin^2\beta \left[1 - exp\left(-\frac{2Kh \tan \varphi}{w sin^2 \beta}\right)\right] \qquad (4.18)$$

$$K = 1.4sin^2\varphi - 2\sin\varphi + 1 \qquad (4.19)$$

Where:

σ_v is the vertical normal stress with inclined narrow stopes

K is the coefficient lateral earth pressure

β is the inclination of stope to horizontal (degree) = dip

Applying the data of the vein and considering inclination 20 degrees, the vertical normal stress would be 0.123 MPa.

In the exponential part of the Inclined stope method ($\left[1 - exp\left(-\frac{2Kh\tan\varphi}{wsin^2\beta}\right)\right]$), with increasing the depth this part will converge to 1, the stress will be a constant value. Figures 22 and 23 show the vertical stress and rate of stress versus depth, respectively. As mentioned before, the free-standing theory is a very conservative estimation and does not include the arching effect on the load distribution. Marston, Terzaghi, and modified Marston theories are used for vertical veins, while the studied vein has an inclination. Therefore, vertical normal stress for a 2 meter diameter and 200 meter depth hole, filling with waste tailings with 2000 kg/m^3 would be 0.123 MPa and using a backfill material with 1 MPa compressive strength is suggested.

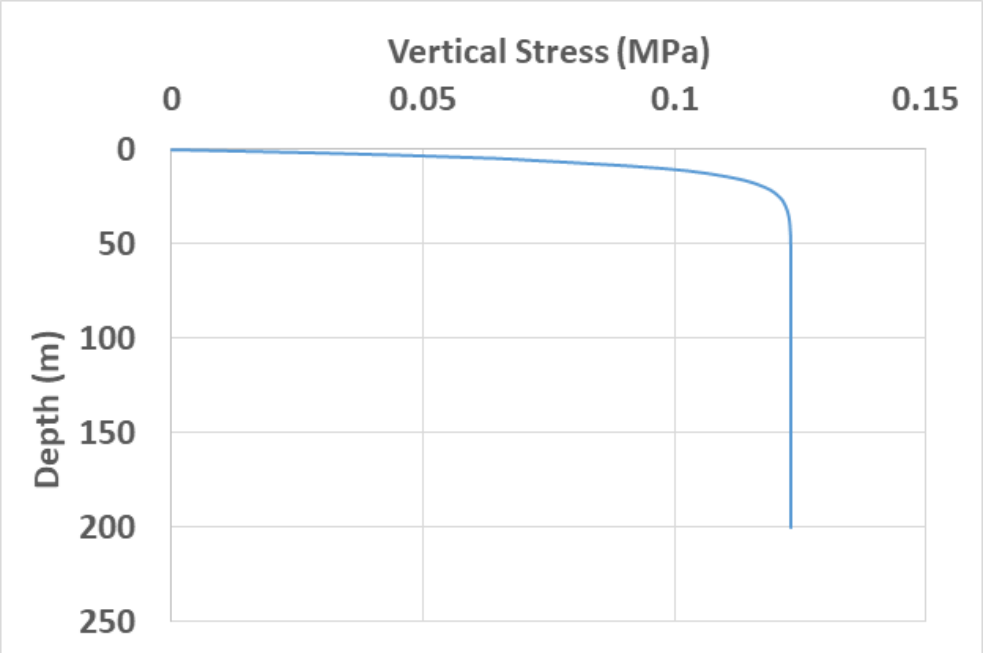

Figure 22-Inclined stope method

Figures 24 and 25 compare the vertical stress versus depth for different methods. As mentioned before, the inclined stope method is being used in the studied vein. Figure 24 shows the depth up to 60 meters, and Figure 25 shows the depth up to 200 meters.

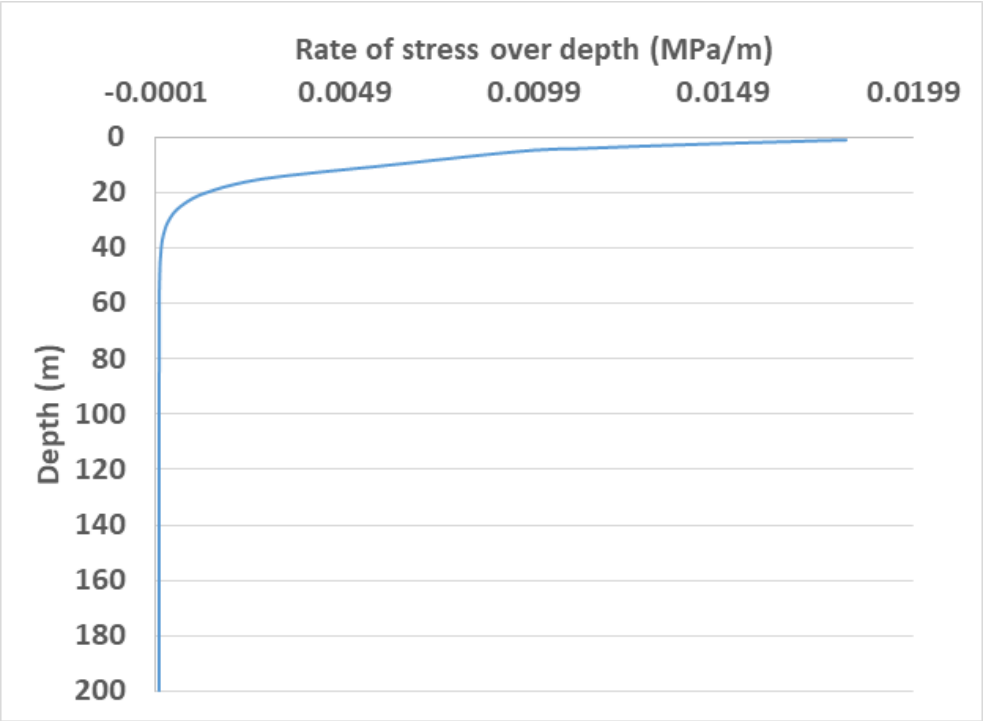

Figure 23-Rate of stress over depth

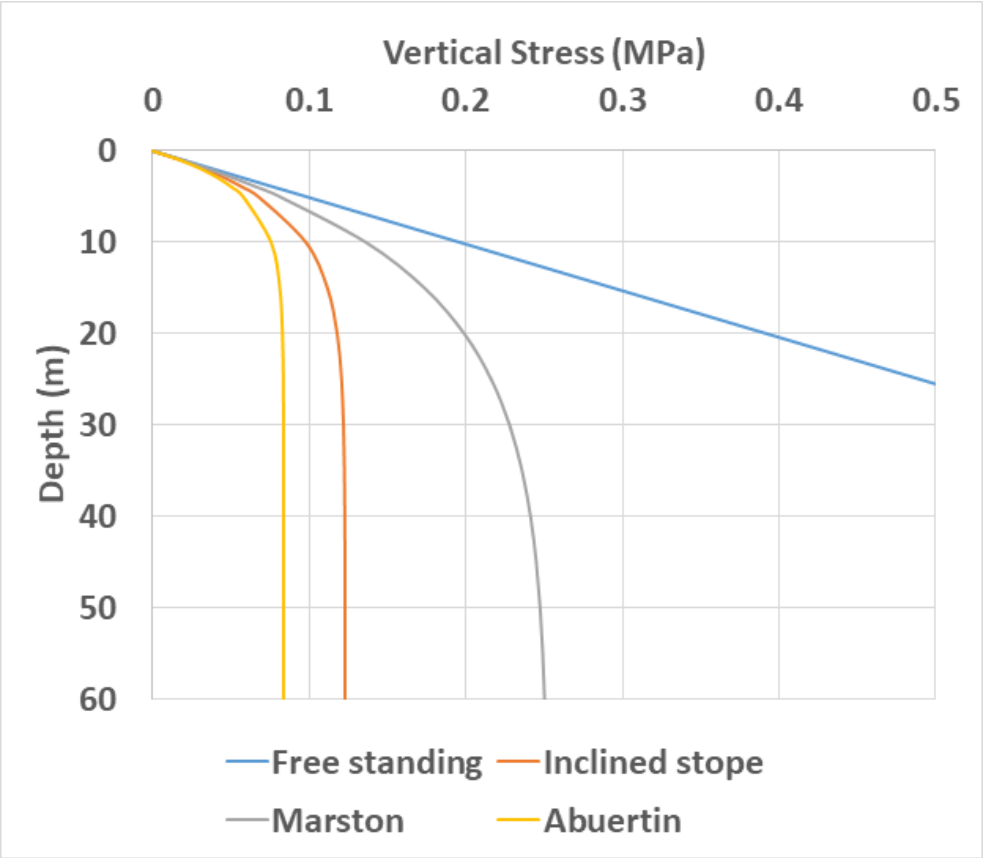

Figure 24-Freestanding, inclined stope, Marston, and Abuertin methods versus

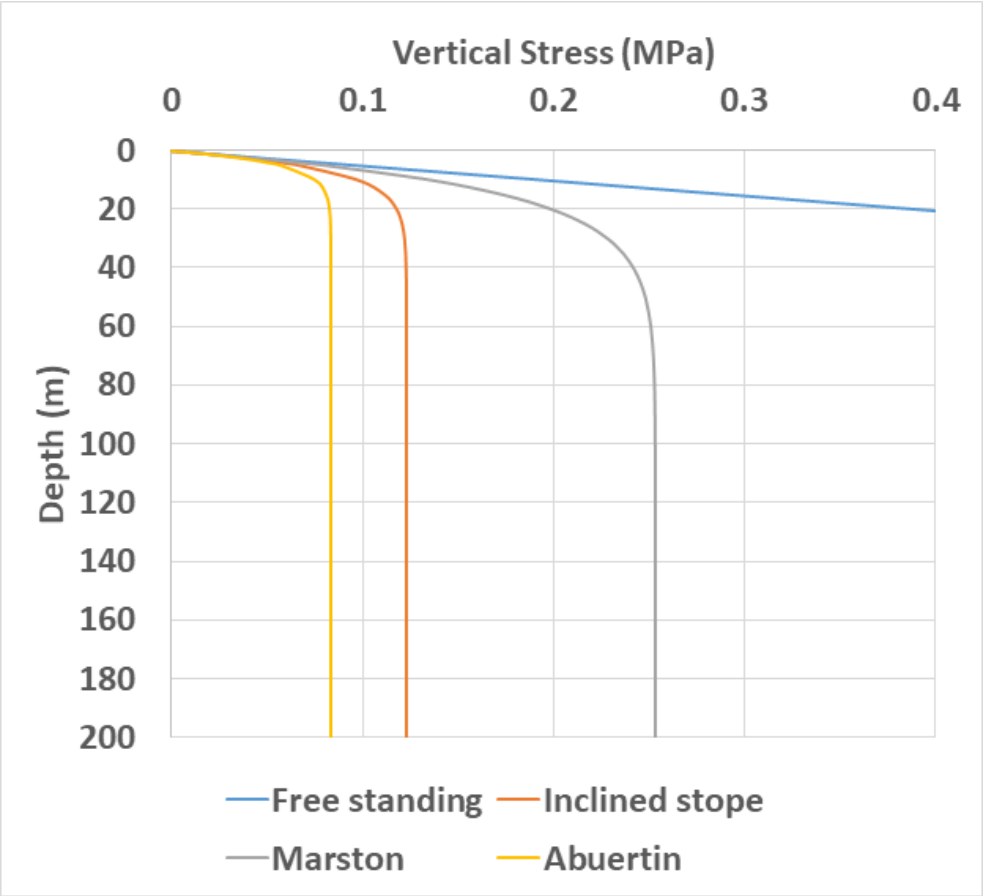

Figure 25-Freestanding, inclined stope, Marston, and Abuertin methods versus

4.5 Summary and conclusions

Every year, 500 million tonnes of tailings and waste rocks are produced in Canada. Paste backfill consists of mill tailings generated throughout ore dressing that have lost water. The CPB method has been increasingly utilized in mining companies. Using the paste fill method not only provides an efficient way to reduce surface tailings impoundment, which prevents environmental issues, but also improves the safety of ore bodies. The arching effect is considered in this study, which enhances the safety and efficiency of the on-site

drilling operation of the vein. In order to minimize backfill failure, freestanding vertical face needs to be calculated, and different methods are suggested. The studied narrow vein has an inclination. Thus the inclined stope is the most suitable method for calculating the freestanding face.

Chapter 05: Backfill Analysis and Parametric Evaluation of the Cement Binder on Cured Strength and Curing Time

Javad Someehneshin[a], Weizhou Quan[a], Dr. Abdelsalam Abugharara[a,b] & Dr. Stephen Butt[a]
a: Memorial University of Newfoundland, St. John's, Newfoundland and Labrador, Canada
b: Department of Oil and Gas Engineering - Sebha University, Sebha, Libya
a: Department of Process Engineering – the University of Newfoundland, St. John's, Newfoundland and Labrador, Canada

This chapter is a paper accepted in the Geocalgary 2020 conference and authored by Javad Someehneshin, Weizhou Quan, Abdelsalam Abugharara & Stephen Butt,. The MEng candidate was involved with the planning and execution of the experiments, design of the binder type and dosage, the experimental data analysis, and the writing of the paper. Lab Test Equipment: Grinder Machine and Geomechanical Loading Frame.

5.1 Abstract

This paper investigates the effects of binder dosage (6%, 8% and 10% wt.), binder composition (Portland cement and fly ash), and curing time (7, 14, and 28 days) on the UCS of backfill materials. At each curing stage, density tests and UCS tests were conducted for each backfill specimens. In total, 72 backfill specimens were prepared by the CPB method. Consequently, the UCS and stiffness of backfill material increased with the increasing binder dosages. The addition of fly ash caused a notable increase in the

compressive strength and stiffness of backfill materials. Also, the compressive strengths for all studied combination backfill materials increase with curing time.

5.2 RÉSUMÉ

Cet article étudie les effets du dosage du liant (6%, 8% et 10% en poids), de la composition du liant (ciment Portland et cendres volantes) et du temps de durcissement (7, 14 et 28 jours) sur la résistance à la compression non confinée (SCU) de matériaux de remblayage. À chaque étape de durcissement, des tests de densité et des tests UCS ont été effectués pour chaque échantillon de remblai. Au total, 72 échantillons de remblai ont été préparés par la méthode du remblai en pâte cimentée (CPB). Par conséquent, le SCU et la rigidité du matériau de remblayage ont augmenté avec l'augmentation des doses de liant. L'ajout de cendres volantes a provoqué une augmentation notable de la résistance à la compression et de la rigidité des matériaux de remblayage. De plus, les résistances à la compression de tous les matériaux de remblayage combinés étudiés augmentent avec le temps de durcissement.

5.3 Introduction

A new innovative method named the method SMD (Lopez-Pacheco, A. 2019) has been proposed and used for mining recently. The SMD method is based on a two-pass drilling procedure. Primary holes, drilled in the intact rock, need to be backfilled. With the expansion of the mining scale, the potential danger caused by the goafs has become a

serious problem. Meanwhile, the tailings discharged from the mines increase annually. In traditional methods, the tailings were directly discharged in the nearby tailings pond by most mining operations. A report by the United Nations Environment Program (UNEP), Canada has more mine tailings than most other countries in the world. The capacity of the tailings pond had difficulty meeting the requirements of expanding production in the future, and the discharged tailings caused many environmental issues, such as water pollution, land-slides, leaching and dust. The mining industry has been under increasing pressure to develop waste management practices, which has resulted in a greater focus on the role of backfill in waste disposal. With the development of backfill technology, the tailings have become the main materials used as backfilling materials to fill the underground goafs. Mine backfilling has many environmental and operational benefits for the mining industry. It provides an environmentally friendly material for backfill and surface disposal by utilizing the tailings. Backfilling with tailings will reduce the tailings pond accumulation on land, and the costs associated with constructing and reclaiming tailings ponds during mining are also reduced. Therefore, backfilling can not only solve the safety and environmental issues caused by mine production and tailings discharge but also maximize the recovery of resources, which is of great significance for the development of SMD.

Gradually, backfilling has attracted more attention, and the percentage of tailings being sent underground has increased. In order to extract a very small portion of ore, a huge amount of waste material needs to be removed from the ground. Also, a great fraction of tailings will be produced after ore processing. The three main types of backfill include hydraulic fill, paste fill, and rock fill. The difficulty of adapting to the environmental

applications and the cost stresses of tailings management led to paste fill method being created as an alternative to rock fill and hydraulic fill. Since the introduction of paste fill in the late 1970s, the use of paste filling has been limited. However, significant advances in paste technology have been made in the past decades, resulting in further achievements of paste backfill systems. In order to meet the strength requirements for ground support, a small amount of binder (Portland cement) is generally added to the backfill material. Because of several environmental and operational advantages, paste fill has become increasingly popular in the past few years (Landriault, 1995; Brackebusch, 1994). The paste fills can obtain a similar strength of rock fills by using less cement than hydraulic fills. It utilizes different size distribution of tailings and consists of high solid contents, resulting in the reduction of surface tailings impoundment requirements. Whereas rock fills and hydraulic fills use less solid content or larger size distribution of tailings. Furthermore, the decant water from paste fills can be virtually eliminated, which lowers costs and reduces associated problems with barricade set-up. The existing bore-hole delivery systems of slurry fills can also be applied to the paste fills delivery.

Currently, the technology of CPB is implemented in many modern mines around the world, especially in Canada (Grice, 1998). CPB is an engineered mixture of wet fine process tailings (75–85% solids by weight), a hydraulic binder (3–7% by dry total paste weight) and mixing water to set the paste solids density of 70–80% at the desired consistency. Binders used within paste backfill aim to produce mechanical strength (Kesimal et al. 2005). Typically, one or two types of cement, such as regular Portland cement, sulphate-resistant cement, ground granulated blast furnace slag (fine-grained smelter slag), and

strong pulverized fly ash are mixed with the tailings as hydraulic binders, to bind the tailings particles and increase the strength of the CPB. If the mixture can give 18-25 cm of slump height, the CPB is ready to transport as a backfill to the underground voids (Helms, 1988; Brackebusch, 1994; Benzaazoua et al., 1999; Yilmaz et al., 2014). The tailings contain very fine, fine, and course proportion grains, some of which are acid generators (reactive), while the rest are non-reactive. Coarse grains are used by many companies for backfilling purposes, while the fine grains must be disposed of on the surface in a tailings pond. However, by utilizing the cemented paste fill method, fine grains (10–30% by weight finer than 45 microns) are used to make paste fill materials (Brummer and Moss, 1991).

Fly ash is a very fine powder composed of spherical particles of less than 50 microns in size and is one of the most widely used pozzolans in the construction industry. Fly ash can be used as a mixture of cement or concrete due to its pozzolanic activity. Under normal temperature, when Portland cement is mixed with water, most of the cement forms insoluble cementitious compounds, and CaOH is also formed in this reaction. After adding the fly ash, it will react with CaOH and produce hydrate with hydraulic cementitious ability. The pozzolanic reaction consumes calcium hydroxide and produces calcium silicate hydrate. Generally, fly ash are categorized by two types: fly ash Class C and fly ash Class F. Class C fly ash typically made from the combustion of younger lignite or subbituminous coal while class F fly ash produced from the burning of harder bituminous coal and older anthracite. In contrast to Class F, self-cementing Class C fly ash does not need an activator.Fly ash can optimize many concrete properties, such as improving

workability and stabilization, flexural and compressive strengths, pumpability, and decreasing permeability when a proper amount is adopted (Thomas, M et al. 1999).

The main purpose of this study is to evaluate the influence of binder dosage, binder composition and curing time on the strength of backfill materials. This paper studied two recipes of backfill materials, 100% Portland cement, and a combination of 80% Portland cement with 20% fly ash. The curing time of the backfilling materials varied from 7 days, 14 days and 28 days after the specimens casting. The tests, including particle size distribution analysis (PSD), and UCS tests were conducted to measure the different parameters. All the performed tests in this study were based on the American Society for Testing and Materials (ASTM) standards.

5.4 Method

One of the essential tasks of the post-mining process is called mine backfilling. Backfill is made by soil, overburden, mine tailing or any kind of aggregate which can be imported as a filler and booster to emplace in the extracted area, which was excavated by mining operations.

There are multiple backfilling methods, and the two most popular types are hydraulic fill and paste fill. Backfill material is categorized as hydraulic fill, paste fill, and rock fill. In order to increase the strength of the backfill material, a small amount of binder (Portland cement) is usually added to the mixture. For designing back-fill and barricades, there are strict rules applied within the procedure of the backfill process. Progressively, hydraulic

backfill is being replaced by CPB wherever strength is needed from backfill or a waste product contain a better quantity of very fine particles.

An extensive amount of tailings and waste rock are produced in Canada annually. The tailings contain very fine, fine, and course proportion grains, some of which are acid generators (reactive), and the rest are non-reactive. Coarse grains are used by many companies for backfilling purposes, while the fine grains must be disposed of on the surface in a tailing pond. However, by utilizing the paste fill method, which is relatively recent, fine grains (10–30% by weight finer than 45 microns) are used to make paste fill materials.

CPB is made by mixing waste tailings, cement, and water. It is a non-homogenous material that contains between 70% and 85% solids, and the utilized water can be either clean water or mine processed water. Usually, a hydraulic binder is added to the mixture to increase the strength of the CPB. The binder fraction is mostly between 3–7% of the total weight. In the mining industry, CPB is improving and expanding every day because it helps to manage the waste tailing in an economical method (Brackebusch, 1994). On the other hand, it provides safety and support for mine and mine workers in the underground. Additionally, CPB develops technology to help solve environmental issues.

5.5 Materials and equipment

5.5.1 Portland cement and fly ash

Portland cement (PC) is the most common type of cement, which is used as a fundamental component of concrete, and it is used in the backfill mixture as a binder to increase the

strength of the backfilling. Considering the high cement and transport cost to the mine site, cement adds high cost to the backfills, even in such small dosages in the order of 2–10%. As a binder, regular type GU Portland cement was used to make specimens in this study. The mines have been trying to replace cement with blended cement, which consists of cement mixed with fly ash and/or slag, with considerable success. A class C fly ash (FA) was used for binder composition with the proportion of 80% PC and 20% FA since the pozzolanic activity of this type FA is 91.3% (Amaratunga, 1992).

5.5.2 Mill tailings and grain size distribution

The Tailings characteristics can be identified by grain (particle) size distribution, which has a great influence on backfill porosity and delivery. The size distribution analysis is based on cumulative function. According to the previous work, the sample tailings were classified by an electric shaker containing 2000, 630, 315, 250, 150, and 75 microns mesh. Figure 26 shows the tailings are well-graded, with 90% of the tailings less than 560-micron, 50% of the tailings less than 350-micron, and 10% of the tailings less than 130-micron. (Someehneshin et al. 2020). The measured bulk density of the waste tailings is 2000 kg/m^3.

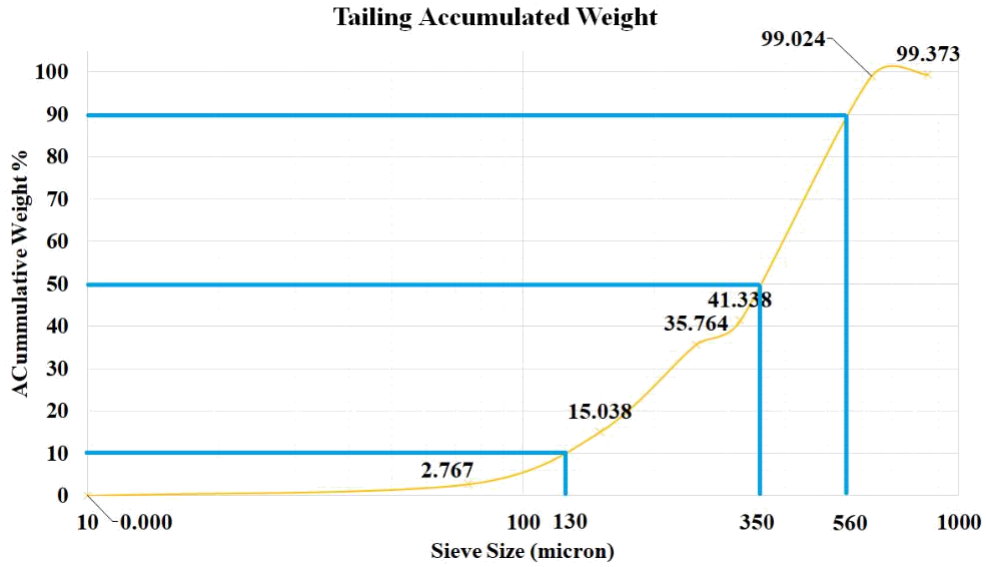

Figure 26-Tailings accumulated weight and grain size distribution

5.5.3 Molds

According to the ASTM Standard C192/C192M-15 and C39/C39M-12, the mixture can be cast in a 2×4 in (5.08 cm by 10.16 cm) molds. The specimen length to diameter ratios is between 2.0:1 and 2.5:1. The molds (kraft tubes) used in the backfill tests were obtained from Uline company. The volume of each mold (2×4 in) is 0.00021 m^3, and the mass of each mold containing backfill is 0.378 kg.

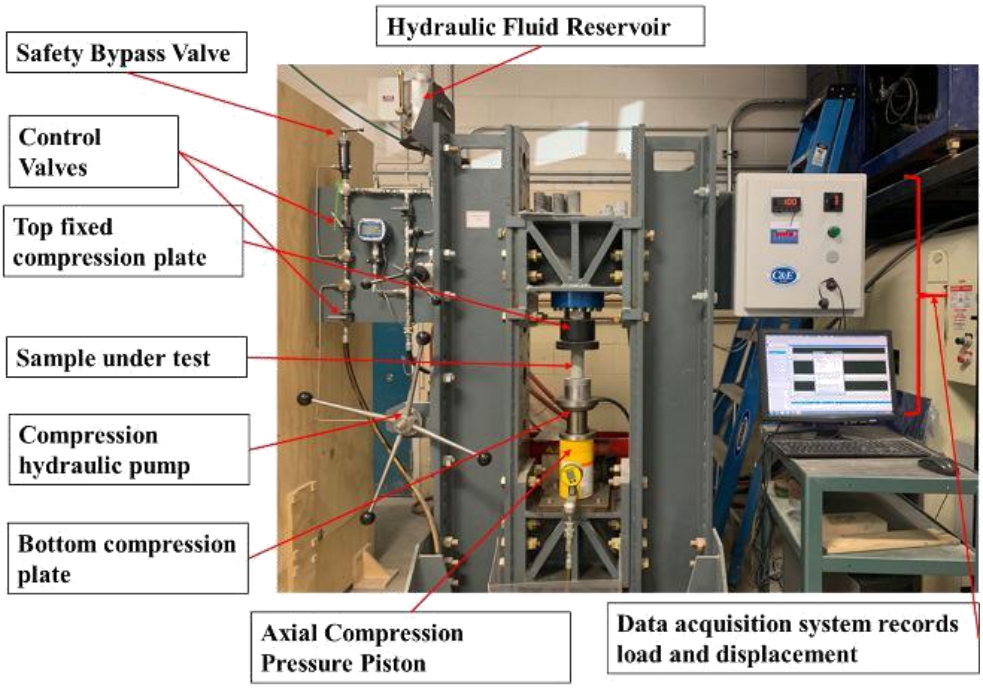

Figure 27-Geomechanical Loading Frame

5.5.4 Geomechanical loading frame

Figure 27 shows the geomechanical loading frame used for UCS measurement. The frame is equipped with Data Acquisition System (DAQ-Sys) that records the main parameters required for constructing stress-strain relationships, including load in Kilo Newton and displacement in millimeters. The DAQ-Sys utilizes LabVIEW software that records at 100 Hz sampling rate for these tests. The compression hydraulic pump is manually operated; however, a fixed loading rate was maintained in all tests. The tests of the same sample types, percentage, parameters, and under the same conditions are repeated at least three times and the strength was estimated based on the average.

5.6 Experimental details

5.6.1 Backfill preparation

The tailings were mixed with Portland cement to give a homogeneous mixture before adding the water. After the addition of water, the mixture was stirred for about 5 minutes before preparing sample specimens. After blending, the mixture was removed to the casting molds. By using a tamping rod, molds would be tamped to reduce the bubbles in the backfill specimens and covered by plastic bags to prevent the evaporation of water. According to ASTM standard C192/C192M-15, the curing temperature is 23±2˚ C. After 24 hours, the specimens were removed from the molds and were kept in the moisture room until the test dates. In order to investigate the influence of binder composition on the strength development of backfill, another group of backfill specimens, which contained Portland cement and fly ash as a binder, were cast following the same procedures. Typically, according to ASTM standard C 1157, three standard samples should be used to do the UCS test after curing periods of 7, 14, and 28 days. In order to observe the development of backfill compressive strength, additional UCS tests were conducted on 21 days with all binder compositions consisting of Portland cement + fly ash. A total of 72 backfill specimens were produced for the tests.

The binder dosages were expressed as a percentage of the total mass of feed materials. Extra 10% of total weight was added to the calculated amount of the backfilling. Table 5gives the dosages of all components without fly ash. Table 6 shows the dosages of all components with fly ash.

Table 5 Cement, tailings, and water percentage

Binder (%)	6%	8%	10%
Mass of tailings (%)	75.2%	73.6%	72%
Mass of cement (%)	4.8%	6.4%	8%
Mass of water (%)	20%	20%	20%

Table 6 Cement, tailings, and water percentage

Binder (%)	6%	8%	10%
Mass of tailings (%)	75.2%	73.6%	72%
Mass of cement (%)	3.8%	5.1%	6.4%
Mass of fly ash (%)	1%	1.3%	1.6%
Mass of water (%)	20%	20%	20%

5.6.2 Backfill testing

One of the most important backfill properties is the UCS. UCS can evaluate the structural stability of the backfill and concretes against static loads. The UCS is the maximum axial compressive stress that a backfill or a concrete specimen can tolerate under zero confining stress. UCS value represents the uniaxial loading capacity of a material. After scheduled timekeeping specimens in the moisture room, both surfaces of each specimen were grinded using a grinding machine to have a smooth and flat surface. Then, a caliper was used to measure the length and diameter of the specimens. All specimens had the same length and

were broken under a constant axial load by a loading frame. The displacement and the load were measured through a LabVIEW software connected to the loading frame (Figure 27). The UCS tests of all backfill specimens, based on ASTM C39/C39M-12, were conducted. The UCS of the backfill samples at different binder dosages, binder compositions and curing time (7, 14 and 28 days) were evaluated.

During the UCS tests, the backfill specimens started failure with small vertical cracks and gradually extended their lengths through the samples. The failure of samples was slow to progress, and most of the fractures on the specimens had a well-formed cone on both ends. Figure 28 (A, B, and C) shows a portion of samples while in the moisture room, one set of samples containing 8% and 10% of cement before and after testing, respectively. This procedure of testing was performed for all samples of cement and fly ash content following the order in Tables 5 and 6.

5.7 Results and discussion

This section analyzes the recorded data, and the stress-strain graph for each specimen was plotted. Each compressive strength value presents an average value obtained from three UCS tests. The maximum peak of the stress-strain graph before failure shows the UCS of the specimen and the slope of the linear part of the graph is the Young's Modulus.

5.7.1 Effect of binder dosage on UCS

Figure 29 shows that the strength of backfill developed with the increasing curing time under all binder combinations. Expediting the mining process is one of the key benefits of achieving high backfill strength over a short curing time. The strengths of the backfill are relatively low when the dosage of Portland cement is 6%-8%. However, the strengths of backfill perform a notable increase when the dosage of Portland cement reaches 8%.

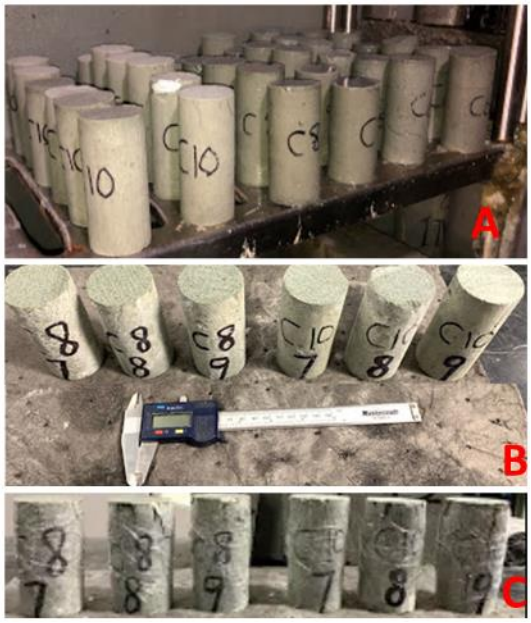

Figure 28-A) Samples while in the moisture room, B) and C) one set of samples before testing and after, respectively

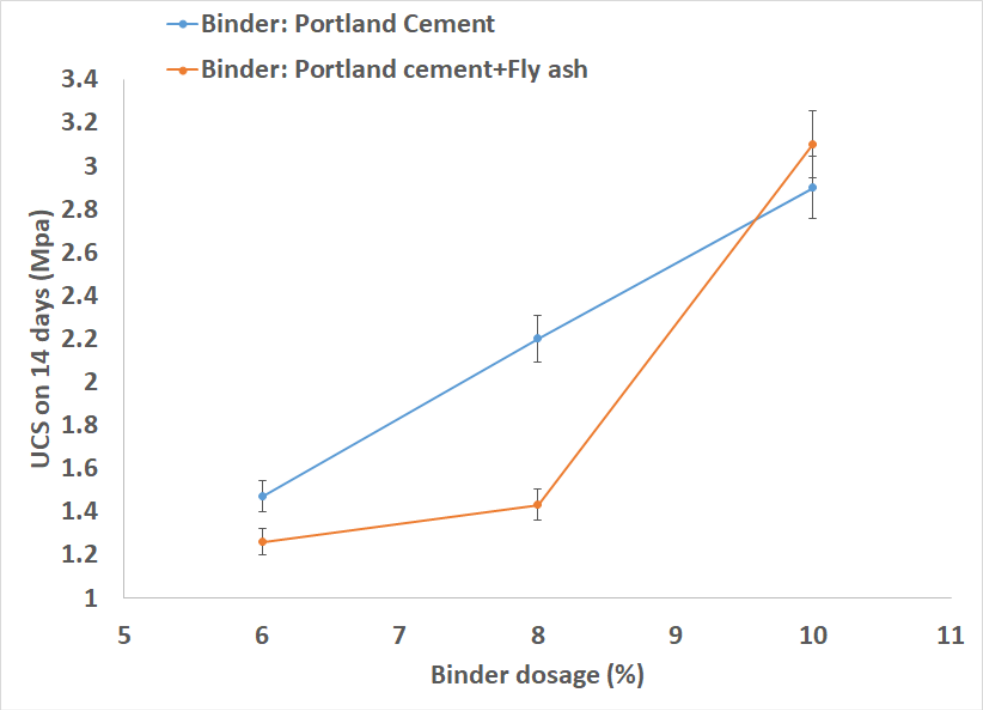

Figure 29-UCS on 14 days versus binder dosage

5.7.2 Effect of binder composition on UCS

Adding a quantity of fly ash into Portland cement instead of pure Portland cement to evaluate the influence of binder composition on UCS is one of the major aims in this paper. Binder composition gives a significant performance on the backfill compressive strength development. Figures 30 and 31 illustrate the short-term strength development of backfill specimens with the addition of fly ash (20% wt. of binder). The sample specimens with the two binder compositions (Portland cement 6%+fly ash and Portland cement 8%+fly ash) show a corresponding 14.8% and 7.7% drop respectively in UCS over the first 7 days. However, after 28 days of curing, an increasing trend in the strength development of the

specimens can be noted obviously. The specimens have obtained about 37.5% and 16.1% strength increase compared with the specimens consisting of pure Portland cement, which illustrates the pozzolanic reaction from the hydration of fly ash and Portland cement.

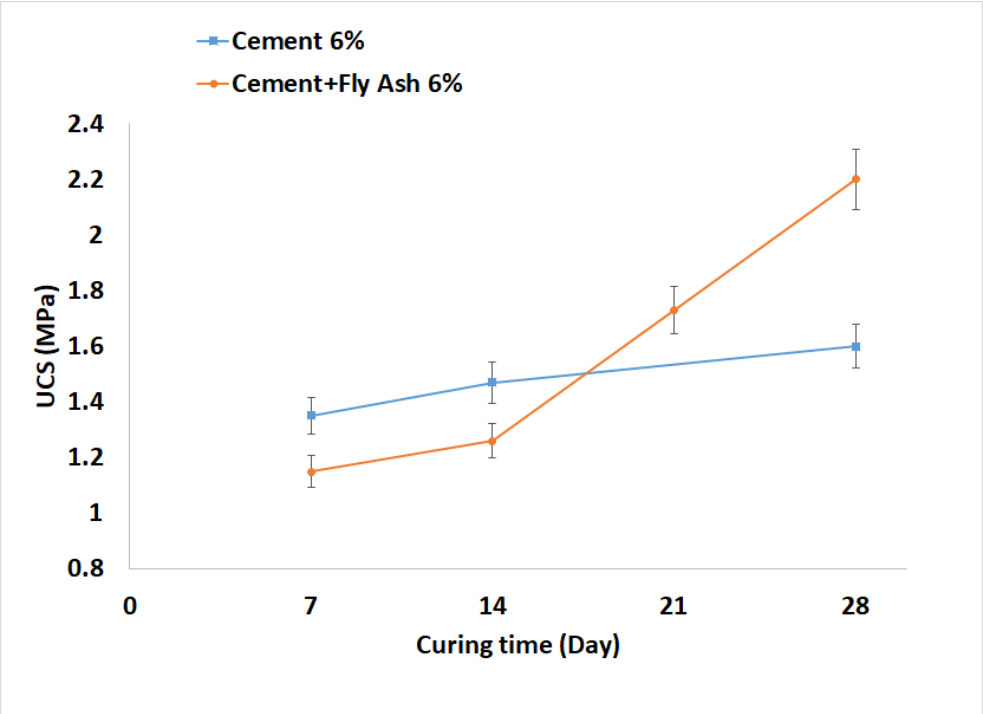

Figure 30-UCS of Cement 6% vs. Cement 6%+ Fly Ash

5.7.3 Effect of curing time on UCS

The effect of curing time with different binder dosages and binder compositions are shown in Figure 32 and 33. From 7 days to 28 days, the strengths for all specimens increase with curing time. It can be observed that the increasing rate from 7days to 14 days is higher than the rate from 14 days to 28 days. The nearly completed hydration of cement around 28 days may account for this performance. Klein and Simon (2006) reported that the shear

velocity of 5% CPB increases with curing time up to 600 h, which means that the 5% cement completed hydration after 600h (25 days) of curing. Ercikdi (2009) states that the UCS of CPB with low cement dosage (5%) keeps constant after 30 days, while the strength of CPB with high cement dosage (7%) keeps increasing till 60 days. Therefore, the strength does not increase, notably after the 28-day curing time.

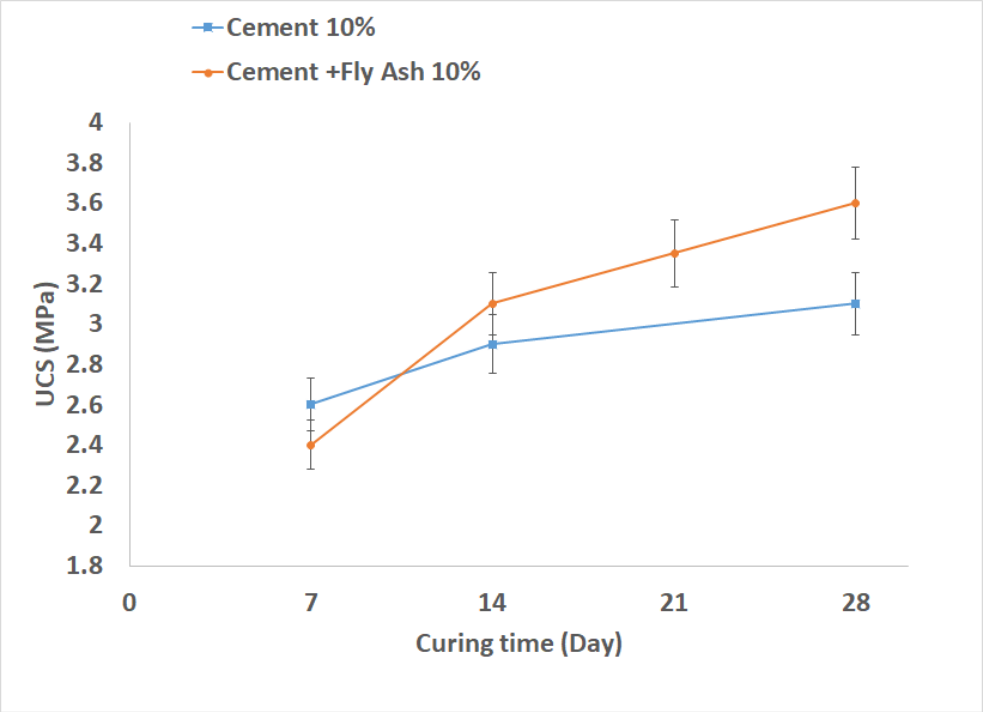

Figure 31-UCS of Cement 10% vs. Cement 10%+ Fly Ash

5.7.4 The stiffness of backfilling materials

Young's modulus E is obtained from an initial linear portion of the stress-strain graphs of backfill specimens and is the sample's resistance against being compressed by uniaxial stress. Young's modulus is the ratio of stress to strain within the elastic region of the stress-

strain curve. It is a measure of the stiffness of a material and is also known as the elastic modulus. Young's Modulus can measure the stiffness of the specimens:

$$E = \frac{\sigma_e}{\varepsilon_e} \qquad (5.1)$$

where:

σ_e is the axial stress and ε_e is the axial strain.

Figures 34 and 35 show the increasing trend of Young's modulus for the backfill specimens with different cement dosages and compositions. It can be found that Young's modulus values of these specimens also follow the same trend as the development of compressive strength.

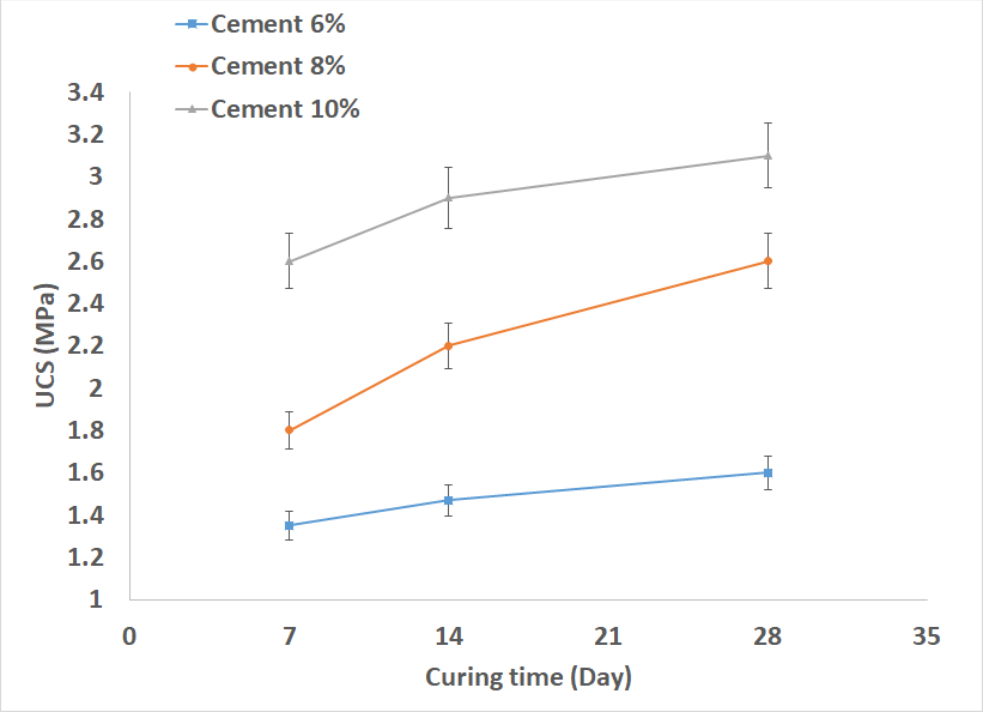

Figure 32-UCS development of Portland cement specimens versus curing time

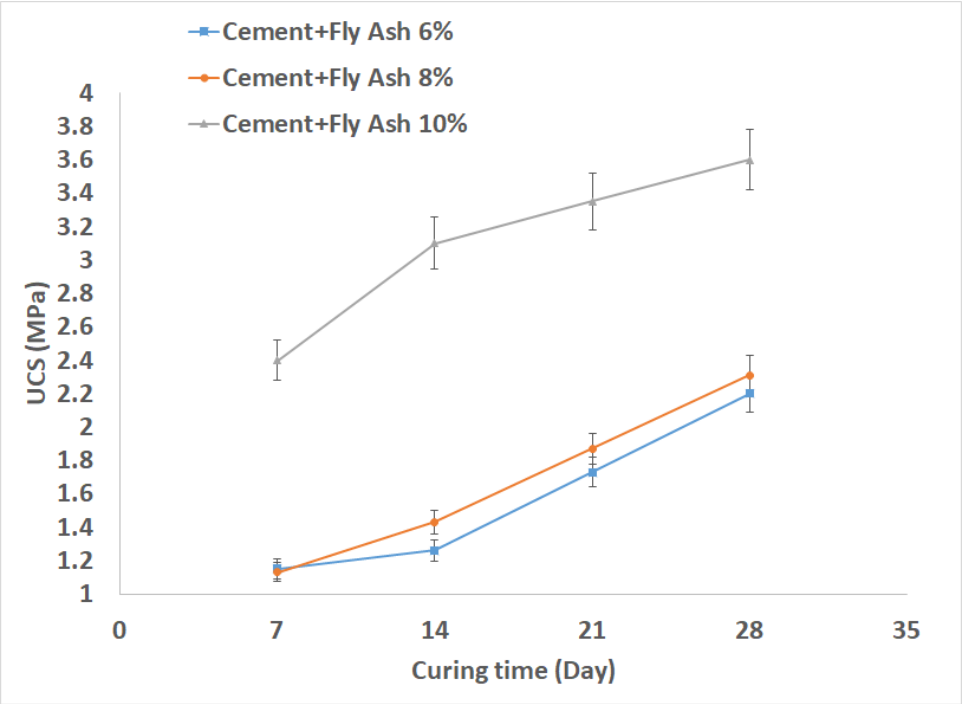

Figure 33-UCS development of binder composition versus curing time

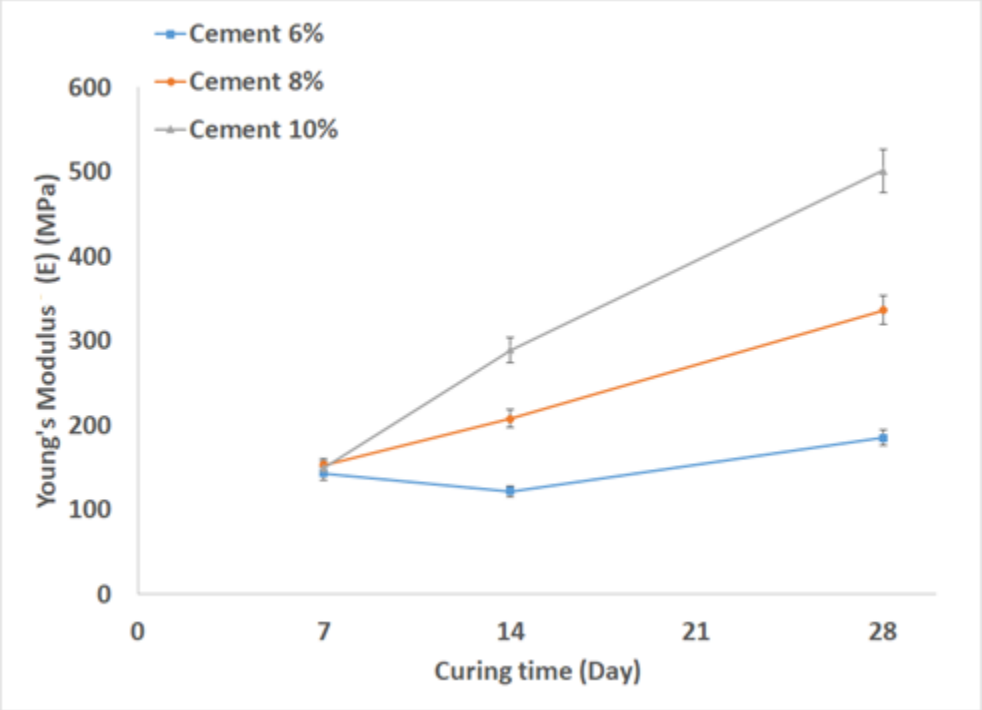

Figure 34-Young's modulus of specimens with only cement

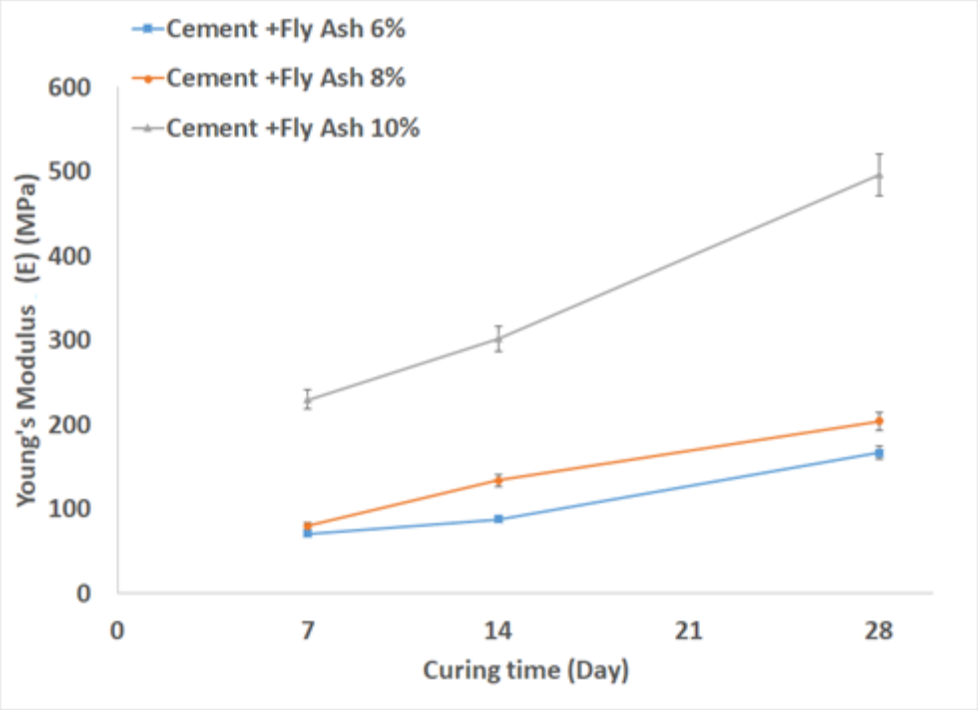

Figure 35-Young's modulus of specimens with cement and fly ash

5.8 Summary and conclusions

In this study, the CPB method was used to prepare the backfill materials based on three main components (tailings, binder, and water). Backfill materials with three different binder dosages and two different binder compositions were prepared to investigate the UCS of the backfilling during the curing time at 7 days, 14 days, and 28 days. From the results, the UCS and stiffness of backfill material increased with the increasing binder dosages. Mixing with fly ash, the backfill material performs with a notable increase in compressive strength and stiffness. For the short-term curing times, the compressive strengths for all studied combination backfill materials increased with curing time. However, increasing the rate of compressive strength decreases with the finished hydration of cement. There is no

typical recipe for all backfill materials. Each type of backfill material is based on laboratory optimization. The characteristics of the three main components play a significant part in the compressive strength development and must be carefully considered in the backfill's design.

Chapter 06: Wellbore Stability of Highly Deviated Well Intervals for Large Diameter Boreholes

Javad Someehneshin[a], Zijian Li[a],Weizhou Quan[a], Dr. Abdelsalam Abugharara[a,b] & Dr. Stephen Butt[a]
a: Memorial University of Newfoundland, St. John's, Newfoundland and Labrador, Canada
b: Department of Oil and Gas Engineering - Sebha University, Sebha, Libya
a: Department of Process Engineering – the University of Newfoundland, St. John's, Newfoundland and Labrador, Canada

This chapter is a paper accepted in the Geocalgary 2020 conference and authored by Javad Someehneshin, Zijian Li, Weizhou Quan, Abdelsalam Abugharara & Stephen Butt,. The MEng candidate was involved with the planning and calculation of the experiments, method selection, the data analysis, and the writing of the paper.

6.1 Abstract

In this paper, analytical study and Discrete Element Method (DEM) simulation were conducted to evaluate the wellbore stability of steeply dipping mining utilizing various wellbore failure criteria. Mining site data of surface and subsurface in-situ stress and rock mechanics properties was collected to support the study. The dimensions of the studied wellbore were 100m maximum depth, 1.3m maximum diameter, and 45 degrees inclination. The wellbore rock failure was analyzed, and the critical wellbore pressure after drilling in four essential azimuths (i.e. 0˚, 90˚, 180˚, and 270˚) using pure water was

calculated. The results of the individual and the analytical-DEM coupled study demonstrated wellbore stability.

6.2 RÉSUMÉ

Dans cet article, une étude analytique et une simulation de la méthode des éléments discrets (DEM) ont été menées pour évaluer la stabilité des puits de forage à forte inclinaison en utilisant divers critères de défaillance des puits de forage. Des données sur le site minier des propriétés in situ et des contraintes in situ et de mécanique des roches ont été recueillies à l'appui de l'étude. Les dimensions du puits de forage étudié étaient de 100 m de profondeur maximum, 1,3 m de diamètre maximum, 45 degrés d'inclinaison. La rupture de la roche de forage a été analysée, la pression critique de forage après le forage dans quatre azimuts essentiels (c.-à-d. 0˚, 90˚, 180˚, et 270˚) en utilisant de l'eau pure a été calculée. Les résultats de l'individu et de l'étude couplée à l'analyse DEM ont approuvé la stabilité du puits de forage.

6.3 Introduction

The conventional development of steeply dipping narrow vein ore bodies (SDNVOB) is always a challenge due to extensive costs, high environmental impacts, and higher risk exposure. As an efficient alternative, the drilling method is introduced to overcome such challenges. In this concept, the SDNVOB will be crushed and transported to the surface in the process of directional drilling. The stability of the wellbores during and after drilling is

critical for the safety of the HW in highly deviated intervals of narrow vein mining and, therefore, requires intensive analysis to be maintained. In the mining industry, the occurrence of wellbore stability problems are frequent, leading to increasing drilling costs and overall non-operational time.

To ensure the wellbore stability, several factors must be considered, including rock mechanical properties, wellbore trajectory, pore pressure, drilling fluid and pore fluid chemicals, temperature, time, mud weight and principal far-field stresses. Moreover, the wellbore formation bedding and natural fracture discontinuities and spacings, as well as the influx of the drilling mud into these fractures, could initiate instability in rock masses. (Aoki et al., 1994; Chen et al., 1998; Last et al., 1995; Okland and Cook, 1998).The borehole diameter is another main parameter that affects the stability of the wellbore. According to the wellbore stability definition, as long as the wellbore and the drill bit have the same diameter, and the drill bit keeps its shape constant, the well will be stable. Zhou et al. (1996) studied the deviated wellbore based on principal horizontal stress and reported that an inclined wellbore could be more stable than a vertical one when $\sigma_v > \sigma_H, \sigma_h$ (extensional stress regime).

Recently, energy demand is increasing intensively. Due to the limited amount of ore bodies near-surface, developing mining resources efficiently and rapidly has become an important research topic for drilling engineering. Nowadays, the open stope mining method with a simple structure is widely used. This method grants simple investor operation, high production efficiency, small dilution and low cost. However, the over break and dilution caused by the stope HW will damage the activity and economy of underground mines.

Therefore, the efficiency of open stope mining is generally determined by the capacity with minimal dilution to achieve maximum extraction (Villaescusa, 2004). It is important to predict HW stability precisely and understand its influencing variables to prevent HW instability and support stable stope design. Wellbore stability requires a proper balance between the uncontrollable factors of earth stresses, rock strength, and pore pressure, wellbore fluid pore pressure, wellbore fluid pressure, and mud chemical composition (J.B. Cheatham Jr. 1984).

Several methods have been developed for the study of HW stability. Mathews et al. (1980) proposed a stability graph approach based on the Mathews stability number and the hydraulic radius to estimate HW stability. The stability of the wellbores during and after drilling is critical in narrow vein mining. In particular, the HW must be stable to avoid wall collapse during drilling caused by inclination and the gravity force. The numerical method calculates the stress around the wellbore at different distances and different azimuths; by using a failure criterion, the wellbore stability can be examined.

The support of the HW in inclined wells is fundamental to the operation and safety of the mine site and areas. Bolting is the primary method of support in many modern mines in the USA and Australia. However, in some cases and for several reasons, rock bolts alone may not be sufficient to support the HW, and secondary support must be installed.

Freezing (if there is water) or cement can be used, however, for the majority of the slopes and HWs, the installation of (Mega long bolts) cable bolts is the standard and most effective method of support.

The discrete element method (DEM) simulation is a good method to estimate the stress condition in a wellbore stability study. It has the advantage of monitoring the stress of every particle in the model and therefore provides a more precise result. For the wellbore instability, distributed stress, and rock strength, two major failure modes can be observed, including shear and tensile failures. Shear fractures occur because of wellbore fluid pressure. Tensile fractures occur as a result of the excessive wellbore fluid pressure has applied parallel to the maximum horizontal stress (σ_H max). This paper studies the stresses around the wellbores in different locations and analyzes their impact on the wellbore stability utilizing a numerical analysis and DEM simulation. A failure criterion has also been applied after calculation of the stress around the wellbore to examine the wellbore stability.

6.4 Theoretical method

The underground formation is always under stress situations, mostly because of overburden and tectonic stresses. The stressed, solid material is removed when a well is drilled. During drilling, a concentration of stresses around the wellbore will be induced, which may cause instability in the wellbores. Therefore the borehole will be supported only by the pressure of the mud or fluid in the bore. Since this support is not exactly the same as the extracted rock and in situ formation stresses, a stress redistribution will occur around the well. In this situation, failure may happen as the stress re-distribution might lead to deviatoric stresses higher than formation support. If we consider the wellbore as a cylindrical shape, in order

to examine the stresses in the rock surrounding a borehole, the stresses and strains in cylindrical coordinates need to be expressed. The stresses of any identified point by r, θ, and z coordination are denoted to radial stress (σ_r), tangential stress (σ_θ), axial stress (σ_z), and the shear stress between them are $\tau_{r\theta}$, τ_{rz}, and $\tau_{\theta z}$, respectively.

6.4.1 Well control and in-situ stress

Well control is a procedure in drill planning to prevent unwanted conditions such as kick and wellbore integrity. The kick occurs when the formation fluids enter the wellbore, and the wellbore integrity is the wellbore failure by fracturing. Both kick and well integrity are related to the bottom hole pressure (BHP). When the BHP is less than formation pore pressure, the kick will happen, and when BHP is greater than formation fracture pressure, wellbore fracturing is expected.

In-situ stress is the natural, local stress within a rock mass formation, and it defines the quantity and direction of compression that is being applied to a rock at a specific location. It is a property of rock mass studied by trenchless construction planners in order to assess potential geotechnical challenges. Most in-situ stresses are caused by body forces (gravity).

The pressure of the drilling fluid (Pmud) in the annulus of the wellbore depends on several factors such as hydraulic mud pressure, annular friction pressure (AFP), and dynamic pressure fluctuations (surge pressure & swab pressure). To stabilize the wellbore while drilling, mud pressure must be larger than formation pore pressure and less than formation fracture pressure.

6.4.2 Wellbore wall failure modes

Minimum well pressure (Pw-min) and maximum well pressure (Pw-max) or fracture pressure are two essential parameters that must be measured to study wellbore stability. Pw-min is generally less than pore pressure, and for weak formations and high in-situ stress zone (deep formations), it has a significant role in most drilling design. When the stress distribution around the wellbore is determined, the wellbore stability can be assessed based on a failure criterion. There are two kinds of failure modes in this context. When the bottom hole pressure (BHP) is greater than maximum well pressure, tensile fractures will occur parallel to the maximum horizontal stress σH. If the BHP is less than minimum well pressure, shear fractures or compressive fractures will develop parallel to the minimum horizontal stress σh (FJÆR et al. 2008).

6.4.3 Transformation formulas

The application of transformation formulas can make the evaluation of the stresses around the wellbore easier. The in situ principal stresses define a coordinate system that we denote as (x', y', z') indicated in Figure 36. We take σv to be parallel to z', σH to be parallel to x', and σh to be parallel to y'.

For inclined wellbore, the directions of the wellbore axis and gravity are not parallel. Thus, a second coordinate system (x, y, z) is introduced. In this coordinate system, the z-axis

points along the axis of the hole, the x-axis points towards the lowermost radial direction of the hole, and the y-axis is horizontal (FJÆR et al. 2008).

$$\sigma_r = \frac{\overset{\circ}{\sigma_x} + \overset{\circ}{\sigma_y}}{2}\left(1 - \frac{R_w^2}{r^2}\right) + \frac{\overset{\circ}{\sigma_x} - \overset{\circ}{\sigma_y}}{2}\left(1 + 3\frac{R_w^4}{r^4} - 4\frac{R_w^2}{r^2}\right)\cos 2\theta$$
$$+\overset{\circ}{\tau_{xy}}\left(1 + 3\frac{R_w^4}{r^4} - 4\frac{R_w^2}{r^2}\right)\sin 2\theta + p_w\frac{R_w^2}{r^2} \qquad (6.1)$$

$$\sigma_\theta = \frac{\overset{\circ}{\sigma_x} + \overset{\circ}{\sigma_y}}{2}\left(1 + \frac{R_w^2}{r^2}\right) - \frac{\overset{\circ}{\sigma_x} - \overset{\circ}{\sigma_y}}{2}\left(1 + 3\frac{R_w^4}{r^4}\right)\cos 2\theta$$
$$-\overset{\circ}{\tau_{xy}}\left(1 + 3\frac{R_w^4}{r^4}\right)\sin 2\theta - p_w\frac{R_w^2}{r^2} \qquad (6.2)$$

$$\sigma_z = \overset{\circ}{\sigma_z} - \nu_{fr}\left[2\left(\overset{\circ}{\sigma_x} - \overset{\circ}{\sigma_y}\right)\frac{R_w^2}{r^2}\cos 2\theta + 4\overset{\circ}{\tau_{xy}}\frac{R_w^2}{r^2}\sin 2\theta\right] \qquad (6.3)$$

$$\tau_{r\theta} = \frac{\overset{\circ}{\sigma_y} - \overset{\circ}{\sigma_x}}{2}\left(1 - 3\frac{R_w^4}{r^4} + 2\frac{R_w^2}{r^2}\right)\sin 2\theta + \overset{\circ}{\tau_{xy}}\left(1 - 3\frac{R_w^4}{r^4} + 2\frac{R_w^2}{r^2}\right)\cos 2\theta \qquad (6.4)$$

$$\tau_{\theta z} = \left(-\overset{\circ}{\tau_{xz}}\sin\theta + \overset{\circ}{\tau_{yz}}\cos\theta\right)\left(1 + \frac{R_w^2}{r^2}\right) \qquad (6.5)$$

$$\tau_{rz} = \left(\overset{\circ}{\tau_{xz}}\cos\theta + \overset{\circ}{\tau_{yz}}\sin\theta\right)\left(1 - \frac{R_w^2}{r^2}\right) \qquad (6.6)$$

Where:

$$\overset{\circ}{\sigma_x} = l_{xx'}^2\sigma H + l_{xy'}^2\sigma h + l_{xz'}^2\sigma v \qquad (6.7)$$
$$\overset{\circ}{\sigma_y} = l_{yx'}^2\sigma H + l_{yy'}^2\sigma h + l_{yz'}^2\sigma v \qquad (6.8)$$
$$\overset{\circ}{\sigma_z} = l_{zx'}^2\sigma H + l_{zy'}^2\sigma h + l_{zz'}^2\sigma v \qquad (6.9)$$
$$\overset{\circ}{\tau_{xy}} = l_{xx'}l_{yx'}\sigma H + l_{xy'}l_{yy'}\sigma h + l_{xz'}l_{yz'}\sigma v \qquad (6.10)$$

$$\tau^{\circ}_{yz} = l_{yx}, l_{zx}, \sigma H + l_{yy}, l_{zy}, \sigma h + l_{yz}, l_{zz}, \sigma v \quad (6.11)$$

$$\tau^{\circ}_{zx} = l_{zx}, l_{xx}, \sigma H + l_{zy}, l_{xy}, \sigma h + l_{zz}, l_{xz}, \sigma v \quad (6.12)$$

σ_r is the radial stress; σ_θ is the tangential stress; σ_z is the axial stress, $\tau_{r\theta}$, τ_{rz}, and $\tau_{\theta z}$, are the shear stress between planes, respectively. Rw is the wellbore radius, r is the distance from the wellbore, θ is the inclination angle, and ν_{fr} is the Poisson ratio. σ_v is normal vertical stress, σ_H is maximum horizontal stress, and σ_h is minimum horizontal stress. Lij' is the cosine of the angle between the i-axis and the j'-axis.

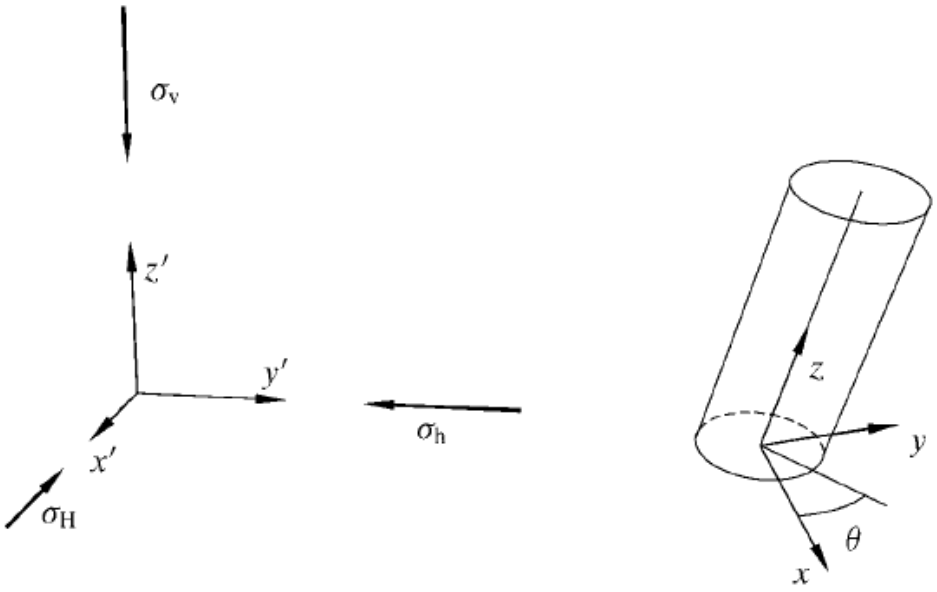

Figure 36-Schematic view of the axis on the wellbore

6.4.4 Critical wellbore pressure

A Closed-form Solution for calculating critical wellbore pressure was conducted. Using the transformed formula that can be found in many references, the in-situ stresses were transformed into the wellbore coordination system. Twenty-three degrees inclination was considered for the wellbore and σ_x, σ_y, σ_{zz}, τ_{xy}, τ_{yz}, and τ_{zx} were calculated, where σ_{zz} is parallel to the direction of the wellbore and σ_x and σ_y act orthogonal to the wellbore direction. The modified Lade criterion is used to calculate the critical wellbore pressure (Pw) that prevents the instability of the wellbores.

$$P\_w = (B - \sqrt{C})/2A \quad (6.13)$$

$$A = \sigma_z + S_1 - P_P \quad (6.14)$$

$$B = A\sigma_{\theta^n} - \tau_{\theta^z}^2 \quad (6.15)$$

$$C = B^2 - 4A\{D - (S_1 - P_P)[A(\sigma_{\theta^n} + S_1 - P_P) - \tau_{\theta^z}]\} \quad (6.16)$$

$$D = (\sigma_{\theta^n} + \sigma_z + 3S_1 - 3P_P)^3/(27 + \eta) \quad (6.17)$$

$$\sigma_{\theta^n} = \sigma_x + \sigma_y - 2(\sigma_x - \sigma_y)cos2\theta - 4\tau_{xy}sin2\theta \quad (6.18)$$

$$\sigma_z = \sigma_{zz} - \mu[2(\sigma_x - \sigma_y)cos2\theta - 4\tau_{xy}sin2\theta] \quad (6.19)$$

$$\tau_{\theta^z} = 2(\tau_{yz}cos\theta - \tau_{zx}sin\theta) \quad (6.20)$$

The critical wellbore pressure must be compensated by mud weight. When the critical wellbore pressure increases, the mud weight must be increased to provide sufficient pressure to the wellbore walls to prevent instability. In this study, the critical wellbore pressure after drilling in four essential azimuths Includes 0, 90, 180, and 270 degrees from the x-axis, was calculated.

Table 7 shows the critical wellbore pressure for this case study in four important azimuths. At the top of the wellbore, the critical wellbore pressure is -9.653, and at the bottom of the wellbore, it is -8.72. It is clear when the critical wellbore pressure is negative, the wellbore is stable, and any mud with the lowest density can be used as drilling fluid.

Table 7 critical wellbore pressure

Azimuth	0	90	180	270
Bottom	-8.72	-8.72	-8.72	-8.72
Top	-9.65	-9.65	-9.65	-9.65

6.5 Case study: Wellbore stability assessment in the target mining zone

In the mining zone, the prospect consists of three quartz veined zones up to 1m to 2m thick, exposed over 300m. The dipping angle varies from 65 to 72 degrees from horizontal. Fine-grained, mafic volcanic, and gabbroic intrusive rocks host the veins. The veins are spatially associated with a north-northeast-trending topographic lineament that continues for several kilometers to the north. Mineralization has been traced for approximately 100m and is open to the east, west, and down dip. For this mining zone, the development plan is to excavate

the vein by sequential borehole drilling mining method. Pure water is planned to be used as mud for the drilling. The drill hole depth could reach 100m. Thus, wellbore stability is of great importance in this project.

6.5.1 Wellbore conditions in the target mining zone

In this study, the target depth of the wellbore is 100m, and the radius of the wellbore (rw) is 0.65m. As the vein has a variable inclination, we studied inclination from 18 to 23 ˚and 45 ˚and the depth from zero (surface) to 100m with a one-meter interval. The stress distribution around the wellbore is studied every 10 ˚from zero to 360 ˚. Several essential distances (R) were selected for the calculation, rw (0.65m), 5rw (3.25m), 10rw (6.5m), and 10m. In general, it is believed that the wellbore has very little influence on the stress distribution further than 5rw (3.25m) away from the wellbore center. Figure 37 shows the different distances from rw to 10m in different colors. Black is the wellbore, brown presents the stresses exactly on the wellbore wall; orange is the stress in 5rw distance, yellow on 10rw and green on 10m distance.

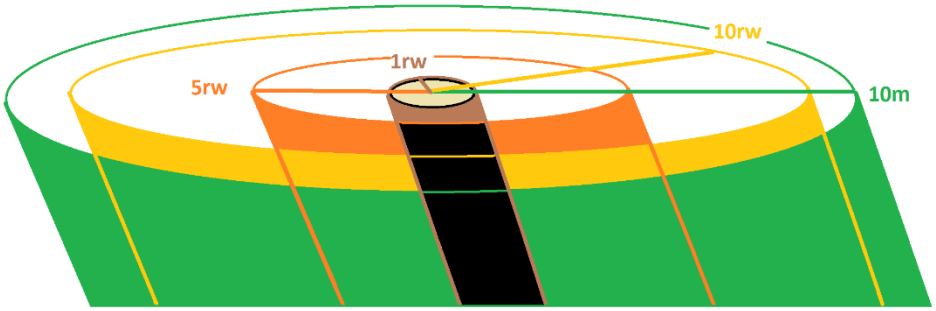

Figure 37-Schematic view of a well and the studied stresses around it on different distance

The results only show the specific 23 degrees inclination at R = rw = 0.65m since the qualitative behavior of stresses for the mentioned inclinations and distances are almost the same.

Each time, the distance (R) is considered constant and by increasing the depth from zero to 100m, σ_r, σ_θ, σ_z, $\tau_{r\theta}$, τ_{rz}, and $\tau_{\theta z}$ are calculated by transformation formulas 6.1 to 6.6 for every 10 degrees around the wellbore. Pw-min and Pw-max from the depth of zero to 100m is calculated. Table 8 shows the input data used to analyze the stress around the well.

Table 8 Geomechanics parameters of the vein used for analyzing stresses

Characteristics	Value	Unit
Rock density	2480	Kg/m^3
UCS of the rock	94	MPa
Poisson ratio	0.25	Unit less
Internal friction angle	55	degree
Cohesion	15	MPa

6.5.2 Joint and GSI (geological strength index) of the host rock

Figure 38 shows the blocky host rock, which is a mafic rock with a good quality surface area. Table 9 summarizes more information such as RQD, and GSI of the host rock.

Table 9 Rock mass characteristic of the host rock

Joint set	1	2
Average Specing	42.75cm	16.2cm
Ja	3	3
Jr	1.5	1.5
Jv	8.5	
RQD	88.7	
GSI	61.6	
Mi (for Quartzite)*	20	

* Marinos, P., and Hoek, H., GSI: A GEOLOGICALLY FRIENDLY TOOL FOR ROCK MASS STRENGTH ESTIMATION (Paul Marinos, Evert Hoek, et al. 2000)

6.6 Numerical results

6.6.1 Pw-min versus Pw-max

Figure 39 shows the minimum well pressure (Pw-min) and maximum well pressure (Pw-max) versus depth. The upper line is the Pw-max, and the lower line is the Pw-min. As expressed before, if the stresses around the wellbore are between these two lines, the wellbore will be stable. If the pressure is beyond this range, the well will fail. In the next step, radial, tangential, axial, and shear stresses surrounding the hole are calculated. If these stresses are higher than minimum well pressure and lower than maximum well pressure, the well is stable.

Figure 38-The host rock of the case study

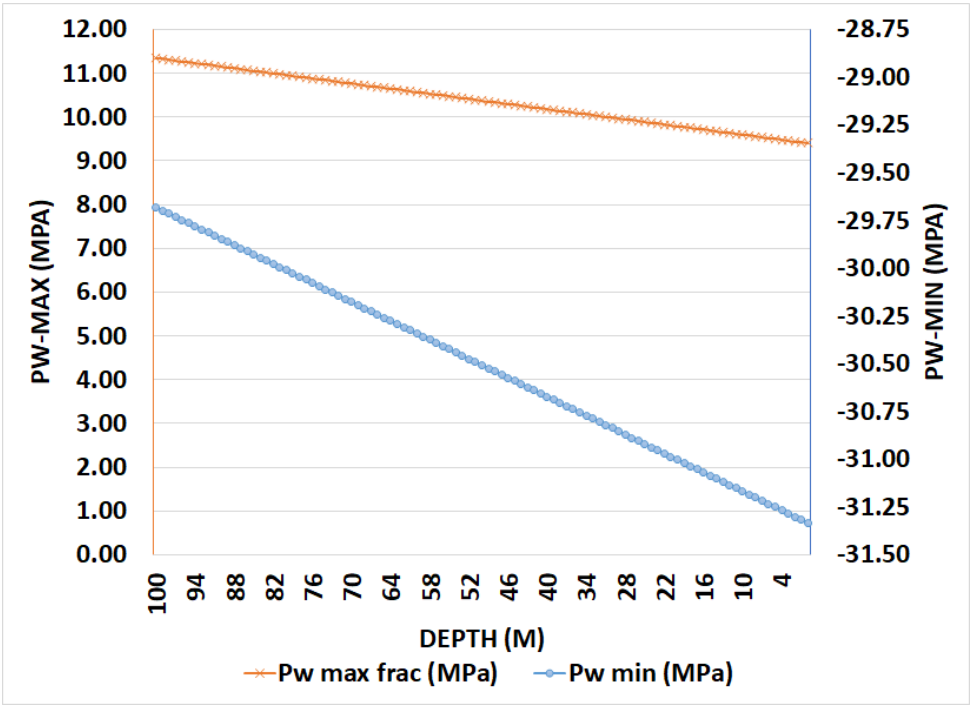

Figure 39-Comparison of the minimum well pressure (Pw-min) and maximum well pressure (Pw-max) as a function of depth

6.6.2 Failure criterion

Mohr-Coulomb and Drucker Prager criterion is the most famous failure criteria used for analyzing wellbore stability. However, they do not consider the effect of intermediate principal stress on rock strength. Modified Lade criterion can provide a closed-form solution for critical wellbore pressure and, consequently, the critical mud weight. It also reflects the influence of intermediate principal stress. In this paper, the Mohr-Coulomb, Ducker Parger (Inner circle, Middle circle, and outer circle), the Modified Lade criterion, and the Modified Hoek and Brown are analyzed. The summary of the failure criterion can be found in the results section. However, the Modified Hoek and Brown failure criterion will be discussed in detail.

6.6.3 Modified Hoek and Brown criterion

Hoek and Brown 1980 developed a failure criterion to estimate jointed rock mass strength. The limitations were derived in 1983 using laboratory triaxial tests on samples of intact rocks. The modified Hoek and Brown criterion was later presented for heavily jointed rock masses.

The GSI was developed by Hoek 1994 and Hoek et al. 1995. In order to link engineering geology observations in the field and the Modified Hoek & Brown criterion. GSI is the rock mass characterization system based on the structure and the condition of the joints.

$$\sigma 1 = \sigma 3 + \sigma ci\ (mb\ \ \sigma 3/\sigma ci\ \ + s)\hat{}a \quad (6.21)$$

$$mb = mi\ \ \exp[(GSI - 100)/(28 - 14D)] \quad (6.22)$$

$$s = \exp[(GSI - 100)/(9 - 3D)] \quad (6.23)$$

$$a = 1/2 + 1/6(e\hat{}(-GSI/15) - e\hat{}(-20/3)) \quad (6.24)$$

Where σ1 and σ3 are the major and minor principal stresses, respectively, σci is the UCS, and mi is a material constant for the intact rock. D is a factor that represents the disturbance degree used for damage by blasting, and for this study, it is considered as zero since the wells are drilled, and no explosives material were used.

6.6.4 Failure criterion results

For all of the mentioned failure criteria, there is a failure index formula that uses principal stress, internal friction angle, pore pressure, and cohesion to evaluate the stability of the wellbore. If the failure index is less than zero (FI<0), then the wellbore fails. The equations are not presented in this paper as they can be found in many references.

The failure index of all failure criteria such as Mohr-Coulomb, Ducker-Prager, Modified Lade, and modified Hoek-Brown criterion was calculated from the top to the bottom of the wellbore at every one-meter intervals. All indicate that the FI is greater than Zero (FI>0), and the wellbore is stable from the surface to the bottom of the well. Table 10 summarizes

the FI for different failure criteria. Note that the bottom of the well shows a greater FI than the top of the well, and this is due to the horizontal stresses that act as confining compressive stress (CCS). By increasing the depth, the magnitude of the horizontal stresses would increase, and consequently, the CCS will increase.

Table 10 Failure index for different failure criterion

Failure Criterion	FI at the Bottom of the well	FI at the Top of the well
Mohr-Coulomb	100.4	95.15
Ducker-Prager (inner circle)	9.76	9.06
Ducker-Prager (Middle circle)	1.12	0.42
Ducker-Prager (Outer circle	1.99	0.74
Modified Lade	147.28	147.33
Modified Hoek-Brown	29.17	11.01

6.6.5 Stress between P_W-min & P_W-max

Figure 40 shows the radial stress (around the well R = rw = 0.65m), Pw-min and Pw-max. The upper surface is Pw-max, and the lower surface is Pw-min. The radial stress is on the middle surface. Since the range of the stresses in Pw-min and Pw-max is much higher than radial stress, the radial stresses are shown as a small picture on the upper left. It is clear that the radial stress is between Pw-min and Pw-max, and as previously mentioned, the wellbore is stable. Figures 41 to 45 show the tangential stress, axial stress, shear stress of the radial and tangential planes, shear stress of the tangential and axial planes, and shear stress of the radial and axial planes (around the well r=Rw=0.65m), respectively, as well as Pw-min, and Pw-max. The insets on the upper left corner of each figure show the

magnified stresses. The figures imply that the same principals discussed above continue to apply and that the wellbore is stable.

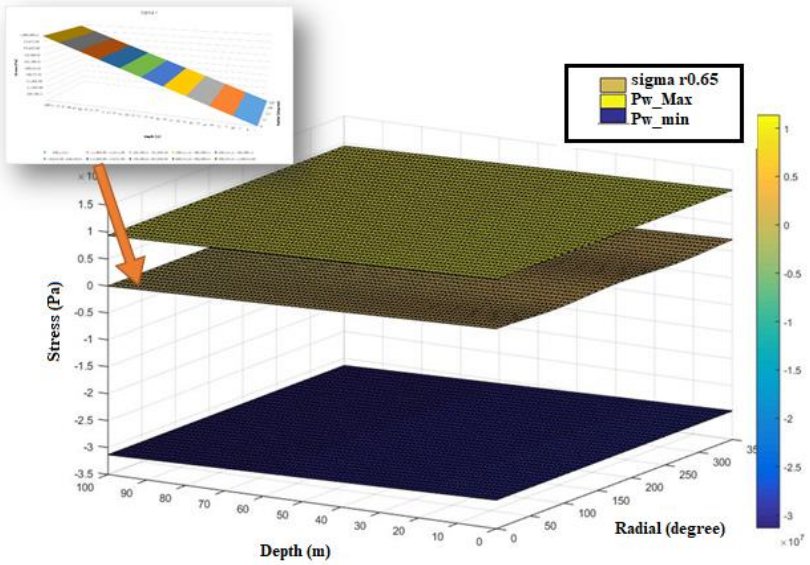

Figure 40-The radial stress (around the well r=Rw=0.65m), Pw-min, and Pw-max

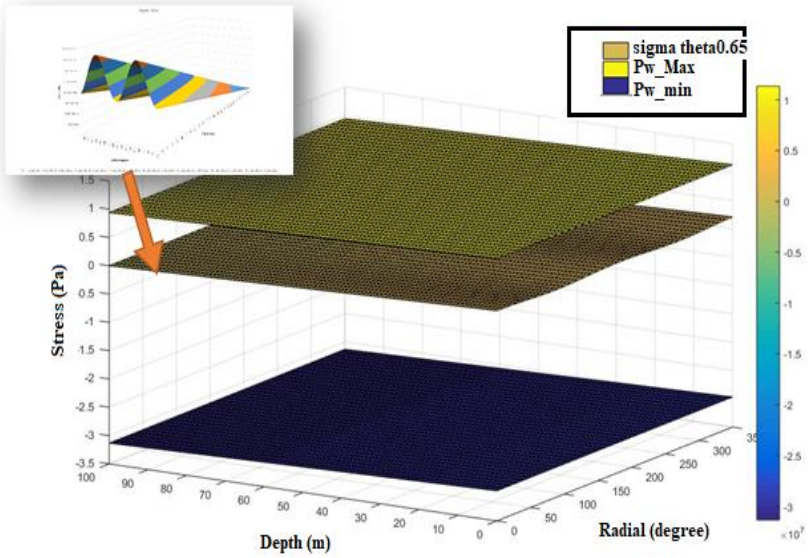

Figure 41-The tangential stress (around the well r=Rw=0.65m) Pw-min, and Pwmax

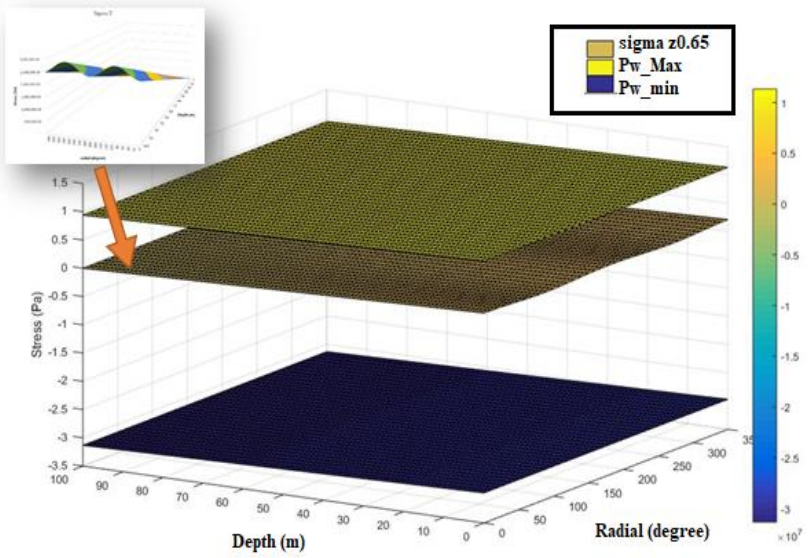

Figure 42-The axial stress (around the well r=Rw=0.65m), Pw-min, and Pw-max

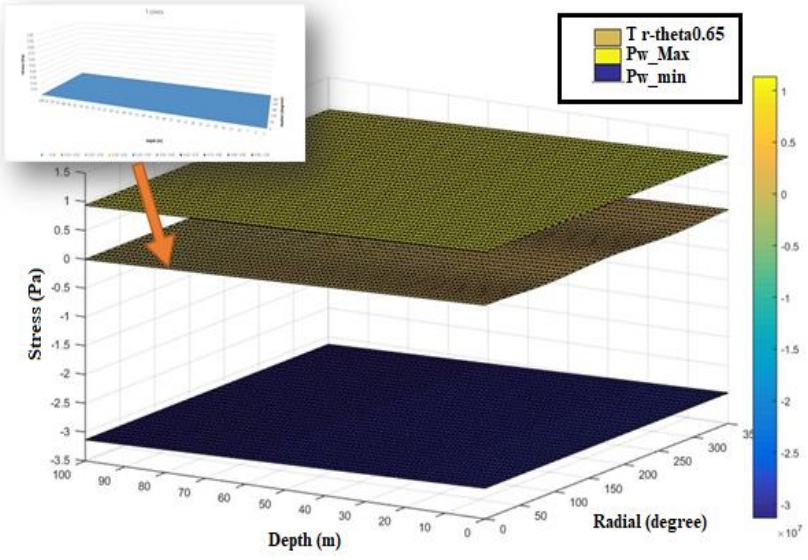

Figure 43-The shear stress of the radial and tangential planes (around the well

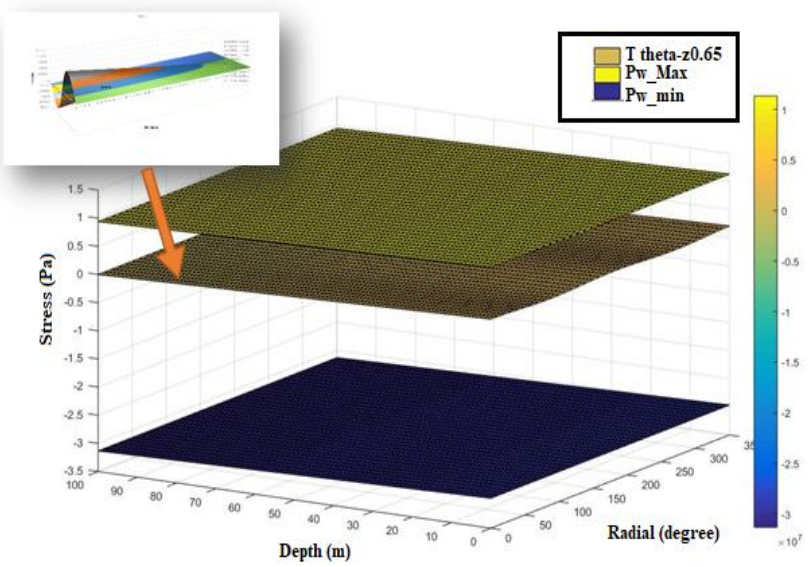

Figure 44-The shear stress of the tangential and axial planes (around the well

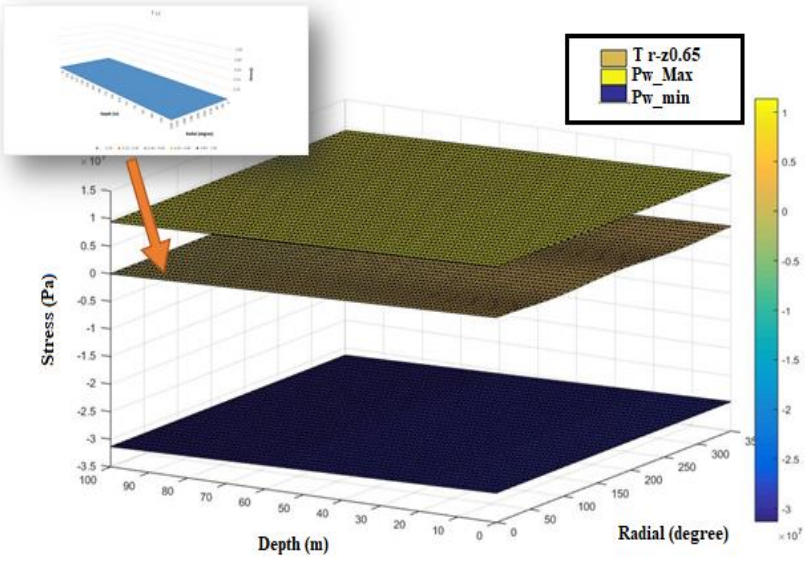

Figure 45-The shear stress of the radial and axial planes (around the well)

6.7 Discrete element method (DEM) simulation of wellbore stability

DEM is a numerical method for calculating the dynamics of discrete elements to obtain the macro property of a target sample. DEM was originally introduced to analyze problems in rock mechanics by Cundall (1971). Today, DEM has been applied in many other fields (Glamheden et al., 2004; Szymakowski, 2004; Konietzky et al., 2004). DEM also has the potential to carry out the wellbore stability analysis because it can trace the dynamics of every particle in the model, in this study, Particle Flow Code 2D (PFC2D) software is used for the DEM simulation.

Before the start of the DEM simulation, a rock model should be created and calibrated. By toning the micro property parameters, the macro property of the rock model should match the rock properties measured in the lab. Then, the rock model is created using the calibrated micro property parameters. After the model generation, the in-situ stresses (maximum and minimum horizontal stresses) are applied to the boundaries of the model. The model reaches the stress equilibrium after running a long time.

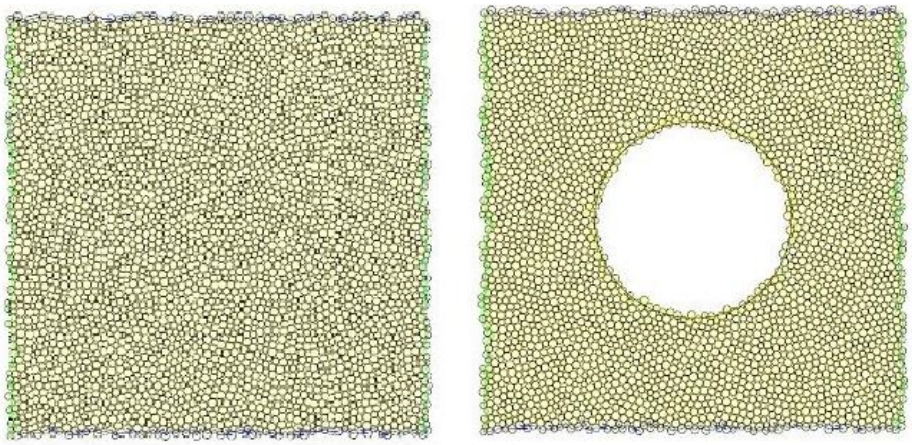

Figure 46-DEM rock model reaches equilibrium with in-situ stress (left) and wellbore drilled in the center (right).

A wellbore is ‘drilled’ in the middle of the model. Mud pressure is applied on the surface of the wellbore. The DEM model is shown in Figure 46. Then, the model starts to run the force-displacement calculation over time. The stress condition of particles at the selected location is monitored and output to the log. The stress distribution at 100m depth and R = rw = 0.65m is presented and compared with the theoretical result. It observed that the average DEM result agrees with the theoretical result. On the other hand, the maximum stresses in the DEM result tend to be higher than the theoretical calculation result. This is because the stress is unevenly distributed in DEM simulations, which is different from the theatrical result. At some point, the stress can be notably higher than the nearby area. The stress concentration is well monitored in DEM simulation. There is no micro fracture observed in the DEM simulation, which suggests that the wellbore is in a safe condition. This result agrees with the theoretical result.

Table 11 Comparison of between theoretical result and DEM simulation result parameters of the vein used for analyzing stresses at 100m depth and R=rw=0.65m

Azimuth (degree)	Radial stress (Theoretical) (MPa)	Radial stress (Maximum value in DEM) (MPa)	Radial stress (Average value in DEM) (MPa)
0	0.05	0.31	0.07
90	0.21	0.79	0.20
180	0.07	0.42	0.08
270	0.23	0.83	0.25
Azimuth (degree)	Tangent stress (Theoretical) (MPa)	Tangent stress (Maximum value in DEM) (MPa)	Tangent stress (Average value in DEM) (MPa)
0	0.08	0.17	0.10
90	0.25	0.32	0.27
180	0.11	0.21	0.09
270	0.28	0.35	0.28

6.8 Conclusions

For a well to be stable during and after drilling, applied, stresses must be studied at different distances. The effective distance is usually considered five times of the well radius. This thesis analyzed the radial stress, tangential stress, axial stress, shear stresses on these planes on the edge of the wellbore, five times of the well radius, ten times of the radius, and ten meters from the wellbore.

Since the inclination of the wellbore understudy is 23 degrees, all stresses mentioned above were studied at 18, 19, 20, 21, 22, 23, and 45 degrees. These stresses were also calculated from surface to 100 m depth at each 1 m depth increment, from wellbore edge to 10 m radial distance, and at each 10 degrees increment from 0 to 360 degrees.

For an efficient drilling process to be applied in steeply dipping mining and optimal stable HWs of wellbores, stresses must be studied at various intervals of depth and radius. For effective radial stress analysis, the distance usually considered is five times the well radius. Moreover, tangential, axial, and shear stresses on planes at the edge of the wellbore involving different scenarios of five times of the well radius, ten times of the radius, and ten meters from the wellbore were determined. The results of the stress analysis by the analytical and DEM methods can be summarized as:

The radial and axial stresses on the edge of the wellbore are linear and will increase by increasing the depth. However, this trend at five times the well radius and more converts to a sinusoidal shape and fluctuate every 90 degrees, while the entire style is a rising trend. The tangential stresses at the wellbore edge, and five times the well radius and more is a

sinusoidal shape and will increase by increasing the depth. This stress also has fluctuations every 90 degrees, but the entire results is a rising trend. The shear stress of the radial and tangential planes is zero on the edge of the wellbore from the surface to 100m depth and all around the wellbore. However, this trend at five times the well radius or more converts to a sinusoidal shape and fluctuate every 90 degrees, while the entire style is a rising trend.

The shear stress of the tangential and axial planes on the edge of the wellbore has one periodic sinusoidal shape. This graph at a zero and 180 degrees has zero value, and at 90 and 270 degrees are its maximum and negative maximum. The shear stress of the radial and axial planes is zero on the edge of the wellbore from the surface to 100m depth and all around the wellbore. However, this trend at five times the well radius or more converts to a curve shape and has a peak at 180 degrees, while the entire style is a rising trend.

The average results of the DEM simulation agreed with the theoretical results. However, the maximum stress near the wellbore obtained by the DEM simulation is higher than that of the theoretical, suggesting that there was a stress concentration phenomenon. In the far-field region from the wellbore center, the stress concentration was decreased.

All failure criteria, the theoretical calculation results, and the DEM simulation result showed that all calculated stresses are between these two surfaces, and the wellbore is stable and safe up to 100m depth.

Chapter 07: Summary and conclusion

Every year, 500 million tonnes of tailings and waste rocks are produced in Canada. Paste backfill consists of mill tailings generated throughout ore dressing that have lost water. The CPB method has been increasingly utilized in mining companies. Using the paste fill method not only provides an efficient way to reduce surface tailings impoundment, which prevents environmental issues, but also improves the safety of ore bodies. The arching effect is considered in this study, which enhances the safety and efficiency of the on-site drilling operation of the vein. In order to minimize backfill failure, freestanding vertical face needs to be calculated, and different methods are suggested. The studied narrow vein has an inclination. Thus the inclined stope is the most suitable method for calculating the freestanding face.

In this study, the CPB method was used to prepare the backfill materials based on three main components (tailings, binder, and water). Backfill materials with three different binder dosages and two different binder compositions were prepared to investigate the UCS of the backfilling during the curing time at 7 days, 14 days, and 28 days. From the results, the UCS and stiffness of backfill material increased with the increasing binder dosages. Mixing with fly ash, the backfill material performs with a notable increase in compressive strength and stiffness. For the short-term curing times, the compressive strengths for all studied combination backfill materials increased with curing time. However, increasing the rate of compressive strength decreases with the finished hydration of cement. There is no typical recipe for all backfill materials. Each type of backfill material is based on laboratory

optimization. The characteristics of the three main components play a significant part in the compressive strength development and must be carefully considered in the backfill's design.

For a well to be stable during and after drilling, applied, stresses must be studied at different distances. The effective distance is usually considered five times of the well radius. This thesis analyzed the radial stress, tangential stress, axial stress, shear stresses on these planes on the edge of the wellbore, five times of the well radius, ten times of the radius, and ten meters from the wellbore.

Since the inclination of the wellbore understudy is 23 degrees, all mentioned stresses were studied at 18, 19, 20, 21, 22, 23, and 45 degrees. These stresses were also calculated from surface to 100 m depth at each 1 m depth increment, from wellbore edge to 10 m radial distance, and at each 10 degrees increment from 0 to 360 degrees.

For an efficient drilling process to be applied in steeply dipping mining and optimal stable HWs of wellbores, stresses must be studied at various intervals of depth and radius. For effective radial stress analysis, the distance usually considered is five times the well radius. Moreover, tangential, axial, and shear stresses on planes at the edge of the wellbore involving different scenarios of five times of the well radius, ten times of the radius, and ten meters from the wellbore were determined. The results of the stress analysis by the analytical and DEM methods can be summarized as:

The radial and axial stresses on the edge of the wellbore are linear and will increase by increasing the depth. However, this trend at five times the well radius and more converts

to a sinusoidal shape and fluctuate every 90 degrees, while the entire style is a rising trend. The tangential stresses at the wellbore edge, and five times the well radius and more is a sinusoidal shape and will increase by increasing the depth. This stress also has fluctuations every 90 degrees, but the entire results is a rising trend.

The shear stress of the radial and tangential planes is zero on the edge of the wellbore from the surface to 100m depth and all around the wellbore. However, this trend at five times the well radius or more converts to a sinusoidal shape and fluctuate every 90 degrees, while the entire style is a rising trend.

The shear stress of the tangential and axial planes on the edge of the wellbore has one periodic sinusoidal shape. This graph at a zero and 180 degrees has zero value, and at 90 and 270 degrees are its maximum and negative maximum. The shear stress of the radial and axial planes is zero on the edge of the wellbore from the surface to 100m depth and all around the wellbore. However, this trend at five times the well radius or more converts to a curve shape and has a peak at 180 degrees, while the entire style is a rising trend.

The average results of the DEM simulation agreed with the theoretical results. However, the maximum stress near the wellbore obtained by the DEM simulation is higher than that of the theoretical, suggesting that there was a stress concentration phenomenon. In the far-field region from the wellbore center, the stress concentration was decreased.

All failure criteria, the theoretical calculation results, and the DEM simulation result showed that all calculated stresses are between these two surfaces, and the wellbore is stable and safe up to 100m depth.

References

- A Henderson, MB Revell, D Landriault, and J Coxon. Handbook on mine fill: paste fill. Perth: Australian Centre for Geomechanics, pages 81–97, 2005.
- A Kesimal, E Yilmaz, and B Ercikdi. Evaluation of paste backfill test results obtained from different size slumps with varying cement contents for sulphur rich mill tailings. Cement and Concrete Research, 34(10):1817–1822, 2004.
- A Lopez-Pacheco. The golden key. 14, No. 5, 2019.
- Alireza Ghirian and Mamadou Fall. Coupled thermo-hydro-mechanical–chemical behavior of CPB in column experiments: Part II: Mechanical, chemical and microstructural processes and characteristics. Engineering Geology, 170:11–23, 2014.
- American Society For Testing and Materials. ASTM C39/C39M-12 Standard test method for compressive strength of cylindrical concrete specimens. ASTM West Conshohocken˚ ePA PA, 2012.
- Amjad Tariq and Moncef Nehdi. Developing durable paste backfill from sulphidic tailings. In Proceedings of the Institution of Civil Engineers-Waste and Resource Management, volume 160, pages 155–166. Thomas Telford Ltd, 2007.
- Anson Marston. The theory of external loads on closed conduits in the light of the latest experiments. In Highway research board proceedings, volume 9, 1930.
- Anthony G Grice. Recent minefill developments in Australia. In Minefill 2001:7 th International Symposium on Mining with Backfill, pages 351–357, 2001.

- ASTM C192. ASTM C192/C192M—16a standard practice for making and curing concrete test specimens in the laboratory. ASTM Standard Book, pages 4–9, 2016.
- ASTM Standard. D4543 (2007). Standard practices for preparing rock core as cylindrical test specimens and verifying conformance to dimensional and shape tolerances," American Society for Testing and Materials.
- ASTM Standard. D7012–10 (2010) Standard test method for compressive strength and elastic moduli of intact rock core specimens under varying states of stress and temperatures. Annual Book of ASTM Standards, American Society for Testing and Materials, West Conshohocken, PA, pages 495–498, 2010.
- ASTM. ASTM C1157 2011: Standard Performance Specification for Hydraulic Cement, 2011.
- Ayhan Kesimal, Erol Yilmaz, Bayram Ercikdi, Ibrahim Alp, and Hacı Deveci. Effect of properties of tailings and binder on the short-and long-term strength and stability of CPB. Materials Letters, 59(28):3703–3709, 2005.
- B Ercikdi, A Kesimal, F Cihangir, H Deveci, and I Alp. Yazıcı M, Sahin B (2009a) An environmentally friendly technology: paste backfill—a case study in Cayeli copper mine 3. In Mining and environment symposium, Ankara, pages139–152.
- B Ercikdi, F Cihangir, A Kesimal, and H Deveci. Waste management method for mill tailings: paste backfill technology. Mining Turkey, 24:70–75, 2012.
- B Slump Tests. Conform to ASTM C143. Perform one test for each load point of discharge and one for each set of compressive strength test specimens, 3330.

- Bayram Ercikdi, Ferdi Cihangir, Ayhan Kesimal, Haci Deveci, and Ibrahim Alp. Utilization of industrial waste products as pozzolanic material in cemented paste backfill of high sulphide mill tailings. Journal of hazardous materials, 168(2-3):848–856, 2009.
- BK Low, SK Tang, and V Choa. Arching in piled embankments. Journal of Geotechnical Engineering, 120(11):1917–1938, 1994.
- BW Ramme. ACI 229R-99 controlled low-strength materials. Am. Concr. Inst, 99:1–15, 2005.
- C ASTM. 1688.". Standard Test Method for Density and Void Content of Freshly Mixed Pervious Concrete," Annual Book of ASTM Standards, 4(2), 2008.
- C Caceres. Effect of backfill on longhole open stoping. MA Sc Thesis, University of British Columbia, 2005.
- C Winch. Geotechnical characteristics and stability of paste backfill at BHP Cannington mine. BE Hons Thesis, James Cook University, Townsville, Australia, 1999.
- D Landriault, R Verburg, W Cincilla, and D Welch. Paste technology for underground backfill and surface tailings disposal applications. In Short course notes, Canadian Institute of Mining and Metallurgy, Technical workshop oe april, volume 27, page 1997, 1997.
- D Landriault. Paste backfill mix design for Canadian underground hard rock mining. In 97th Annual General Meeting of CIM. Rock Mechanics and Strata Control Session. Halifax, Nova Scotia, pages 239–238, 1995.

- D Okland, JM Cook, et al. Bedding-related borehole instability in high-angle wells. In SPE/ISRM rock mechanics in petroleum engineering. Society of Petroleum Engineers,1998.
- D2166 ASTM. 2166/D 2166M (2013) Standard test method for unconfined compressive strength of cohesive soil. ASTM International, West Conshohocken.
- David F McCarthy and David F McCarthy. Essentials of soil mechanics and foundations, volume 505. Reston Publishing Company Virginia, 1977.
- David M Chambers and Bretwood Higman. Long term risks of tailings dam failure. Center for Science in Public Participation, Bozeman, Montana, 2011.
- DF Coates. Caving, subsidence, and ground control. Rock Mechanics Principles, CANMET, Department of Energy, Mines and Resources, Canada, pages 5–1,1981.
- Dragana Simon. Microscale analysis of cemented paste backfill. University of Toronto, 2005.
- DS Webbstock, MA Keen, and RA Bradley. Backfilling operations at Cooke 3 shaft. In Proc. 5th Int. Symp. on Mining with backfill, Johannesburg, South Africa, pages 295–305, 1993.
- E Villaescusa. Quantifying open stope performance. Proceedings of Mass Min, pages 96–104, 2004.
- Emel Guney Cetiner, Bahtiyar Unver, and Mehmet Ali Hindistan. Regulations related with mining wastes: European community and turkey. Madencilik, 45(1):23–34, 2006.

- Erling Fjar, Rachel M Holt, AM Raaen, and P Horsrud. Petroleum related rock mechanics. Elsevier, 2008.
- Erol Yilmaz and Mamadou Fall. Introduction to paste tailings management. In Paste Tailings Management, pages 1–5. Springer, 2017.
- Erol Yilmaz, Tikou Belem, and Mostafa Benzaazoua. Effects of curing and stress conditions on hydromechanical, geotechnical and geochemical properties of cemented paste backfill. Engineering Geology, 168:23–37, 2014.
- Eva Jiránková. Utilisation of surface subsidence measurements in assessing failures of rigid strata overlying extracted coal seams. International journal of rock mechanics and mining sciences (1997), 53:111–119, 2012.
- Ferdi Cihangir, Bayram Ercikdi, Ayhan Kesimal, Alp Turan, and Haci Deveci. Utilisation of alkali-activated blast furnace slag in paste backfill of high-sulphide mill tailings: effect of binder type and dosage. Minerals Engineering, 30:33–43, 2012.
- FP Hassani and D Bois. Economic and technical feasibility for backfill design in Quebec underground mines. Final report 1/2, Canada-Quebec Mineral Development Agreement. Research & Development in Quebec Mines. Contract no. EADM, 1992, 1989.
- FW Brackebusch. Basics of paste backfill systems. In International Journal of Rock Mechanics and Mining Sciences and Geomechanics Abstracts, volume 3, page 122A, 1995.

- Geraldo R Iglesia, Herbert H Einstein, and Robert V Whitman. Determination of vertical loading on underground structures based on an arching evolution concept. In Geo-Engineering for underground facilities, pages 495–506. ASCE, 1999.
- Heinz Konietzky, Lothar te Kamp, T Groeger, and C Jenner. Use of DEM to model the interlocking effect of geogrids under static and cyclic loading. Numerical modeling in micromechanics via particle m*ethods*, pages 3–12, 2004.
- J Naylor, RA Farmery, and RA Tenbergen. Paste backfill at the Macassa mine with flash paste production in a paste production and storage mechanism. In Proceedings 29th annual meeting of the Canadian mineral processors, Ottawa, Ontario, January, pages 21–23, 1997.
- Jabulani S Mahlaba, Elsabé P Kearsley, Richard A Kruger, and Pieter Corne Pretorius. Evaluation of workability and strength development of fly ash pastes prepared with industrial brines rich in SO4= and Cl- to expand brine utilisation. Minerals Engineering, 24(10):1077–1081, 2011.
- Javad Someehneshin, Weizhou Quan, Abdelsalam Abugharara, and Stephen Butt. Assessment of Freestanding Vertical Face for the Backfill Using the Run of the Mine Tailings and Portland Cement. ARMA, Canada, 2020.
- JB Cheatham Jr et al. Wellbore stability. Journal of petroleum technology, 36(06):889–896, 1984.
- JB Szymakowski. UDEC modeling of constant normal stiffness direct shear tests. In Numerical Modelling of Discrete Materials in Geotechnical Engineering, Civil Engineering and Earth Sciences: Proceedings of the First International

UDEC/3DEC Symposium, Bochum, Germany, 29 September-1 October 2004, page 145. CRC Press, 2004.

- JR Barrett, MA Coulthard, and PM Dight. Determination of fill stability. 1978.
- K Been, ET Brown, and N Hepworth. Liquefaction potential of paste fill at Neves Corvo mine, Portugal. Mining Technology, 111(1):47–58, 2002.
- K Le Roux, WF Bawden, and MW Grabinsky. Liquefaction analysis of early age cemented paste backfill. In Proceedings of the 8th International Symposium on Mining with Backfill, Beijing, China, pages 19–21, 2004.
- K Mathews, E Hoek, DC Wyllie, and SBV Steward. Prediction of stable excavation spans for mining at depths below 1000 Meters in hard rock mines. CANMET Report DSS Serial, 1981.
- Kandiah Pirapakaran and Nagaratnam Sivakugan. A laboratory model to study arching within a hydraulic fill stope. Geotechnical Testing Journal, 30(6):496– 503, 2007.
- Kandiah Pirapakaran. Load-deformation characteristics of minefills with particular reference to arching and stress developments. PhD thesis, James Cook University, 2008.
- Karl Terzaghi. Theoretical soil mechanics. johnwiley & sons. New York, pages 11–15, 1943.
- Katherine Klein and Dragana Simon. Effect of specimen composition on the strength development in cemented paste backfill. Canadian Geotechnical Journal, 43(3):310–324, 2006.

- Le Huynh, DA Beattie, D Fornasiero, and J Ralston. Effect of polyphosphate and naphthalene sulfonate formaldehyde condensate on the rheological properties of dewatered tailings and cemented paste backfill. Minerals engineering, 19(1):28–36, 2006.
- Libardo Orejarena and Mamadou Fall. Artificial neural network based modeling of the coupled effect of sulphate and temperature on the strength of cemented paste backfill. Canadian Journal of Civil Engineering, 38(1):100–109, 2011.
- LM Amaratunga and DN Yaschyshyn. Development of a high modulus paste fill using fine gold mill tailings. Geotechnical & Geological Engineering, 15(3):205–219, 1997.
- M Aubertin, LSTBM Li, S Arnoldi, T Belem, B Bussière, M Benzaazoua, and R Simon. Interaction between backfill and rock mass in narrow stopes. Soil and rock America, 1:1157–1164, 2003.
- M Fall, M Benzaazoua, and EG Saa. Mix proportioning of underground cemented tailings backfill. Tunnelling and Underground space technology, 23(1):80– 90, 2008.
- M Fall, M Benzaazoua, and S Ouellet. Experimental characterization of the influence of tailings fineness and density on the quality of cemented paste backfill. Minerals engineering, 18(1):41–44, 2005.
- M Pokharel and M Fall. Combined influence of sulphate and temperature on the saturated hydraulic conductivity of hardened cemented paste backfill. Cement and Concrete Composites, 38:21–28, 2013.

- Mayte Rico, Gerardo Benito, AR Salgueiro, Andrés Díez-Herrero, and HG Pereira. Reported tailings dam failures: a review of the European incidents in the worldwide context. Journal of hazardous materials, 152(2):846–852, 2008.
- MDA Thomas, MH Shehata, and SG Shashiprakash. The use of fly ash in concrete: classification by composition. Cement, concrete and aggregates, 21(2):105–110, 1999.
- Mehmet Yumlu. Mining with paste fill. In AusIMM Cobar Mining Seminar, 26p, 2010.
- MG Karfakis and E Topuz. Post mining subsidence abatements in Wyoming abandoned coal mines.[USA-Wyoming]. 1991.
- MG Spangler. Culverts and conduits. Chapter 11, Foundation engineering, GA Leonards, ed, 1962.
- Mostafa Benzaazoua, Jacques Ouellet, Stéphane Servant, Phil Newman, and Rens Verburg. Cementitious backfill with high sulfur content physical, chemical, and mineralogical characterization. Cement and concrete research, 29(5):719– 725, 1999.
- N Sivakugan, RM Rankine, KJ Rankine, and KS Rankine. Geotechnical considerations in mine backfilling in Australia. Journal of Cleaner Production, 14(12-13):1168–1175, 2006.
- Nasir and M Fall. Coupling binder hydration, temperature and compressive strength development of underground cemented paste backfill at early ages. Tunnelling and Underground Space Technology, 25(1):9–20, 2010.

- NC Gay, AJ Jager, and PS Piper. A quantitative evaluation of fill performance in South African gold mines. In Proceedings of a Symposium on Backfill in South African Mines. South African Institute of Mining and Metallurgy, Randburg, 1986.
- Ne Last, R Plumb, R Harkness, P Charlez, J Alsen, M McLean, et al. An integrated approach to evaluating and managing wellbore instability in the Cusiana field, Colombia, South America. In SPE annual technical conference and exhibition. Society of Petroleum Engineers, 1995.
- O Nasir and M Fall. Shear behavior of cemented pastefill-rock interfaces. Engineering Geology, 101(3-4):146–153, 2008.
- Olena Medelyan, David Milne, Catherine Legg, and Ian H Witten. Mining meaning from Wikipedia. International Journal of Human-Computer Studies, 67(9):716–754, 2009.
- Paul Marinos, Evert Hoek, et al. GSI: a geologically friendly tool for rock mass strength estimation. In ISRM international symposium. International Society for Rock Mechanics and Rock Engineering, 2000.
- Peter A Cundall. A computer model for simulating progressive, large-scale movement in blocky rock system. In Proceedings of the International Symposium on Rock Mechanics, 1971.
- PR Helm, CT Davie, and S Glendinning. Numerical modelling of shallow abandoned mine working subsidence affecting transport infrastructure. Engineering Geology, 154:6–19, 2013.

- QD Nguyen and DV Boger. Application of rheology to solving tailings disposal problems. International Journal of Mineral Processing, 54(3-4):217–233, 1998.
- R Cooke. Backfill pipeline distribution systems-design methodology review. CIM Magazine, 2(5), 2007.
- R Glamheden, H Hökmark, and R Christiansson. Modeling creep in jointed rock masses, 1st International UDEC/3DEC Symposium: Numerical Modeling of Discrete Materials in Geotechnical Engineering. Civil Engineering and Earth Science, Bochum, Germany, 2004.
- Resat Ulusay and Candan Gokceoglu. The modified block punch index test. Canadian Geotechnical Journal, 34(6):991–1001, 1997.
- RG Gürtunca, AR Leach, G York, and ML Treloar. In situ performance of cemented backfill in a deep-level South African gold mine. In Minefill, volume 93, pages 121–8, 1993.
- Richard Brummer. Paste: the fill of the future?(Part I). Canadian Mining Journal, pages 112, 31–5, 1991.
- RJ Mitchell. Stability of cemented tailings backfill. Computer and physical modelling in geotechnical engineering. Balkema, Rotterdam, pages 501–507, 1989.
- Robert J Mitchell, Richard S Olsen, and John D Smith. Model studies on cemented tailings used in mine backfill. Canadian Geotechnical Journal, 19(1):14– 28, 1982.
- S Clayton, TG Grice, and DV Boger. Analysis of the slump test for on-site yield stress measurement of mineral suspensions. International journal of mineral processing, 70(1-4):3–21, 2003.

- Shahid Azam and Qiren Li. Tailings dam failures: a review of the last one hundred years. Geotechnical news, 28(4):50–54, 2010.
- Shaohua Zhou, Richard Hillis, Mike Sandiford, et al. On the Mechanical Stability of lnclined Wellbores. SPE Drilling & Completion, 11(02):67–73, 1996.
- Sven Knutsson. Stresses in the hydraulic backfill from analytical calculations and in-situ measurements. In Conference on the Application of Rock Mechanics to Cut and Fill Mining: 01/06/1980-03/06/1980, pages 261–268. The Institution of Mining and Metallurgy, 1981.
- T Aoki, CP Tan, and WE Bamford. Stability analysis of inclined wellbores in saturated anisotropic shales. 1994.
- Tikov Belem and Mostafa Benzaazoua. Design and application of underground mine paste backfill technology. Geotechnical and Geological Engineering, 26(2):147–174, 2008.
- Tony Grice. Underground mining with backfill. 2nd Annual Summit oe Mine Tailings Disposal Systems, Brisbane, Nov, pages 24–25, 1998.
- UP WISE. Chronology of major tailings dam failures, 2016.
- W Helms. Preparation and transportation systems for cemented backfill. Mining Science and Technology, 7(2):183–193, 1988.
- W Hustrulid, Y Qianyuan, and N Krauland. Modelling of cut-and-fill mining systems-Näsliden revisited. In International Symposium on mining with backfill. 4, pages 147–164, 1989.

- Xi Chen, Chee P Tan, CM Haberfield, et al. A comprehensive practical approach for wellbore instability management. In SPE International Oil and Gas Conference and Exhibition in China. Society of Petroleum Engineers, 1998.
- Yi Ming Wang, Ming Qing Huang, Ai Xiang Wu, Gao Hui Yao, and Kai Jian Hu. Rock backfill and hazard control of abandoned stopes: A case study. In Applied Mechanics and Materials, volume 368, pages 1726–1731. Trans Tech Publ, 2013.
- Yuan Yao and Henghu Sun. A novel silica alumina-based backfill material composed of coal refuse and fly ash. Journal of hazardous materials, 213:71–82, 2012.
- Yves Potvin, Ed Thomas, and Andy Fourie. Handbook on mine fill. In Not available, page 179. Australian Centre for Geomechanics, 2005.
- Zdzisław Tadeusz Bieniawski. Engineering rock mass classifications: a complete manual for engineers and geologists in mining, civil, and petroleum engineering. John Wiley & Sons, 1989.